

UNITARIZING HIGH-ENERGY SCATTERING AMPLITUDES
IN YANG-MILLS THEORY

by

JOHN A. DICKINSON

B.A., City College of New York
(1973)

M.A., City College of New York
(1973)

SUBMITTED IN PARTIAL FULFILLMENT
OF THE REQUIREMENTS FOR THE
DEGREE OF

DOCTOR OF PHILOSOPHY

at the

MASSACHUSETTS INSTITUTE OF TECHNOLOGY

JULY, 1978

© Massachusetts Institute of Technology

ARCHIVES
MASSACHUSETTS INSTITUTE
OF TECHNOLOGY

AUG 28 1978

LIBRARIES

Signature of Author.....
Department of Mathematics, July 13, 1978

Certified by.....
Thesis Supervisor

Accepted by.....
Chairman, Department Committee

UNITARIZING HIGH-ENERGY SCATTERING AMPLITUDES
IN YANG-MILLS THEORY

by

JOHN A. DICKINSON

Submitted to the Department of Mathematics
on July 13, 1978 in partial fulfillment of the requirements
for the Degree of
Doctor of Philosophy

ABSTRACT

A new calculational scheme for unitarizing S-matrix amplitudes in the high-energy limit is applied to a Yang-Mills theory with SU(2) symmetry. The vector-meson-vector-meson elastic scattering amplitude is calculated through the eighth order in the coupling constant and it is shown that the result can be expressed in the exponential form $S = \exp(iV)$, where the potential V is an infinite-dimensional hermitian matrix whose individual entries are of the Regge-pole form. This result is explicitly unitary in all channels.


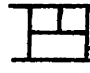
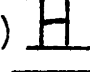

Thesis Supervisor: Hung Cheng

Title: Professor of Mathematics

ACKNOWLEDGEMENTS

The work described in this thesis is part of a general theory of high-energy scattering which has been developed by a group headed by Professor Hung Cheng. Many of the ideas presented here are due to Professor Cheng. I sincerely thank him for his contribution and also for the encouragement, benevolence and support he has shown me while I have been his advisee. Other members of the group were C.Y. Lo, Patrick Yeung and Kaare Olaussen. I am grateful for the many useful discussions we have had and, more specifically, for their contributions to an earlier version of the calculation presented here.

TABLE OF CONTENTS

	<u>Page</u>
Abstract.....	2
Acknowledgements.....	3
I. Introduction.....	5
II. The Feynman Diagram Calculation. Second Through Sixth Orders.....	17
i) The Isospin Calculation.....	17
ii) The Second and Fourth Order Calculations.....	20
iii) The Sixth Order Calculation.....	22
III. The Feynman Diagram Calculation. Eighth Order.....	31
i)  Type Diagrams.....	32
ii)  Type Diagrams.....	34
iii)  Type Diagrams.....	46
iv)  Type Diagrams.....	59
IV. The Feynman Diagram Calculation. Summary.....	84
V. The Calculation from Exponentiation.....	86
VI. The Eikonal Form in Impact-Distance Space.....	98
VII. Conclusion.....	103
Appendix I. Feynman Rules.....	106
Appendix II. On the Infinite-Momentum Space Technique and Momentum-Flow Diagrams.....	108
Appendix III. Transverse-Momentum Diagrams.....	124
Appendix IV. Identities Involving Sums of Products of Propagators.....	126
References.....	131

I. Introduction

There are two general methods that have been used in the past to study high-energy scattering. These are model building and calculations in field theories. Examples of models are the Regge-pole model,¹⁴ the droplet model,¹⁵ the parton model,¹⁶ and multiperipheral models.¹⁷ The procedure is to start with some assumptions which are motivated by a variety of physical reasons and to see what consequences can be deduced. One advantage of this method is that it is often possible to make definite physical statements that can then be compared with experiments. The disadvantage of the method is that the starting point is an assumption -- it may be plausible but it is not on a firm theoretical basis. And if it is not true, the whole structure built on it collapses. For example, the Regge-pole model and the droplet model are based on generalizations from non-relativistic potential theory. And since we believe that the strong interactions are properly described by a fully relativistic quantum field theory, it is questionable how valid the starting points in these models are.

The other general method for studying high-energy scattering, which is the one that is used in this thesis, is to do a calculation in field theory. Over the last decade very extensive computations have been done in two field theories: quantum-electrodynamics (QED)¹ and Yang-Mills theories.^{2,3}

The advantage to such an approach is that we really believe in the starting point. In particular, QED has had very impressive successes both theoretically and experimentally, and Yang-Mills theories provide the general framework for most present day fundamental work on the weak, electromagnetic and strong interactions.

The Yang-Mills theories¹⁸ are based on the idea of generalizing local gauge invariance to non-Abelian groups. From this principle it is possible to deduce the existence of gauge vector mesons. One outstanding success of the Yang-Mills theory is the unification of the weak and electromagnetic interactions based on the coupling of the weak and electromagnetic currents with these gauge vector mesons.¹⁹ It is also believed that a Yang-Mills theory involving an octet of colored gauge mesons accurately describes the strong interaction. And it is hoped that future theoretical progress will succeed in unifying all three interactions in terms of a single Yang-Mills theory. Other advantages of Yang-Mills theories are that they are renormalizable,²⁰ that they possess asymptotic freedom,²¹ and that they can account for Bjorken scaling.

In the high-energy realm many physical features are realized in Yang-Mills theories: the approximate conservation of helicity, the fact that the amplitudes for quantum number exchange processes are much smaller than the amplitude for no exchange of quantum numbers, and the fact that the real

part of the scattering amplitude is small. This last feature implies that the one-vector exchange amplitude, which is real, is forbidden, and hence that the vector meson involved carries some forbidden quantum number, such as color. Finally, the near constancy of the total cross-section suggests that the diffractive process is mediated by a vector meson.

The disadvantages of doing a perturbative calculation in field theory are first, that there are certain non-perturbative effects which may not be accurately accounted for, and second, that it is necessary to assume that the sum of the terms ignored, which are individually large, is small compared to the sum of the terms kept.

It is very difficult to do these calculations, and, once done, to deduce physical consequences from the calculated scattering amplitude. However, this cannot be considered a flaw in field theoretic calculations themselves -- rather, it is a difficulty inherent in nature. These calculations are perturbative calculations in powers of the coupling constant g , which is assumed to be small. But unlike standard perturbative calculations in quantum mechanics, for example, we cannot get a good approximation by taking just the first few terms in the expansion. The reason is that the scattering amplitude is a function not only of g , which is small, but also of the energy of the system, which is large. And so the perturbative expansion is really

a double power series in both of these variables.

In these computations the most difficult general principle to satisfy is unitarity. It is not hard to understand why. Dispersion relations are automatically incorporated into individual Feynman diagrams, and crossing symmetry can be satisfied by including crossed diagrams. But the unitarity condition interrelates the amplitudes of an infinite number of Feynman diagrams. And any approximation scheme which includes one Feynman diagram must include all others related to it, if the scheme is to be unitary. In both QED¹ and Yang-Mills theory^{3,4} it has turned out that the amplitudes in the leading logarithm approximation violate the Froissart bound,⁵ a limit placed on the size of the scattering amplitude by unitarity. In particular, for an SU(2) Yang-Mills theory with an isospin-1/2 Higgs doublet, Fadin, Kuraev and Lipatov⁴ and Cheng and Lo³ have separately found that for elastic scattering, $W + W \rightarrow W + W$, the sum of the leading logarithmic terms violates the Froissart bound in the $I = 0$ channel (no exchange of isospin).

Therefore it is necessary to develop a calculational

scheme which goes beyond the approximation of summing leading terms and which includes a larger set of Feynman diagrams. Of course, the choice of which diagrams to include and which to exclude cannot be arbitrary but must be consistent with the general principles of unitarity and crossing symmetry. In a previous series of letters^{6,7} Cheng, Lo, Olaussen, Yeung and the present author have formulated a new approximation scheme for high-energy scattering in both QED and Yang-Mills theories. A procedure was developed which incorporates s-channel unitarity and t-channel unitarity at every step and which treats elastic and inelastic scattering processes side by side. Here we will explicitly show that for a Yang-Mills theory with an isodoublet of Higgs bosons, using the approximations discussed below, the high-energy elastic scattering amplitude agrees, through the eighth order in the coupling constant g , with the Taylor series expansion of the matrix elements of $i(1 - e^{iV})$. The potential V is a hermitian operator whose matrix elements for a given process are the sum of the lowest order amplitudes with the propagators of the exchanged mesons replaced by Regge-poles. This result is explicitly unitary in all channels. The scattering amplitude may equivalently be written in the eikonal form in impact-distance space (\vec{b}) space

$$M_{fi} = 2s \int d^2\vec{b}_1 e^{i\vec{A}_1 \cdot \vec{b}_1} i \left(1 - e^{iU(\vec{b}_1, s)} \right)_{fi}, \quad (1.1)$$

where $U(\vec{b}_\perp, s)$ is defined by

$$V_{fi} = (2\pi)^4 \delta^{(4)}(P_i - P_f) 2 \int d^2\vec{b}_\perp e^{i\vec{\Delta}_\perp \cdot \vec{b}_\perp} \left(U(\vec{b}_\perp, s) \right)_{fi}, \quad (1.2)$$

where s is the square of the center-of-mass energy, $\vec{\Delta}_\perp$ is the transverse momentum transferred to one of the incident particles, and where P_i and P_f are the sums of the initial and final four-momenta. This will be discussed more fully below.

In any approximate calculation in perturbation theory, the crucial question to be answered is: "Which terms from the amplitudes of which Feynman diagrams are to be included in the calculation and why these terms and not others?" In the leading logarithm approximation (which is a weak coupling approximation) real terms of the order $g^2 s (g^2 \ln s)^n$ and imaginary terms of the order $i g^4 s (g^2 \ln s)^n$ were kept and terms with extra positive powers of g were neglected.* As we shall see below, such a scheme can never satisfy unitarity. In order to determine which scheme will, we must look at the unitarity condition itself. The scattering matrix S and the scattering amplitude \mathcal{M} are related according to

$$S = 1 + i (2\pi)^4 \delta^{(4)}(P_i - P_f) \frac{\mathcal{M}}{\sqrt{\pi} \lambda^n} \quad (1.3)$$

* Whenever we write $\ln s$ we really mean $\ln\left(\frac{s}{\lambda^2}\right)$ where λ is some appropriate mass scale, such as the mass of the vector-meson. Likewise, s^{-a} really means $\left(\frac{s}{\lambda^2}\right)^{-a}$.

where

$$f_n = \begin{cases} \frac{E_n}{m} & \text{for a fermion with energy } E_n \text{ and mass } m, \\ 2E_n & \text{for a boson.} \end{cases}$$

The product $\prod f_n$ in (1.3) is over all external particles. In terms of \mathcal{M} , the unitarity condition is

$$\text{Im } \mathcal{M}_{fi} = \frac{1}{2} \sum_n (2\pi)^4 \delta^{(4)}(P_i - P_n) \frac{\mathcal{M}_{fn}^* \mathcal{M}_{ni}}{\prod_m f_m} \quad (1.4)$$

where P_i and P_n are the total four-momenta of the incoming and intermediate states respectively and where there is a kinematic factor f_m for each particle in the intermediate state.

As a starting point, let us take the leading lowest order amplitudes for each process, elastic and inelastic, in which, in the center-of-momentum system, two incoming and two outgoing particles have extremely high energies and all other particles have much smaller (although perhaps still large) energies. The justification for considering these processes that contribute to the creation of intermediate energy particles in the CM system (pionization products) is that they give the dominant contributions to the total cross-section and to the imaginary part of an amplitude calculated via unitarity. The amplitude for $2+m$ particles going into $2+n$ particles is then of the order $g^{2+m+n} s$. Amplitudes with extra positive powers of g or with smaller

energy dependence are dropped. Thus we are considering the weak coupling limit. Examples of diagrams kept and diagrams ignored are given in Fig. 1. (These diagrams are all evaluated in the Feynman gauge and all extremely energetic particles are transversely polarized. By convention, the extremely energetic particles are at the top and bottom of each graph.)

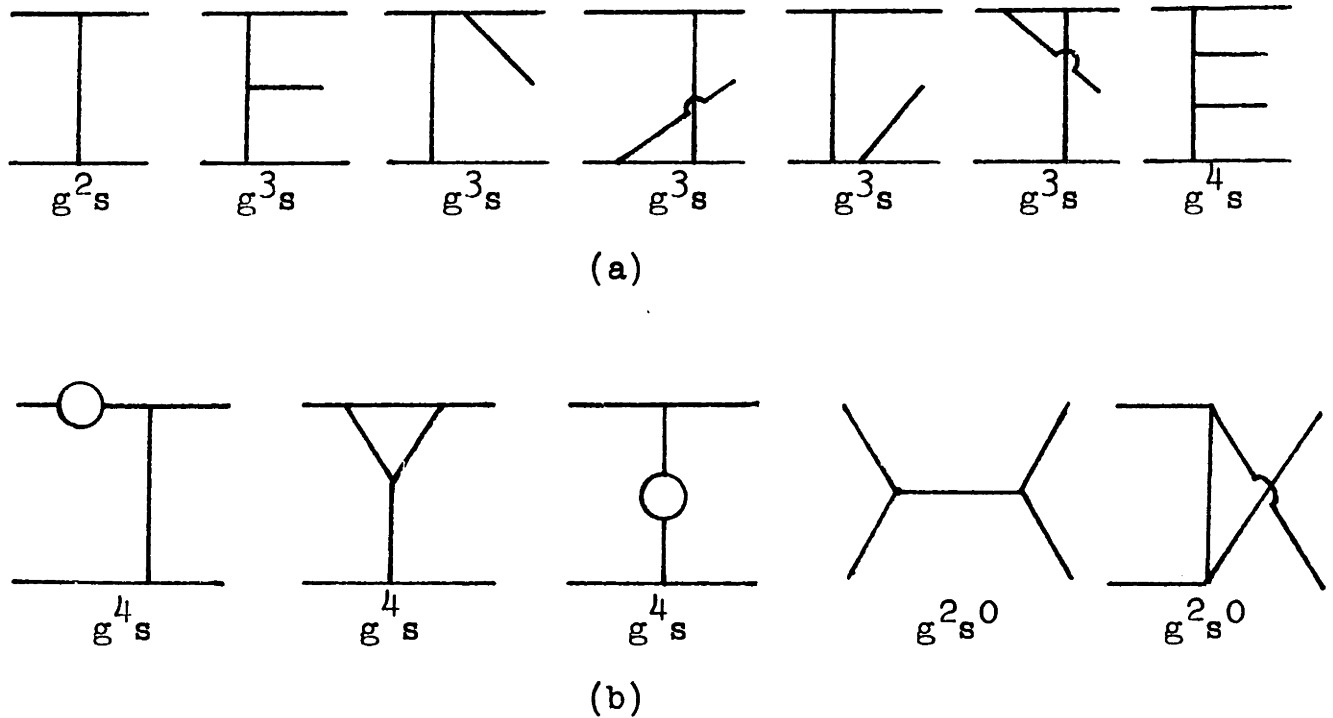


Fig. 1

(a) Examples of diagrams kept. (b) Examples of diagrams dropped. The order of each diagram is indicated.

If we put these leading lowest order amplitudes into the right-hand side of eqn. (1.4) then the leading imaginary parts of a new set of diagrams are generated. A subset of these diagrams which contribute to elastic scattering are shown in Fig. 2; these are the so-called tower diagrams. The imaginary parts

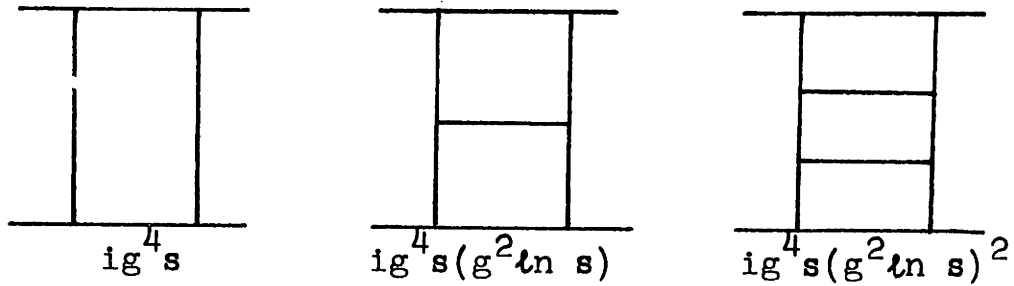


Fig. 2

The size of the imaginary parts of the amplitudes is indicated. The real parts are in fact larger by a factor of $\ln s$.

of the amplitudes of these tower diagrams are all of the order $ig^4 s (g^2 \ln s)^n$ for some n . These amplitudes must be included in any scheme which is to satisfy the unitarity condition, and they are included in the leading logarithm approximation. However, if we iterate once more by putting these amplitudes into the right-hand side of eqn. (1.4) we get amplitudes whose imaginary parts are of the order $ig^8 s (g^2 \ln s)^n$ (the corresponding diagrams are indicated in Fig. 3 -- of course there are other unitarity cuts which also contribute to the imaginary parts of these diagrams). These amplitudes

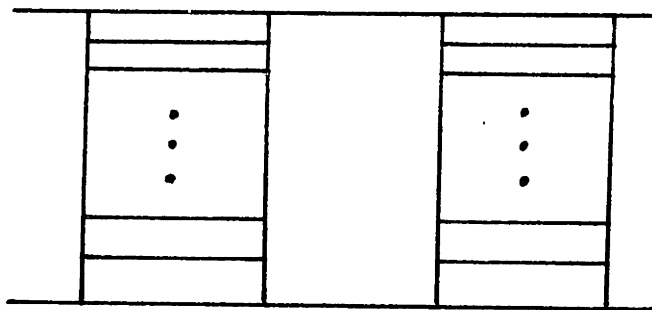


Fig. 3

are not included in the leading logarithm calculation and we must keep them in order to get a unitary answer. But we have already dropped terms of the same order of magnitude! For example, in the tower diagrams, unitarity dictated only that we keep the leading terms of order $ig^4s(g^2\ln s)^n$ but that terms with extra positive powers of g could be dropped. The way out of this paradox is to realize that the diagram in Fig. 3 has more vertices on the top and bottom horizontal lines (representing the extremely energetic particles) than the tower diagrams in Fig. 2. If we consider the extremely energetic particles to be carrying a "charge" T , then the tower diagrams are of the order $(gT)^4$ and the diagrams depicted in Fig. 3 are of the order $(gT)^8$. Thus, if $gT \sim 1$ and $g^2 \ll 1$ it is consistent to keep the terms from the diagrams in Fig. 3 and drop the non-leading terms from the tower diagrams.

In Yang-Mills theories there is a natural candidate for the "charge" T -- namely, isospin. Each scattering amplitude \mathcal{M} is the product of an isospin factor I and a space-time factor M (which is independent of isospin), $\mathcal{M} = M \cdot I$. If the two extremely energetic particles have isospin T then the isospin factor for any Feynman diagram is a polynomial in T whose degree is at most the number of vertices on the high-energy lines. Therefore, in the anticipation that it gives a unitary result (it does), we adopt the following calculational scheme for elastic scattering: terms of the order $(gT)^m s(g^2 \ln s)^n$ are kept and terms with extra positive powers of g are neglected.

Mathematically, the region where this approximation is valid is one where

$$gT \sim 1, \quad (1.5a)$$

$$g^2 \ln s \sim 1, \quad (1.5b)$$

and

$$g^2 \ll 1. \quad (1.5c)$$

In other words, g^2 is small and $\ln s$ and T are large. All terms in the leading logarithm approximation are included in the new approximation. This is because, as will be apparent below, all the leading logarithm real terms are of the order T^2 and all the leading logarithm imaginary terms are of the order T^4 . Since the potential U in eqn. (1.1) is of order T^2 , this means that the leading logarithm terms are just the first two terms in the power series expansion of $i(1 - e^{iU})$. Since successive terms in this expansion are larger and larger and the series is divergent it is clearly not a valid approximation to truncate it after any finite number of terms.

We emphasize that we calculate all diagrams by Feynman rules, keeping or discarding terms according to the above prescription. The above discussion of the unitarity condition is heuristic -- its purpose was to deduce a scheme which will give a unitary answer, not to actually calculate that answer.

Before writing down the explicit form of the potential we need some preliminaries. In the center-of-momentum system, where the total energy is $\sqrt{s} = 2\omega$, $s \rightarrow \infty$, precisely two particles have energies $\sim \omega$, and any other particles have much smaller energies. Thus the extremely energetic particles

have approximately equal and opposite momenta of magnitude $\sim \omega$. Let these momenta be oriented predominantly along the z-axis, and for an arbitrary four-vector $k = (k_0, k_1, k_2, k_3)$ define $k_{\pm} = k_0 \pm k_3$. Then one of these extremely energetic particles has + momentum $\sim 2\omega$ and - momentum $O(\frac{1}{\omega})$, and vice versa for the other one.

At high-energies, the helicities in the CM system are conserved. Let ϵ_1, ϵ_2 ($\epsilon_{1'}, \epsilon_{2'}$) be the polarization vectors for the incoming (outgoing) extremely energetic particles. If the W-mesons are transversely polarized, then in each amplitude there is a factor of $(\vec{\epsilon}_{1\perp} \cdot \vec{\epsilon}_{1'\perp})(\vec{\epsilon}_{2\perp} \cdot \vec{\epsilon}_{2'\perp})$, which will hereafter be suppressed. For each pair of W-mesons which are longitudinally polarized, the $\vec{\epsilon}_1 \cdot \vec{\epsilon}_1$ factor is replaced by a factor of 1/2. We will treat the case where the W-mesons are transversely polarized since when there is longitudinal polarization the calculations are complicated by the fact that many more diagrams contribute in the Feynman gauge.

The conclusion of the calculation is that in the high-energy limit, at least for elastic processes through the eighth order, the scattering matrix can be written in the form

$$S = e^{iV} \quad (1.6)$$

where

$$V = (2\pi)^4 \delta^{(4)}(P_i - P_f) \frac{\overline{\mathcal{M}}}{\sqrt{\prod_n f_n}} \quad , \quad (1.7)$$

and where the matrix elements of $\overline{\mathcal{M}}$ are given below. Consider scattering from a state with $m+2$ particles to a state with $n+2$ particles. Let \vec{k}_i , $i=1,2,\dots,n+m$ be the momenta of the n created and m annihilated particles, ordered so that $k_{i-} \gg k_{j-}$ if $i > j$, and let \vec{p}_1 and \vec{p}_2 (\vec{p}'_1 and \vec{p}'_2) be the momenta of the incoming (outgoing) extremely energetic particles with large + momentum and large - momentum respectively. (The states are normalized so that $\langle \vec{k} | \vec{k}' \rangle = (2\pi)^3 \delta^{(3)}(\vec{k} - \vec{k}')$.) Then the $\overline{\mathcal{M}}$ matrix element for this process is (suppressing isospin indices and the polarization vectors of the extremely energetic particles)

$$\langle \vec{p}'_1, \vec{p}'_2, n | \overline{\mathcal{M}} | \vec{p}_1, \vec{p}_2, m \rangle = 2g^2 s \left[\prod_{i=1}^{n+m} \frac{s_i^{-\alpha(\vec{\Delta}_i)}}{\vec{\Delta}_i^2 + \lambda^2} g V(\Delta_i, \Delta_{i+1}, k_i) \right] \frac{s_{n+m+1}^{-\alpha(\vec{\Delta}_{n+m+1})}}{\vec{\Delta}_{n+m+1}^2 + \lambda^2} I. \quad (1.8)$$

In the above equation λ is the mass of the W-meson,

$$\Delta_1 = p_1 - p_{1'}, \quad (1.9a)$$

$$\Delta_{i+1} = \begin{cases} \Delta_i - k_i & \text{if the } i^{\text{th}} \text{ particle is created,} \\ \Delta_i + k_i & \text{if the } i^{\text{th}} \text{ particle is annihilated,} \end{cases} \quad (1.9b)$$

$i=1, 2, \dots, n+m$

$$s_i = (p_{1'} + k_1)^2 \sim \omega k_{1-}, \quad (1.10a)$$

Fig. 4. The form of the vertex factor (1.12) is based on the calculation of the two-body to three-body scattering amplitude.^{4,8} Note that it is gauge invariant, that is, $\Gamma \cdot k = 0$. Eqn. (1.8) is also the matrix element when any number of intermediate energy particles pass through without interacting (see Fig. 4 for an example).

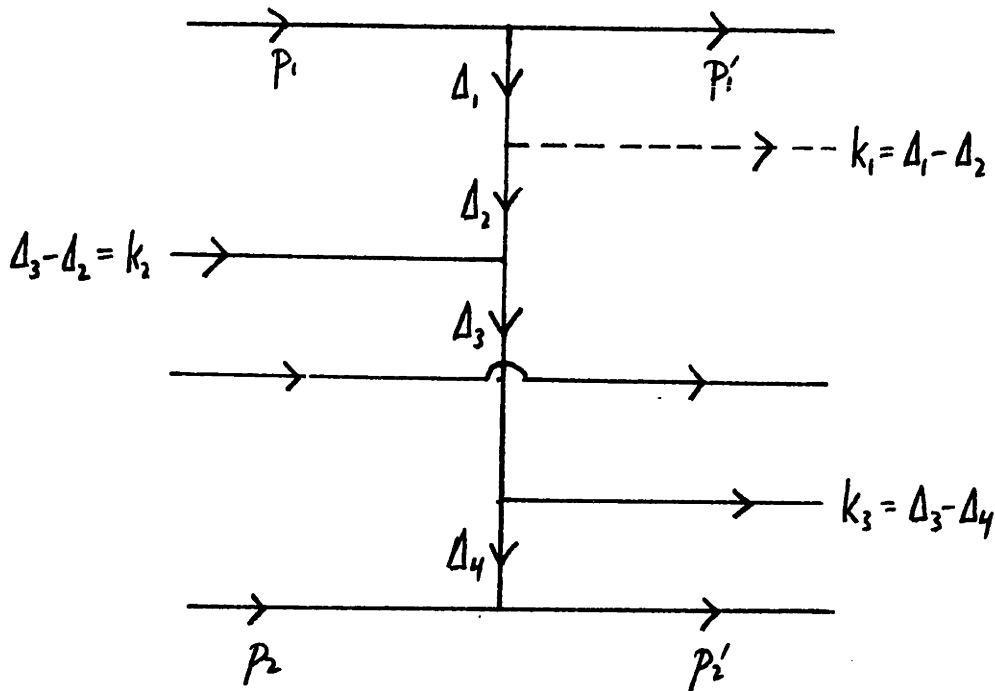


Fig. 4

An example of a matrix element of \mathcal{M} . $\langle \vec{p}_1, \vec{p}_2, \vec{k}_1, \vec{k}_3 | \mathcal{M} | \vec{p}_1, \vec{p}_2, \vec{k}_2 \rangle$
 $= 2sg^5 \prod_{i=1}^4 (s_i^{-\alpha(\vec{\Delta}_{i\perp})} (\Delta_{i\perp}^2 + \lambda^2)^{-1}) (-\lambda) \Gamma(\Delta_2, \Delta_3, k_2) \cdot \epsilon(k_2)$

$\times \Gamma(\Delta_3, \Delta_4, k_3) \cdot \epsilon(k_3)$ I. The isospin factor I is represented diagrammatically by precisely this diagram. Solid lines represent W-mesons and the dashed line represents the scalar Z.

A NOTE ON THE MANNER OF PRESENTATION

When this calculation was originally done, in collaboration with Hung Cheng and with the assistance of C. Y. Lo and Kaare Olaussen, the momentum dependence of the Feynman diagrams was calculated using the infinite-momentum technique and momentum-flow diagrams and the contribution of each diagram to the different isospin channels was calculated in terms of polynomials of the isospin generators. Subsequent to that, C. Y. Lo redid the isospin calculation²², expressing the isospin factors in terms of diagrams²³. This method makes the presentation clearer and has the additional advantage that it automatically verifies the eikonal form for all possible values of the t-channel isospins I , whereas previously this was established only for $I = 0$ and $I = 1$. However, only the $I = 0, 1, \text{ or } 2$ channels have any physical relevance, since in the scattering processes under consideration all external particles have isospin $\frac{1}{2}$ or 1 . The diagrammatic representation of isospin factors is used in this thesis.

II. The Feynman Diagram Calculation. Second Through Sixth Orders

The calculation via Feynman rules has already been done through the tenth order in the coupling constant g -- but only in the leading logarithm approximation, which corresponds to the real T^2 and imaginary T^4 terms of our new scheme. It is obvious that there are no imaginary T^2 terms, but it is not at all obvious what happens to the real T^4 terms. It is an important result of this calculation that the real T^4 terms cancel identically. Likewise, we will see that the T^6 terms are purely real and the T^8 terms are purely imaginary. This is clearly a necessary condition for the exponential form to hold, since successive terms in the Taylor series expansion of $i(1 - e^{iV})$ are alternately purely real and purely imaginary.

The necessary Feynman rules for the Yang-Mills $SU(2)$ theory with an isodoublet of Higgs bosons are given in Appendix I. The calculation will be done using the infinite-momentum technique throughout. For a background discussion of this technique and some sample calculations see Appendix II.

i) The Isospin Calculation

The isospin factors will be calculated diagrammatically. This procedure has the advantages of i) easy comparison with the exponential result, ii) not having to separately check the $I = 0, 1, 2, \dots$ channels of isospin exchange, and, most important,

iii) being generalizable to other gauge groups, since most of the manipulations of the isospin diagrams involve the Jacobi identity which is valid for all such groups.

The isospin factor associated with each Feynman diagram can be represented by precisely that diagram. Each line then carries an isospin index and the indices corresponding to all internal lines are summed over, from one to three. Each external line also has an isospin wave function, denoted χ . And each vertex has a numerical factor associated with it, as shown in Fig. 5. There, T_i are the isospin matrices which

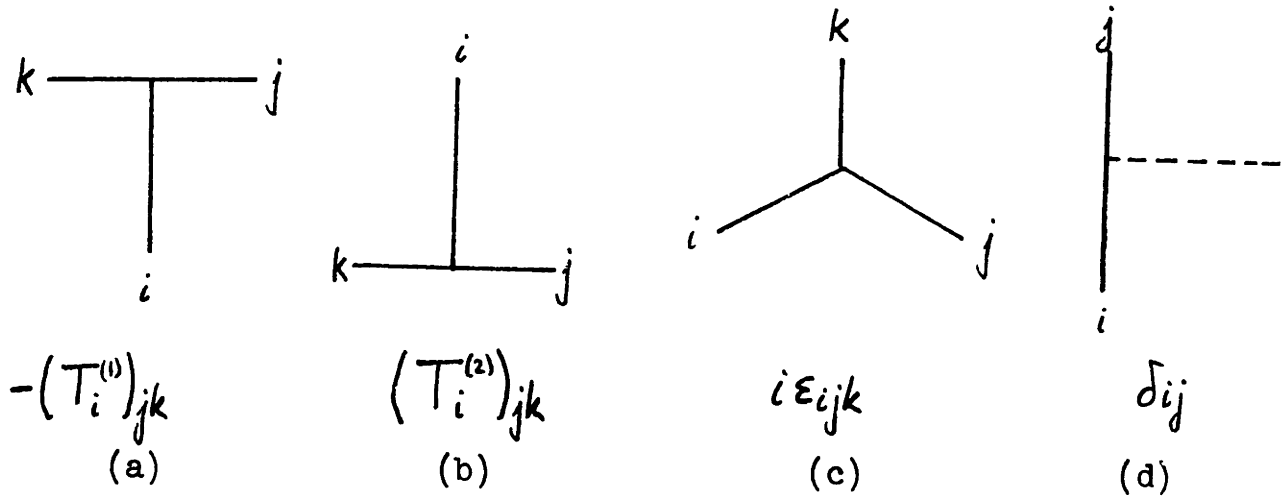


Fig. 5

(a) Top high-energy line, (b) bottom high-energy line, (c) internal three-vector-meson vertex, (d) internal vector-meson-scalar vertex.

satisfy the commutation rule

$$[T_i, T_j] = i\epsilon_{ijk}T_k, \quad (2.1)$$

and where

$$(T_i T_i)_{jk} = T(T+1)\delta_{jk}. \quad (2.2)$$

In eqns. (2.1) and (2.2) and in the sequel a sum (from one to three) over repeated indices is assumed. If $T = 1$, $(T_i)_{jk} = -i\epsilon_{ijk}$. Then the assignments given in Fig. 5(a,b,c) are all consistent.

As an example, the isospin factor corresponding to the diagram in Fig. 6 is

$$-\left(\chi_{1'}^\dagger T_i^{(1)} \chi_1\right)\left(\chi_{2'}^\dagger T_i^{(2)} \chi_2\right), \quad (2.3)$$

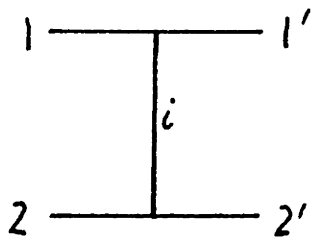


Fig. 6

and is, of course, $O(T^2)$.

The diagrammatic expression of eqn. (2.1), which is called the Jacobi identity, is given in Fig. 7. Another

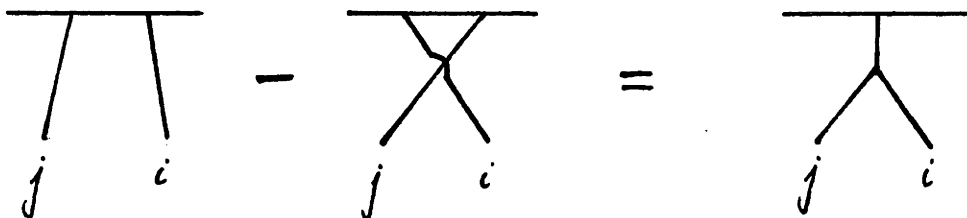


Fig. 7

useful identity, derived from (2.1), is

$$i\epsilon_{ijk} T_i T_j = \frac{1}{2} i\epsilon_{ijk} (T_i T_j - T_j T_i) = \frac{1}{2} i\epsilon_{ijk} (i\epsilon_{ijl} T_l) = -T_k \quad (2.4)$$

This is expressed diagrammatically in Fig. 8 and is called the triangle contraction. Both of the identities in Figs. 7 and 8

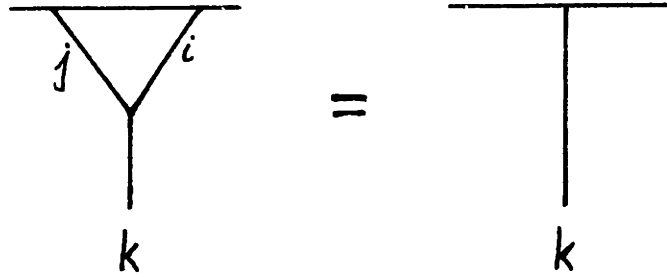


Fig. 8

can be turned upside down and remain valid.

ii) The Second and Fourth Order Calculations

The space-time amplitude for the second order diagrams (see Appendix II) is

$$2s g^2 \frac{1}{\Delta_1^2 + \lambda^2} \quad (2.5)$$

and the isospin factor is represented diagrammatically by the diagram in Fig. 6. The two fourth order Feynman diagrams which contribute in the high-energy limit are shown in Fig. 9(a) and 9(b). Call their space-time amplitudes M_a and M_b respectively. Using the isospin identities of Figs. 7 and 8, the isospin factor of the diagram shown in Fig. 9(b) can be

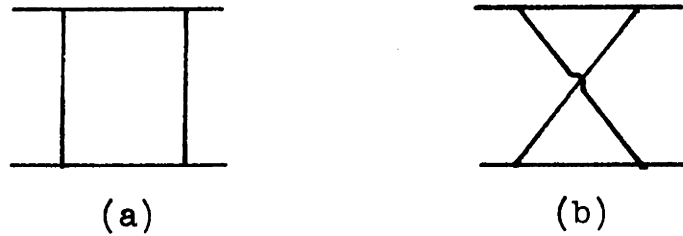


Fig. 9

expressed in terms of the isospin factors of Figs. 6 and 9(a). See Fig. 10. This identity exemplifies the general procedure

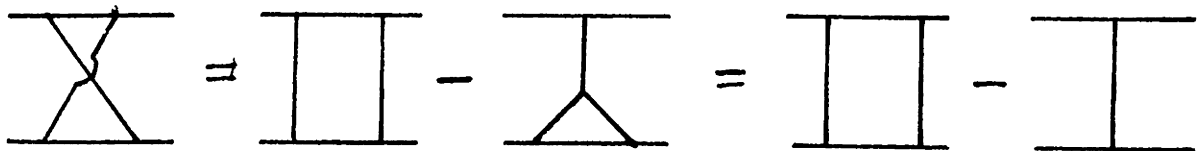


Fig. 10

to be used in this calculation. All isospin factors will be represented as linear combinations of isospin factors whose corresponding diagrams have only vertical and horizontal lines; for purposes of future identification these isospin factors will be called "box" factors. The advantage in this procedure is that the isospin factors generated from the exponential formula are all of this form and so the result of the Feynman diagram calculation can be easily compared with the result from exponentiation. Now the sum of the fourth order amplitudes equals

$$(M_a + M_b) \text{II} - M_b \text{I} \tag{2.6}$$

using an obvious notation for the isospin factors. From

Appendices II and IV,

$$M_b \sim 2g^2 s \frac{g^2 \ln s}{2\pi} K \quad (2.7)$$

and

$$M_a + M_b \sim ig^4 s K \quad (2.8)$$

where

$$K = \int \frac{d^2 \vec{q}_\perp}{(2\pi)^2} \frac{1}{(\vec{q}_\perp^2 + \lambda^2) [(\Delta_\perp - \vec{q}_\perp)^2 + \lambda^2]} \quad (2.9)$$

The integral K can be represented diagrammatically by a "transverse-momentum" diagram as shown in Fig. 11. See Appendix III for details. As claimed above the T^2 terms

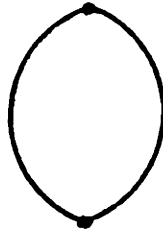


Fig. 11

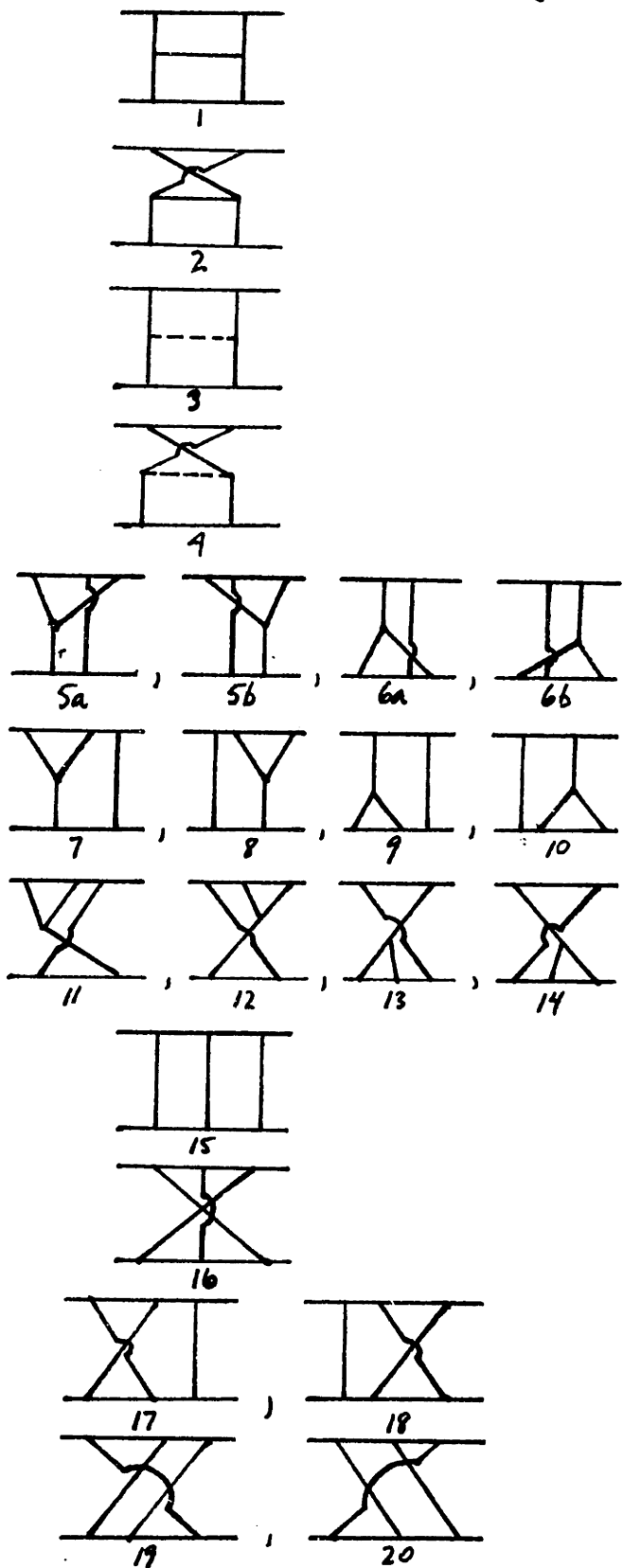
in (2.5) and (2.7) are real whereas the T^4 term in (2.8) is imaginary and contains no real terms proportional to s .

iii) The Sixth Order Calculation

The first step is to express the isospin factors of all diagrams which contribute in the high-energy limit in terms of the "box" factors. For the twenty contributing sixth order

Feynman diagrams

Isospin factors



0	0	1	0
-1	0	1	0
0	1	0	0
-1	1	0	0
0	1	-1	0
0	1	0	0
-1	1	0	0
0	0	0	1
1	-3	1	1
0	-1	0	1
0	-2	1	1

Table I (see next page for caption)

Caption to Table I: In the left column are the twenty contributing sixth order Feynman diagrams (or equivalently, their corresponding isospin diagrams). The isospin factors are expressed as linear combinations of the box isospin factors with coefficients given above. (Diagrams 5a and 5b (6a and 6b) are topologically equivalent but have different flows of the extremely energetic particles which by convention are represented by the top and bottom horizontal lines.)

Feynman diagrams this is done in Table I. Then, for each box isospin factor, the sum of the space-time factors multiplying it is evaluated to the appropriate order in $g^2 \ln s$. From Table I, the amplitude of the T^2 terms is

$$\left(-M_2 - M_4 - M_{11} - M_{12} - M_{13} - M_{14} + M_{16}\right) \mathbb{I}.$$

From the previous leading logarithm calculation it is known that

$$M_2 \sim -\frac{1}{2} g^2 s \left(\frac{g^2 \ln s}{2\pi}\right)^2 \left(2 \textcircled{8} + \lambda^2 \textcircled{8} - 4 \textcircled{8}\right), \quad (2.11a)$$

$$M_4 \sim \frac{1}{2} g^2 s \left(\frac{g^2 \ln s}{2\pi}\right)^2 \left(\lambda^2 \textcircled{8}\right), \quad (2.11b)$$

$$M_{11} \sim M_{12} \sim M_{13} \sim M_{14} \sim -\frac{1}{2} g^2 s \left(\frac{g^2 \ln s}{2\pi}\right)^2 \textcircled{8}, \quad (2.11c)$$

and

$$M_{16} = O(\ln s) \quad (2.11d)$$

so that (2.10) becomes

$$g^2 s \left(\frac{g^2 \ln s}{2\pi} \right)^2 \textcircled{\text{O}} \text{I} . \quad (2.12)$$

(See Appendix III for a discussion of the meaning of the transverse-momentum diagrams.) Notice that the divergences in the transverse-momentum integrations cancel out exactly and that the T^2 terms through the sixth order, from (2.5), (2.7) and (2.12), are exactly equal to the first three terms in the power series expansion of

$$2sg^2 \frac{1}{\vec{\Delta}_1^2 + \lambda^2} s^{-g^2(\vec{\Delta}_1^2 + \lambda^2) \frac{1}{2\pi}} \textcircled{\text{O}} \text{I} . \quad (2.13)$$

This indicates that the vector-meson Reggeizes.

Next consider the T^4 terms. From Table I, one such term is

$$(M_1 + M_2 - M_{5a} - M_{5b} - M_{6a} - M_{6b} + M_{16} + M_{19} + M_{20}) \text{I} \text{I} \quad (2.14)$$

Using the methods of Appendices II and IV, and especially the identity

$$\frac{1}{q_- + i\varepsilon} + \frac{1}{-q_- + i\varepsilon} = -2i\pi \delta(q_-), \quad (2.15)$$

we find that

$$M_1 + M_2 \sim -\frac{1}{2} ig^4 s \frac{g^2 \ln s}{2\pi} \left(2 \textcircled{\text{O}} + \lambda^2 \textcircled{\text{O}} - 4 \textcircled{\text{O}} \right). \quad (2.16)$$

Notice that separately M_1^1 and M_2 each contain real terms proportional to $\ln^2 s$ and $\ln s$ but they cancel out in the sum.

Likewise, using (2.15) again, we find that

$$M_{5a} + M_{5b} \sim M_{6a} + M_{6b} \sim ig^4 s \frac{g^2 \ln s}{2\pi} \bigcirc. \quad (2.17)$$

M_{5a}, M_{5b}, M_{6a} and M_{6b} each separately contain real terms proportional to $\ln s$ but, as above, they cancel out in the sum. The divergent parts of (2.16) and (2.17) also cancel.

Now consider the sum of the space-time amplitudes of diagrams 16, 19 and 20. Using the notation of Fig. 12,

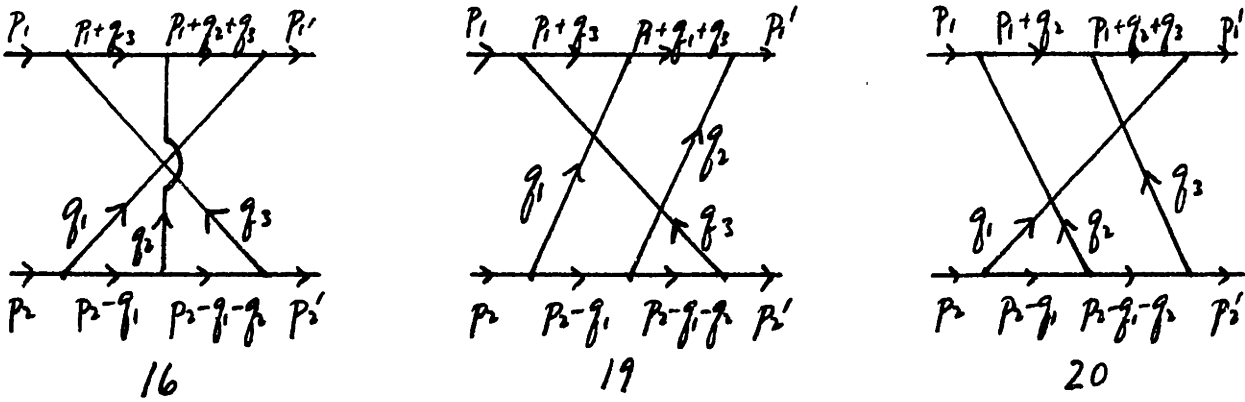


Fig. 12

$$\begin{aligned}
 M_{16} + M_{19} + M_{20} &\sim (-i)^{1+6+7} g^6 \frac{1}{2^2} \int \prod_{i=1}^2 \frac{d^2 \vec{q}_{i\perp}}{(2\pi)^2} \int \prod_{i=1}^3 \frac{dq_{i-}}{2\pi} \frac{dq_{i+}}{2\pi} \\
 &\times (2\pi) \delta\left(\sum_{i=1}^3 q_{i+}\right) (2\pi) \delta\left(\sum_{i=1}^3 q_{i-}\right) (-2s)^3 \frac{1}{p_{1+}^2 p_{2-}^2} \frac{1}{(-q_{1+}+i\epsilon)(-q_{1+}-q_{2+}+i\epsilon)} \\
 &\times \left(\prod_{i=1}^3 \frac{1}{q_{i+} q_{i-} - \vec{q}_{i\perp}^2 - \lambda^2 + i\epsilon} \right) \left\{ \frac{1}{(q_{3-}+i\epsilon)(q_{3-}+q_{2-}+i\epsilon)} \right. \\
 &\left. + \frac{1}{(q_{3-}+i\epsilon)(q_{3-}+q_{1-}+i\epsilon)} + \frac{1}{(q_{2-}+i\epsilon)(q_{2-}+q_{3-}+i\epsilon)} \right\}. \quad (2.18)
 \end{aligned}$$

From Appendix IV,

$$\delta\left(\sum_{i=1}^3 q_{i-}\right) \times \left\{ \text{sum in above brackets} \right\} = (-2\pi i) \frac{1}{q_{3-} + i\epsilon} \delta(q_{3-} + q_{1-}) \delta(q_{2-}). \quad (2.19)$$

This means that there is only one non-zero momentum-flow diagram corresponding to the integrals in (2.18) it is given in Fig. 13. It can be evaluated using the standard techniques

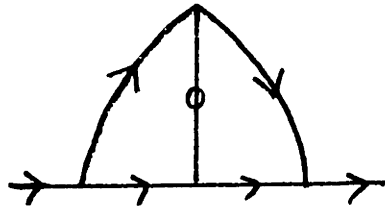


Fig. 13

The circle on the line means it carries no - momentum.

explained in Appendix II; the result is

$$M_{16} + M_{19} + M_{20} \sim 2ig^4s \frac{g^2 \ln s}{2\pi} \bigcirc. \quad (2.20)$$

Therefore (2.14) becomes

$$ig^4s \frac{g^2 \ln s}{2\pi} \left(-\bigcirc - \frac{1}{2} \lambda^2 \bigcirc + 2 \bigcirc \right) \square.$$

And again there is no real part.

The other term proportional to T^4 is

$$\left(M_3 + M_4 + M_{5a} + M_{5b} + M_{6a} + M_{6b} + M_7 + M_8 + M_9 + M_{10} \right. \\ \left. + M_{11} + M_{12} + M_{13} + M_{14} - 3M_{16} - M_{17} - M_{18} - 2M_{19} - 2M_{20} \right) \square.$$

Using (2.15) we readily find that

$$M_3 + M_4 \sim \frac{1}{2} i g^4 s \frac{g^2 \ln s}{2\pi} \lambda^2 \bigcirc \quad (2.23)$$

$$M_7 + M_{11} \sim M_8 + M_{12} \sim M_9 + M_{13} \sim M_{10} + M_{14} \sim -\frac{1}{2} i g^4 s \frac{g^2 \ln s}{2\pi} \bigcirc. \quad (2.24)$$

From Fig. 14 it is clear that

$$\begin{aligned} -3 M_{16} - M_{17} - M_{18} - 2 M_{19} - 2 M_{20} &\sim (i)^{1+6+7} g^6 \frac{1}{2^2} (-2s)^3 \frac{1}{s^2} \int \prod_{i=1}^2 \frac{d^2 \vec{q}_{i\perp}}{(2\pi)^2} \\ &\times \int \prod_{i=1}^3 \frac{dq_{i+}}{2\pi} \prod_{j=1}^3 \frac{dq_{j-}}{2\pi} (2\pi) \delta\left(\sum_{i=1}^3 q_{i+}\right) (2\pi) \delta\left(\sum_{i=1}^3 q_{i-}\right) \frac{1}{(-q_{1+}+i\varepsilon)(-q_{1+}-q_{2+}+i\varepsilon)} \\ &\times \prod_{i=1}^3 \frac{1}{q_{i+} q_{i-} - \vec{q}_{i\perp}^2 - \lambda^2 + i\varepsilon} \left\{ \frac{-3}{(q_{3-}+i\varepsilon)(q_{3-}+q_{2-}+i\varepsilon)} + \frac{-1}{(q_{2-}+i\varepsilon)(q_{2-}+q_{1-}+i\varepsilon)} \right. \\ &\left. + \frac{-1}{(q_{1-}+i\varepsilon)(q_{1-}+q_{3-}+i\varepsilon)} + \frac{-2}{(q_{3-}+i\varepsilon)(q_{3-}+q_{1-}+i\varepsilon)} + \frac{-2}{(q_{2-}+i\varepsilon)(q_{2-}+q_{3-}+i\varepsilon)} \right\}. \end{aligned} \quad (2.25)$$

From Appendix IV,

$$\begin{aligned} &\delta\left(\sum_{i=1}^3 q_{i-}\right) \left\{ \text{term in brackets in eqn. (2.25)} \right\} = \\ &(-2\pi i) \left(\frac{-1}{q_{2-}+i\varepsilon} \delta(q_{2-}+q_{1-}) \delta(q_{3-}) + \frac{-1}{q_{3-}+i\varepsilon} \delta(q_{3-}+q_{1-}) \delta(q_{2-}) + \frac{-1}{q_{3-}+i\varepsilon} \delta(q_{3-}+q_{2-}) \delta(q_{1-}) \right). \end{aligned} \quad (2.26)$$

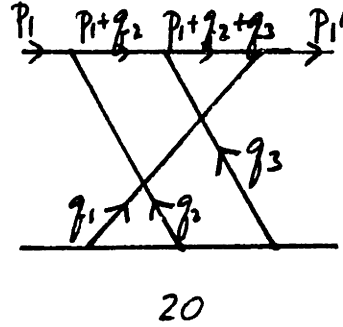
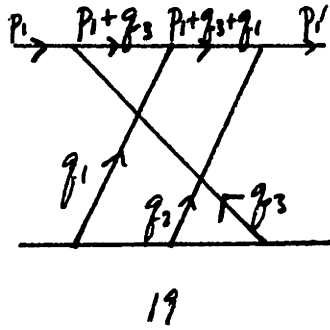
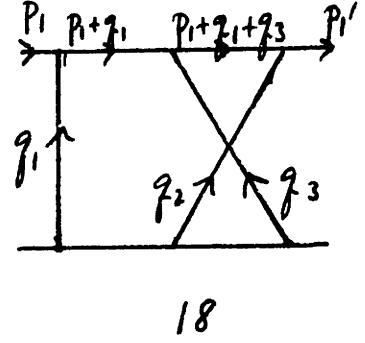
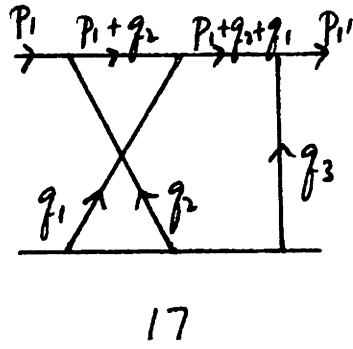
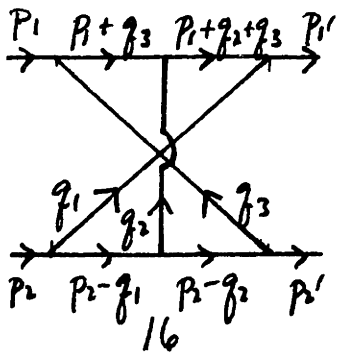


Fig. 14

The only term in (2.26) which leads to a result proportional to $\ln s$ is $(-2\pi i) \frac{-1}{g_3+i2} \delta(g_3+g_1) \delta(g_2-)$; the flow diagram is the same as the one in Fig. 13. Thus (2.25) becomes

$$-3M_{16} - M_{17} - M_{18} - 2M_{19} - 2M_{20} \sim -2ig^4s \frac{g^2 \ln s}{2\pi} \textcircled{\text{I}}. \quad (2.27)$$

And, from (2.17), (2.23), (2.24) and (2.27), (2.22) becomes

$$ig^4s \frac{g^2 \ln s}{2\pi} \left(\frac{1}{2} \lambda^2 \textcircled{\text{II}} - 2 \textcircled{\text{I}} \right) \text{III}. \quad (2.28)$$

Once again the divergent terms and real $\ln s$ terms cancel out.

Finally we consider the T^6 terms. From Table I they are

$$\left(M_{15} + M_{16} + M_{17} + M_{18} + M_{19} + M_{20} \right) \text{III}. \quad (2.29)$$

Using the methods of Appendix IV, (2.29) becomes

$$-\frac{1}{3} g^6 s \textcircled{\text{I}} \text{III} . \quad (2.30)$$

which is pure real as expected. This completes the calculation through the sixth order. Note that in the leading logarithm approximation, the amplitude in (2.30) is dropped. This is the first (non-zero) difference between our present scheme and the leading logarithm calculation.

III. The Feynman Diagram Calculation. Eighth Order

We showed above that all divergences from integrations over the transverse-momenta cancelled exactly through the sixth order. And it has been previously shown that these divergences also cancel in the eighth order of the leading logarithm calculation.⁹ Since there is no ambiguity in extracting the convergent terms from any amplitude we will henceforth simply assume all divergences cancel and ignore divergent terms whenever they appear.

There are four general classes of diagrams that contribute to the convergent part of the amplitude in the eighth order. They are indicated in Fig. 15. All other diagrams

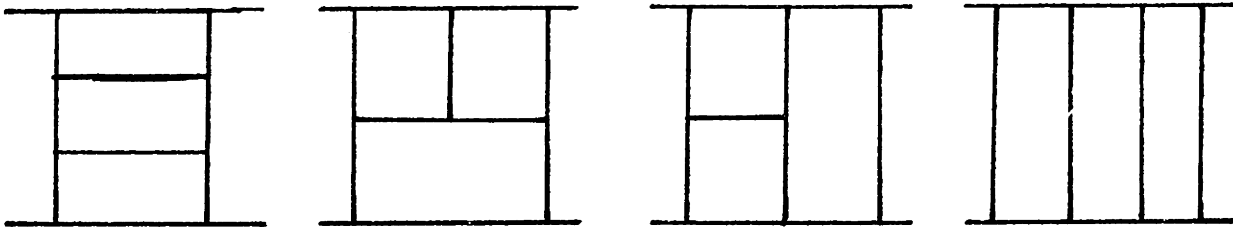



Fig. 15

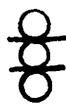


formed from those shown by up-down inversion, by replacing a horizontal vector-meson line by a scalar or by a four-vertex, by rearranging the order in which the mesons attach to the high-energy lines, or by any combination of these processes also contribute.

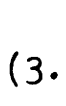

i)  Type Diagrams

We will first calculate the contributions from the tower diagrams of which there are eight in the eighth order. These are shown in Table II, where their isospin factors are decomposed into box factors. From the table we see that the T^2 amplitude is


$$- (M_2 + M_4 + M_6 + M_8) \text{  } . \quad (3.1)$$

From the leading logarithm calculation we know that (discarding divergent terms)


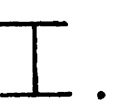
$$M_2 \sim \frac{1}{2} g^2 s \frac{1}{3!} \left(\frac{g^2 \ln s}{2\pi} \right)^3 \left(4 \text{  } + 4 \lambda^2 \text{  } + \lambda^4 \text{  } \right), \quad (3.2)$$

$$M_4 = M_6 \sim -\frac{1}{2} g^2 s \frac{1}{3!} \left(\frac{g^2 \ln s}{2\pi} \right)^3 \left(2 \lambda^2 \text{  } + \lambda^4 \text{  } \right), \quad (3.3)$$

and

$$M_8 \sim \frac{1}{2} g^2 s \frac{1}{3!} \left(\frac{g^2 \ln s}{2\pi} \right)^3 \left(\lambda^4 \text{  } \right). \quad (3.4)$$

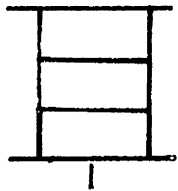
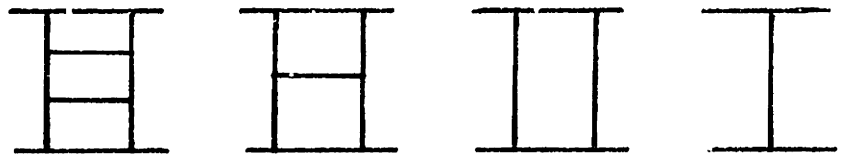
Thus (3.1) becomes

$$-\frac{1}{3} g^2 s \left(\frac{g^2 \ln s}{2\pi} \right)^3 \text{  } \text{  } . \quad (3.5)$$

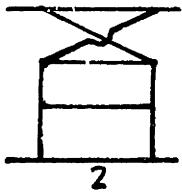
No other eighth order diagrams contribute to the T^2 terms.

The amplitude in (3.5) is also the fourth term in the

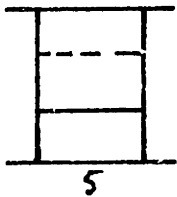
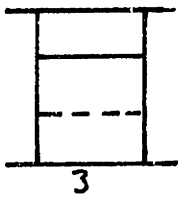
Feynman diagrams / isospin diagrams



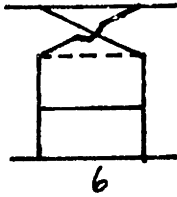
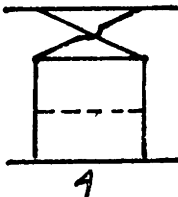
1 0 0 0



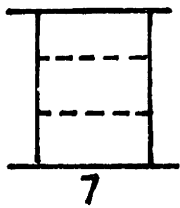
1 0 0 -1



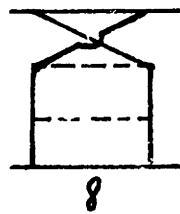
0 1 0 0



0 1 0 -1



0 0 1 0



0 0 1 -1

Table II

expansion of (2.13).

The T^4 contribution from these diagrams is, from Table II,

$$(M_1 + M_2) \text{H} + (M_3 + M_4 + M_5 + M_6) \text{H} + (M_7 + M_8) \text{II} \quad (3.6)$$

Using the methods of Appendices II and IV,

$$M_1 + M_2 \sim \frac{1}{8} ig^4 s \left(\frac{g^2 \ln s}{2\pi} \right)^2 \left(4 \text{H} + 4 \lambda^2 \text{H} + \lambda^4 \text{H} \right), \quad (3.7)$$

$$M_3 + M_4 + M_5 + M_6 \sim -\frac{1}{4} ig^4 s \left(\frac{g^2 \ln s}{2\pi} \right)^2 \left(2 \lambda^2 \text{H} + \lambda^4 \text{H} \right), \quad (3.8)$$

and

$$M_7 + M_8 \sim \frac{1}{8} ig^4 s \left(\frac{g^2 \ln s}{2\pi} \right)^2 \left(\lambda^4 \text{H} \right). \quad (3.9)$$

ii) III Type Diagrams

Next we consider the diagrams shown in Table III. First we note that

$$(M_{14} + M_{19} + M_{20}) \text{I} = O(s \ln^2 s) \text{I} \quad (3.10)$$

so that these terms do not contribute to the T^2 amplitude.

There are three other box isospin diagrams in Table III. The sum of the space-time amplitudes multiplying each of them is of the form (see Fig. 16)

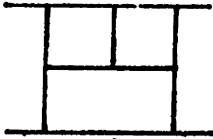
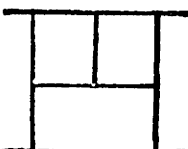
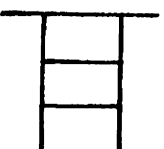
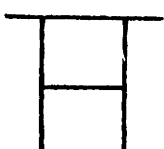

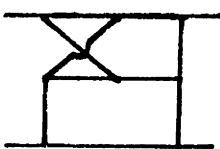
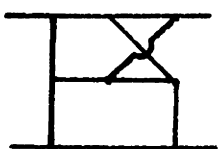
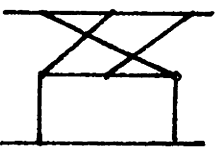
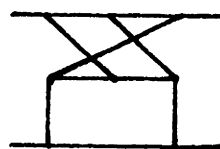
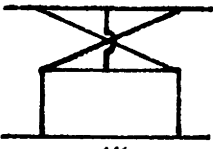
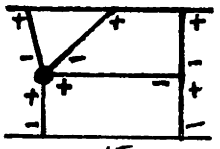
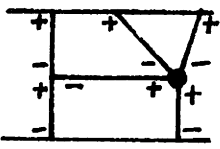
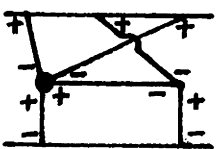
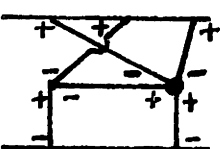
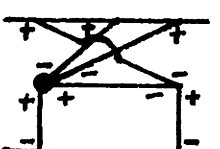
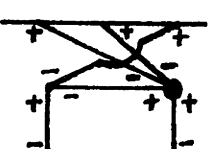
Feynman diagrams	Isospin diagrams				
					
9	1	0	0	0	
		1	0	-1	0
10	11				
		1	1	-2	0
12	13				
	1	1	-3	1	
14					
		2	0	-1	0
15	16				
		2	1	-3	0
17	18				
		2	2	-5	1
19	20				

Table III

In diagrams 15 - 20, use has been made of the polarization to eliminate one of the three terms from a four-vertex.

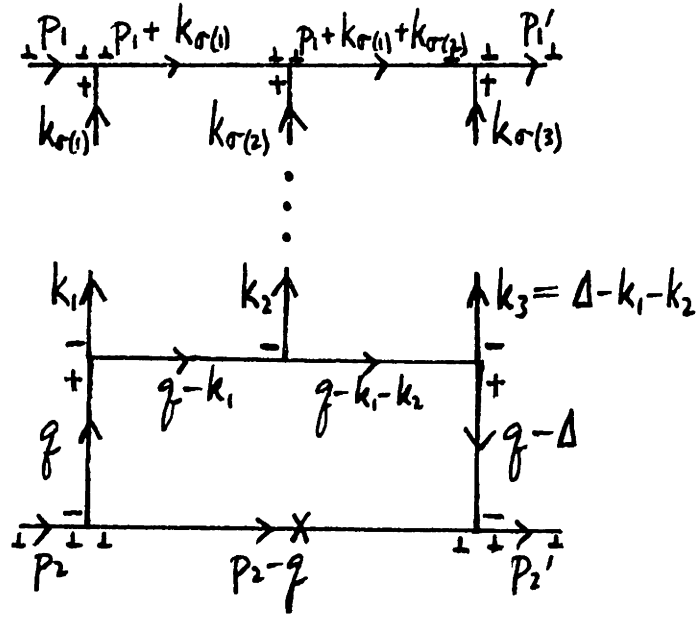


Fig. 16

$$\begin{aligned}
 & (-i)^{1+8+10} g^8 (-2s)^3 \left(\frac{2p_{1+}}{\sqrt{2}} \right) \frac{1}{p_{1+}^2 p_{2-}} \frac{1}{2^3} (-i) \int \frac{d\vec{q}_\perp}{(2\pi)^2} \frac{d\vec{k}_{1\perp}}{(2\pi)^2} \frac{d\vec{k}_{2\perp}}{(2\pi)^2} \\
 & \int \frac{dk_{1+}}{2\pi} \frac{dk_{2+}}{2\pi} \int \frac{dq_-}{2\pi} \frac{dk_{1-}}{2\pi} \frac{dk_{2-}}{2\pi} \frac{dk_{3-}}{2\pi} 2\pi \delta(k_{1-} + k_{2-} + k_{3-}) \frac{1}{\vec{q}_\perp^2 + \lambda^2} \\
 & \times \frac{1}{(\vec{q}_\perp - \vec{k}_{1\perp})^2 + \lambda^2} \frac{1}{(q_- - k_{1-})(-k_{1+}) - (\vec{q}_\perp - \vec{k}_{1\perp})^2 - \lambda^2 + i\epsilon} \\
 & \times \frac{1}{(q_- - k_{1-} - k_{2-})(-k_{1+} - k_{2+}) - (\vec{q}_\perp - \vec{k}_{1\perp} - \vec{k}_{2\perp})^2 - \lambda^2 + i\epsilon} \left(\prod_{i=1}^3 \frac{1}{k_i - k_{i+} - \vec{k}_{i\perp}^2 - \lambda^2 + i\epsilon} \right) \\
 & \times \sum_{\sigma} I_{\sigma} \frac{1}{(k_{\sigma(1)} - i\epsilon)(k_{\sigma(1)} + k_{\sigma(2)} - i\epsilon)} N, \tag{3.11}
 \end{aligned}$$

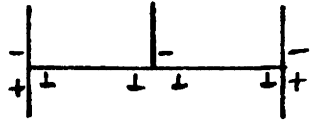
where N is the numerator factor from the three vertices on the horizontal line in the middle of Fig. 16, where σ runs over the appropriate Feynman diagrams, and where I_σ is the appropriate isospin factor as given in Table III. The q_+ integration has already been performed, with $q_+ = O(\frac{1}{p_{2-}})$.

N is calculated in Fig. 17 where the contribution from each polarization of the internal lines is shown separately. The result is

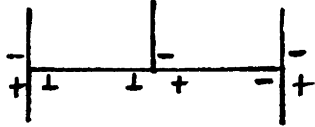
$$\begin{aligned}
 N \sim & \frac{1}{2\sqrt{2}} \left\{ (q_- - 2k_{1-} + 2k_{2-}) \left[(-k_{1-} - k_{2-})(-k_{1+} - k_{2+}) - (\vec{\Delta}_\perp - \vec{k}_{1\perp} - \vec{k}_{2\perp})^2 - \lambda^2 \right] \right. \\
 & + (q_- - 2k_{1-} - 4k_{2-}) \left[k_{1-} k_{1+} - \vec{k}_{1\perp}^2 - \lambda^2 \right] \\
 & \left. + (q_- - 4k_{1-} - 2k_{2-}) \left[k_{2-} k_{2+} - \vec{k}_{2\perp}^2 - \lambda^2 \right] \right\} \\
 & + \frac{1}{\sqrt{2}} q_- \left[3(\vec{q}_\perp^2 + \lambda^2) + 3((\vec{q}_\perp - \vec{\Delta}_\perp)^2 + \lambda^2) + \frac{3}{2}(\vec{k}_{1\perp}^2 + \lambda^2) + \frac{3}{2}(\vec{k}_{2\perp}^2 + \lambda^2) \right. \\
 & \quad \left. + \frac{3}{2}((\vec{\Delta}_\perp - \vec{k}_{1\perp} - \vec{k}_{2\perp})^2 + \lambda^2) - 4\vec{\Delta}_\perp^2 - 7\lambda^2 \right] \\
 & + k_{1-} \left[\text{a function of the transverse momenta} \right] \\
 & + k_{2-} \left[\text{a function of the transverse momenta} \right]. \quad (3.12)
 \end{aligned}$$

Consider the term

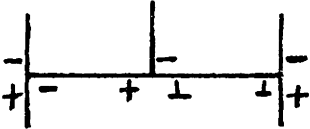
$$\left(\sum_{i=9}^{14} M_i + 2 \sum_{i=15}^{20} M_i \right) \text{III}. \quad (3.13)$$



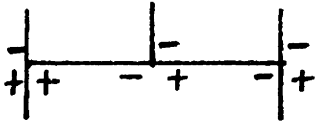
$$-(\vec{q}_1 + \vec{k}_{1\perp}) \cdot (\vec{q}_1 + \vec{k}_{1\perp} + \vec{k}_{2\perp} - 2\vec{A}_1) \frac{-2q_- + 2k_{1-} + k_{2-}}{\sqrt{2}}$$



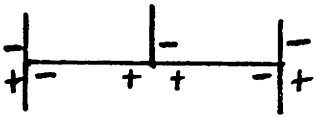
$$-(\vec{q}_1 + \vec{k}_{1\perp}) \cdot (\vec{q}_1 - \vec{k}_{1\perp} - 2\vec{k}_{2\perp}) \frac{2k_{1-} + 2k_{2-} - q_-}{\sqrt{2}}$$



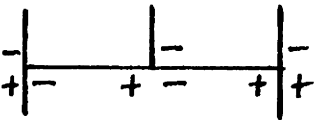
$$-(\vec{q}_1 - \vec{k}_{1\perp} + \vec{k}_{2\perp}) \cdot (\vec{q}_1 + \vec{k}_{1\perp} + \vec{k}_{2\perp} - 2\vec{A}_1) \frac{2k_{1-} - q_-}{\sqrt{2}}$$



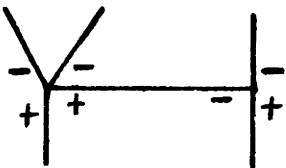
$$\frac{-k_{1+}}{\sqrt{2}} \quad \frac{k_{1-} - k_{2-} - q_-}{\sqrt{2}} \quad \frac{2k_{1-} + 2k_{2-} - q_-}{\sqrt{2}}$$



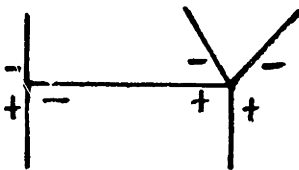
$$\frac{2k_{1-} - q_-}{\sqrt{2}} \quad \frac{-2k_{1+} - k_{2+}}{\sqrt{2}} \quad \frac{2k_{1-} + 2k_{2-} - q_-}{\sqrt{2}}$$



$$\frac{2k_{1-} - q_-}{\sqrt{2}} \quad \frac{k_{1-} + 2k_{2-} - q_-}{\sqrt{2}} \quad \frac{-k_{1+} - k_{2+}}{\sqrt{2}}$$



$$\frac{2k_{1-} + 2k_{2-} - q_-}{\sqrt{2}} \left[(q_- - k_{1-})(-k_{1+}) - (\vec{q}_1 - \vec{k}_{1\perp})^2 - \lambda^2 \right]$$



$$\frac{2k_{1-} - q_-}{\sqrt{2}} \left[(q_- - k_{1-} - k_{2-})(-k_{1+} - k_{2+}) - (\vec{q}_1 - \vec{k}_{1\perp} - \vec{k}_{2\perp})^2 - \lambda^2 \right]$$

Fig. 17

The contribution to the numerator N from each polarization of the internal lines.

The isospin factor in (3.13) appears to be $O(T^5)$ -- but in fact it is only $O(T^4)$. This can be seen by the isospin manipulations in Fig. 18(a), where we have used the isospin identity (valid for our $SU(2)$ model)

$$(i\epsilon_{eba})(i\epsilon_{ecd}) = \delta_{ac}\delta_{bd} - \delta_{ad}\delta_{bc} \quad (3.14)$$

which is illustrated diagrammatically in Fig. 18(b).

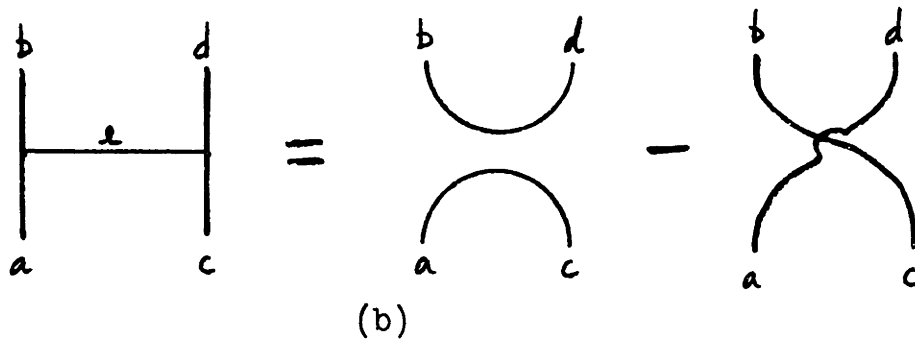
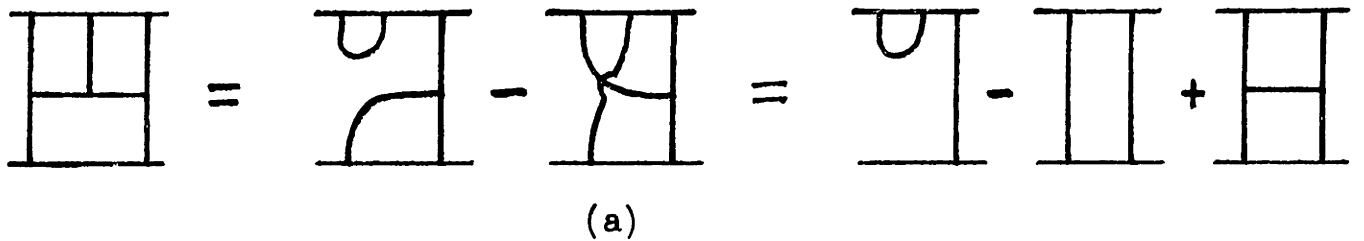


Fig. 18

So in order for the amplitude given by (3.13) to contribute, the sum of the space-time amplitudes must be as large as $s \ln^2 s$. Using the methods of Appendix IV,

$$\delta\left(\sum_{i=1}^3 k_i\right) \sum_{\sigma} I_{\sigma} \frac{1}{(k_{\sigma(1)} + i\epsilon)(k_{\sigma(1)} + k_{\sigma(2)} + i\epsilon)} = (-2\pi i)^2 \delta(k_+) \delta(k_2) \delta(k_3) \quad (3.15)$$

In N the terms proportional to $q_-^2 k_{1+}$ and $q_-^2 k_{2+}$ cancel exactly, so that $N \sim q_- x$ (a function of the transverse-

momenta). Thus the s dependence of (3.11) is

$$s \int_{p_{1-}}^{p_{2-}} \frac{dq_-}{2\pi} \frac{1}{q_-^2} q_- \sim s \frac{\ln s}{2\pi} \quad (3.16)$$

and consequently (3.13) does not contribute at all.

Next we calculate

$$(M_{12} + M_{13} + M_{14} + M_{17} + M_{18} + 2M_{19} + 2M_{20}) \underline{\text{II}}. \quad (3.17)$$

Using the methods of Appendix IV we see in this case

$$\delta\left(\sum_{i=1}^3 k_{i-}\right) \sum_{\sigma} I_{\sigma} \frac{1}{(k_{\sigma(1)-} + i\varepsilon)(k_{\sigma(1)-} + k_{\sigma(2)-} + i\varepsilon)} = (-2\pi i) \frac{1}{k_{3-} + i\varepsilon} \delta(k_{3-} + k_{1-}) \delta(k_{2-}) \quad (3.18)$$

Therefore there is only one non-zero flow diagram and it is illustrated in Fig. 19. The terms in (3.12), such as

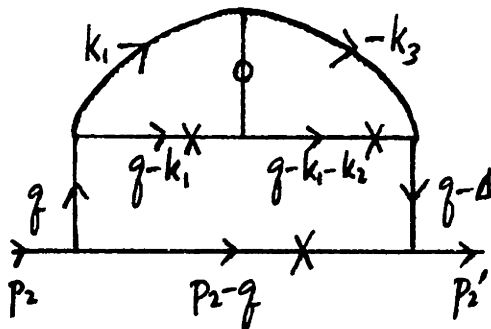


Fig. 19

$q_{-}(k_{1-} k_{1+} - \vec{k}_{1\perp}^2 - \lambda^2)$, which cancel propagators from the denominator are all divergent in the transverse-momentum integration, so they are dropped. The terms like $q_{-}(\vec{q}_{\perp}^2 + \lambda^2)$ are also divergent and are dropped. Thus N becomes

$$N \Rightarrow \frac{1}{\sqrt{2}} q_{-} (-4(\vec{q}_{\perp}^2 + \lambda^2) - 3\lambda^2) \quad (3.18)$$

where the double arrow indicates divergences have been ignored.

And (3.11) becomes

$$\begin{aligned}
 & \frac{i}{2} g^8 s \int \frac{d^2 \vec{q}_\perp}{(2\pi)^2} \frac{d^2 \vec{k}_{1\perp}}{(2\pi)^2} \frac{d^2 \vec{k}_{2\perp}}{(2\pi)^2} \int_{p_-}^{p_-} \frac{dq_-}{2\pi} \int_{p_-}^{p_-} \frac{dk_-}{2\pi} \frac{1}{(\vec{q}_\perp^2 + \lambda^2) ((\vec{q}_\perp - \vec{\Delta}_\perp)^2 + \lambda^2) (\vec{k}_{2\perp}^2 + \lambda^2)} \\
 & \times \frac{1}{k_- (q_- - k_-)^2} \frac{1}{k_{1-} \left(\frac{(\vec{q}_\perp - \vec{k}_{1\perp})^2 + \lambda^2}{q_- - k_-} \right) + \vec{k}_{1\perp}^2 + \lambda^2} \frac{1}{k_{1-} \left(\frac{(\vec{q}_\perp - \vec{k}_{1\perp} - \vec{k}_{2\perp})^2 + \lambda^2}{q_- - k_{1-}} \right) + (\vec{\Delta}_\perp - \vec{k}_{1\perp} - \vec{k}_{2\perp})^2 + \lambda^2} \\
 & \times q_- (-4(\vec{\Delta}_\perp^2 + \lambda^2) - 3\lambda^2). \tag{3.19}
 \end{aligned}$$

Evaluating this, (3.17) becomes

$$-ig^4 s \left(\frac{g^2 \ln s}{2\pi} \right)^2 \left(\text{⊙} + \frac{3}{4} \lambda^2 \text{⊙} \right) \text{⊠}. \tag{3.20}$$

Now we consider the amplitude (see Table III)

$$-\left(M_{10} + M_{11} + 2M_{12} + 2M_{13} + 3M_{14} + M_{15} + M_{16} + 3M_{17} + 3M_{18} + 5M_{19} + 5M_{20} \right) \text{⊠}. \tag{3.21}$$

For this particular sum,

$$\begin{aligned}
 & \delta\left(\sum_{i=1}^3 k_{i-}\right) \sum_{\sigma} I_{\sigma} \frac{1}{(k_{\sigma(1)-} + i\varepsilon)(k_{\sigma(1)-} + k_{\sigma(2)-} + i\varepsilon)} = (-2\pi i) \left\{ \frac{-1}{k_{3-} + i\varepsilon} \delta(k_{3-} + k_{1-}) \delta(k_{2-}) \right. \\
 & \left. + \frac{-1}{k_{2-} + i\varepsilon} \delta(k_{2-} + k_{1-}) \delta(k_{3-}) + \frac{-1}{k_{3-} + i\varepsilon} \delta(k_{3-} + k_{2-}) \delta(k_{1-}) \right\}, \tag{3.22}
 \end{aligned}$$

as shown in Appendix IV. The leading contributions from

$\frac{-1}{k_2 - i\epsilon} \delta(k_2 + k_1) \delta(k_3)$ and $\frac{-1}{k_3 - i\epsilon} \delta(k_3 + k_2) \delta(k_1)$ are divergent and are dropped. This leaves only the $\frac{-1}{k_3 - i\epsilon} \delta(k_3 + k_1) \delta(k_2)$ term. As before, numerator terms of the form $q_-(k_{1-} k_{1+} - \vec{k}_{1\perp}^2 - \lambda^2)$ or $q_-(\vec{k}_{1\perp}^2 + \lambda^2)$ or $q_-(\vec{q}_{1\perp}^2 + \lambda^2)$ lead to divergences. Again the only flow diagram is given by Fig. 19 and N is given by (3.18).

Thus (3.21) becomes

$$ig^4 s \left(\frac{g^2 \ln s}{2\pi} \right)^2 \left(\text{Diagram I} + \frac{3}{4} \lambda^2 \text{Diagram II} \right) \text{Diagram III}. \quad (3.23)$$

Thus (3.20) and (3.23) give the complete contribution from the diagrams of Table III.

Now consider those diagrams given in Table IV, which are similar to those in Table III except that a scalar line replaces one of the vector-meson lines. Eqn. (3.11) still applies if we make two modifications due to the scalar propagator: M^2 replaces λ^2 in that propagator and there is an extra overall minus sign. The T^2 terms

$$\left(-M_{27} - M_{28} + M_{31} + M_{32} \right) \text{Diagram I} \quad (3.24)$$

do not contribute since they are not as large as $s \ln^3 s$. The T^4 terms proportional to the isospin diagram **II** are

$$\left(M_{22} + M_{24} - M_{26} + M_{28} - M_{30} - M_{32} \right) \text{Diagram II} \quad (3.25a)$$

and

$$\left(M_{21} + M_{23} - M_{25} + M_{27} - M_{29} - M_{31} \right) \text{Diagram II}. \quad (3.25b)$$

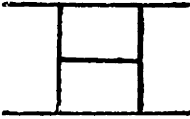
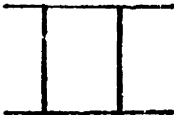

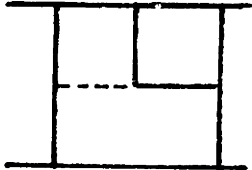
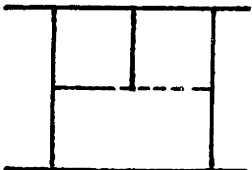
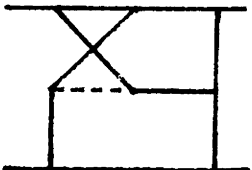
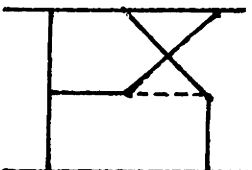
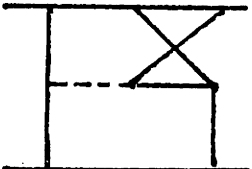
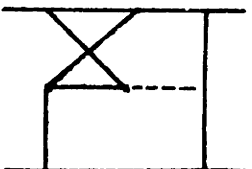
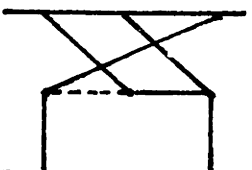
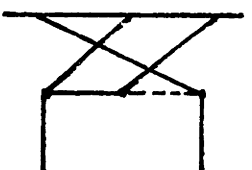
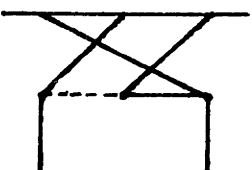
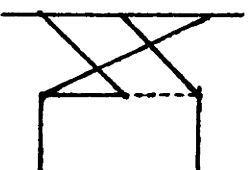
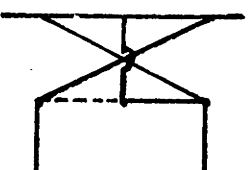
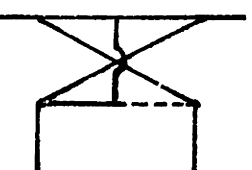
<i>Feynman diagrams</i>		<i>Isospin diagrams</i>					
	21)		22	0	1	0
	23)		24	-1	1	0
	25)		26	0	-1	0
	27)		28	0	1	-1
	29)		30	1	-1	0
	31)		32	0	-1	1

Table IV

From Appendix IV, for the amplitude given in (3.25a),

$$\delta\left(\sum_{i=1}^3 k_{i-}\right) \sum_{\sigma} I_{\sigma} \frac{1}{(k_{\sigma(1)-} + i\varepsilon)(k_{\sigma(1)-} + k_{\sigma(2)-} + i\varepsilon)} = (-2\pi i) \left\{ \frac{1}{k_{1-} + i\varepsilon} \delta(k_{1-} + k_{2-}) \delta(k_{3-}) \right. \\ \left. - \frac{1}{k_{2-} + i\varepsilon} \delta(k_{2-} + k_{1-}) \delta(k_{3-}) \right\}. \quad (3.26)$$

This leads to a contribution proportional to $\text{sln } s$, not $\text{sln}^2 s$, so is dropped. Likewise, the amplitude in (3.25b) is too small. Finally, the amplitudes proportional to the isospin diagram \mathbb{H} are

$$(-M_{24} + M_{30}) \mathbb{H} \quad (3.27a)$$

and

$$(-M_{23} + M_{29}) \mathbb{H}. \quad (3.27b)$$

We easily establish the following facts about the amplitude in (3.27a): first,

$$N \sim \lambda^2 \frac{2k_{1-} - q_-}{\sqrt{2}}; \quad (3.28)$$

second, from Appendix IV,

$$\delta\left(\sum_{i=1}^3 k_{i-}\right) \sum_{\sigma} I_{\sigma} \frac{1}{(k_{\sigma(1)-} + i\varepsilon)(k_{\sigma(1)-} + k_{\sigma(2)-} + i\varepsilon)} \\ = (-2\pi i) \left(\frac{1}{k_{2-} + i\varepsilon} \delta(k_{2-} + k_{3-}) \delta(k_{1-}) - \frac{1}{k_{1-} + i\varepsilon} \delta(k_{1-} + k_{3-}) \delta(k_{2-}) \right); \quad (3.29)$$

third, only the second term on the right-hand side of (3.29) contributes; and fourth, the only flow diagram is shown in Fig. 19. Thus (3.27a) becomes

$$\frac{1}{4} i g^4 s \left(\frac{g^2 l m s}{2\pi} \right)^2 \lambda^2 \textcircled{\text{H}} \quad (3.30)$$

Likewise, the amplitude in (3.27b) gives a contribution equal to (3.30).

To summarize, the total contribution from the diagrams of Tables III and IV plus the contribution from the diagrams formed from them by an up-down inversion (this leads to a factor of two) equals, from (3.20), (3.23) and (3.30),

$$\begin{aligned} & -i g^4 s \left(\frac{g^2 l m s}{2\pi} \right)^2 \left(2 \textcircled{\text{H}} + \frac{3}{2} \lambda^2 \textcircled{\text{H}} \right) \textcircled{\text{H}} \\ & + i g^4 s \left(\frac{g^2 l m s}{2\pi} \right)^2 \left(2 \textcircled{\text{H}} + \frac{3}{2} \lambda^2 \textcircled{\text{H}} \right) \textcircled{\text{H}} \\ & + i g^4 s \left(\frac{g^2 l m s}{2\pi} \right)^2 \left(\lambda^2 \textcircled{\text{H}} \right) \textcircled{\text{H}}. \end{aligned} \quad (3.31)$$

This result can be manipulated using the isospin identity shown in Fig. 20 which itself can be established by using the identity of Fig. 18(b). Then (3.31) becomes

$$- \textcircled{\text{H}} + \textcircled{\text{H}} + 2 \textcircled{\text{H}} - \textcircled{\text{H}} = 0$$

Fig. 20

$$\left\{ ig^4 s \left(\frac{g^2 \ln s}{2\pi} \right)^2 \left(2 \textcircled{1} + \lambda^2 \textcircled{2} \right) (-\text{III} + \text{II}) \right. \\ \left. + ig^4 s \left(\frac{g^2 \ln s}{2\pi} \right)^2 \lambda^2 \textcircled{3} (\text{II} - \text{II}) \right\} \\ + ig^4 s \left(\frac{g^2 \ln s}{2\pi} \right)^2 \frac{1}{2} \lambda^2 \textcircled{4} \text{I}$$

$$\sim \left\{ \text{term in brackets above} \right\}. \quad (3.32)$$

In (3.32) the term proportional to the isospin diagram I has been dropped since it is of the order $g^2 (gT)^2 s (g^2 \ln s)^2$.

iii) $\overline{\text{III}}$ Type Diagrams

Table V lists the diagrams of this type which have no four-vertices or scalar propagators. The letters A, B or C in the diagrams' names refer to whether the internal horizontal vector-meson line connects the first and second, the second and third, or the first and third lines emerging from the bottom high-energy line, respectively. The three digits in the name refer to the order in which these lines attach to the top high-energy line. A bar over the letter of the name refers to the same diagram but viewed as if it had been rotated 180° so that the top and bottom are reversed. The table expresses

<i>Feynman diagrams</i> / <i>Isospin diagrams</i>							
A123, $\bar{B}123$	1						
A132, $\bar{C}213$	1		-1				
A213, $\bar{B}132$	1					-1	
A231, $\bar{C}231$	1		-1		1	-1	
A321, $\bar{A}321$	1			1	-2	-1	1
$\bar{A}312, \bar{A}312$	1			1	-2		
B123, $\bar{A}123$	1						
B132, $\bar{A}213$	1					-1	
B213, $\bar{C}132$	1		-1				
B231, $\bar{B}231$	1			1	-2		
B321, $\bar{B}321$	1			1	-2	-1	1
B312, $\bar{C}312$	1		-1		1	-1	
C123, $\bar{C}123$	1	-1	-1		1		
C132, $\bar{B}213$	1	-1					
C213, $\bar{A}132$	1	-1					
C231, $\bar{A}231$	1	-1			1	-1	
C321, $\bar{C}321$	1	-1	-1	-1	3	-1	
C312, $\bar{B}312$	1	-1			1	-1	

Table V

Blank entries stand for zeros.

the isospin factors of each diagram in terms of box isospin factors.

For each of the diagrams in Table V the horizontal vector-meson line can be shrunk to a point so that the two lines which it connected are fused to form a four-vertex. There are nine such diagrams with four-vertices. The isospin factor of each of these diagrams is the sum of two terms which are themselves precisely the isospin factors of the two diagrams from Table V which, when the horizontal vector-meson line is shrunk, reproduce the four-vertex diagram. This is illustrated in Fig. 21. (According to the Feynman rules for a four-vertex

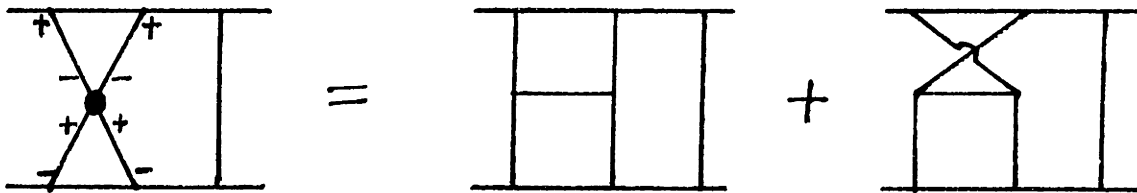


Fig. 21

there should be a third isospin diagram on the right-hand side of Fig. 21 -- but because of the polarization of the lines emerging from the high-energy lines, the coefficient in front of this third isospin diagram is zero.) Therefore there is a one-to-one correspondence between the isospin factors of the diagrams in Table V and the isospin factors of the four-vertex diagrams. So the amplitudes of the four-vertex diagrams can be taken care of by simply adding together the space-time

amplitude of a diagram in Table V and the space-time amplitude of the corresponding four-vertex diagram. (This is precisely what was done in the treatment of the diagrams of Table III.) In other words, always treat the space-time factors shown in Fig. 22 together, as a unit.



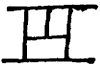
Fig. 22

The T^6 term from the diagrams in Table V is then

$$\left\{ \text{the sum of all space-time amplitudes in Table V along with their four-vertex contributions} \right\} \text{III}. \quad (3.33)$$

This is calculated in Appendix II and equals

$$g^6_5 \frac{g^2_{lms}}{2\pi} \left(\text{III} + \frac{1}{2} \lambda^2 \text{III} \right) \text{III}. \quad (3.34)$$

The terms proportional to the isospin diagram  are

$$-(C_{123} + C_{132} + C_{213} + C_{231} + C_{321} + C_{312}) \text{III} \quad (3.35)$$

where we have used C_{123} to stand for that diagram's space-

time amplitude, etc. Using the methods of Appendix IV it is clear that in (3.35) the sum of the propagators on the top high-energy line is a product of delta functions in the momenta of the three lines attaching to the top line. The corresponding flow diagram is given in Fig. 23. Its amplitude

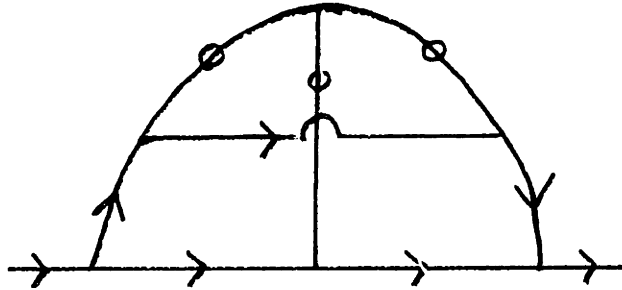


Fig. 23

is $O(s \ln s)$ so is too small. Likewise the terms proportional to the isospin diagram III are all of the \bar{C} type and are again too small.

Those terms proportional to the isospin diagram II are, from Table V,

$$\begin{aligned}
 & - \left[(A_{213} + A_{231} + A_{321}) + (B_{132} + B_{321} + B_{312}) + (C_{231} + C_{321} + C_{312}) \right] \text{II} \\
 & \equiv - \left[A(2>1) + B(3>2) + C(3>1) \right] \text{II} \quad (3.36)
 \end{aligned}$$

in an obvious notation. The C type terms are of the form (see Fig. 24)

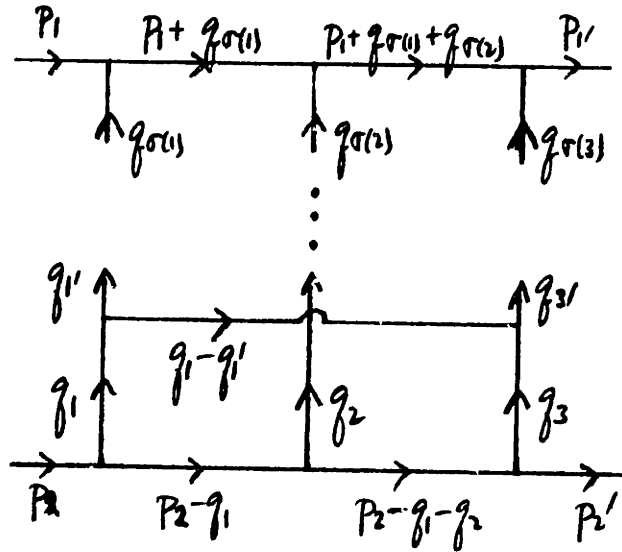


Fig. 24

$$\begin{aligned}
 & (-i)^{1+8+10} g^8 \frac{1}{2^3} (-2s)^3 \frac{1}{P_1^2 P_2^2} \int \frac{d^2 \vec{q}_{1\perp}}{(2\pi)^2} \frac{d^2 \vec{q}_{2\perp}}{(2\pi)^2} \frac{d^2 \vec{q}_{3\perp}}{(2\pi)^2} \int \frac{dq_{1+}}{2\pi} \frac{dq_{2+}}{2\pi} \frac{dq_{3+}}{2\pi} \\
 & \times \int \frac{dq_{1-}}{2\pi} \frac{dq_{2-}}{2\pi} \frac{dq_{3-}}{2\pi} \frac{dq_{1'}}{2\pi} \frac{dq_{3'}}{2\pi} 2\pi \delta(q_{1-} + q_{2-} + q_{3-}) 2\pi \delta(q_{1+} + q_{3+} - q_{1'} - q_{3'}) \\
 & \times \left(\sum_{\sigma} I_{\sigma} \frac{1}{q_{\sigma(1)} + i\epsilon} \frac{1}{q_{\sigma(1)} + q_{\sigma(2)} + i\epsilon} \right) \left(\prod_{i=1}^3 \frac{1}{q_{i+} q_{i-} - \vec{q}_{i\perp}^2 - \lambda^2 + i\epsilon} \right) \frac{1}{q_{1+} q_{1-} - \vec{q}_{1\perp}^2 - \lambda^2 + i\epsilon} \\
 & \frac{1}{q_{3+} q_{3-} - \vec{q}_{3\perp}^2 - \lambda^2 + i\epsilon} \frac{1}{(q_{1-} - q_{1'}) (q_{1+} - q_{1'}) - (\vec{q}_{1\perp} - \vec{q}_{1'\perp})^2 - \lambda^2 + i\epsilon} N \quad (3.37)
 \end{aligned}$$

where N is the numerator factor (with a change of notation it is given in Appendix II, eqn. II.26). From Appendix IV, for $C(3>1)$,

$$\delta\left(\sum_{i=1}^3 q_{\sigma(i)}\right) \sum_{\sigma} I_{\sigma} \frac{1}{(q_{\sigma(1)} + i\epsilon)(q_{\sigma(1)} + q_{\sigma(2)} + i\epsilon)} = (-2\pi i) \frac{1}{q_{3+} + i\epsilon} \delta(q_{3-} + q_{1-}) \delta(q_{2-}), \quad (3.38)$$

and the only non-zero flow diagram is given in Fig. 25.

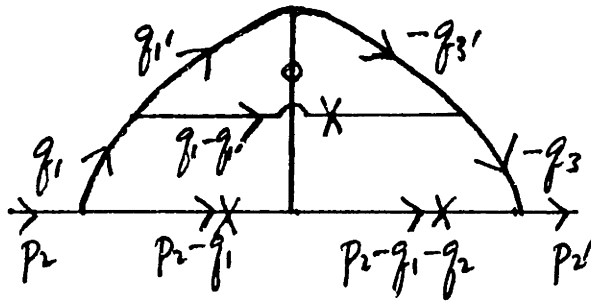


Fig. 25

There are corresponding flow diagrams for the A and B type terms but they are all zero! For example, for the A(2>1) terms, some potential flow diagrams are shown in Fig. 26 (where $q_{3-} = q_{1'-} + q_{2'-} = 0$).



Fig. 26

The loops which integrate to zero are indicated.

The contributing region in the flow diagram of Fig. 25 is $p_{2-} \gg q_{1-} \gg q_{1'-} \gg p_{1-}$, so

$$N \Rightarrow 2((\vec{q}_{11} + \vec{q}_{31})^2 + \lambda^2) + \lambda^2 \quad (3.39)$$

and (3.36) becomes

$$ig^4 s \left(\frac{g^2 \ln s}{2\pi} \right)^2 \left(\text{Diagram 1} + \frac{1}{2} \lambda^2 \text{Diagram 2} \right) \text{II}. \quad (3.40)$$

Next consider the terms in Table V proportional to the isospin diagram III :

$$\begin{aligned} & (A_{321} + A_{312} + B_{231} + B_{321} - C_{321}) \text{III} \\ &= \left\{ \begin{aligned} & (A_{123} + A_{132} + A_{231} + A_{321} + A_{312} + A_{213}) \\ & + (A_{123} + A_{213} + B_{231} + B_{321} + C_{132} + C_{312}) \\ & - (A_{123} + A_{213} + C_{312}) - (A_{123} + A_{213} + C_{132}) \\ & - (A_{132} + A_{231} + B_{213} + B_{312} + C_{123} + C_{321}) \\ & + (B_{213} + B_{312} + C_{123}) \end{aligned} \right\} \text{III} \\ &= \left(A + \bar{B} - \bar{B}(1>2) - \bar{B}(1>3) - \bar{C} + \bar{C}(1>2) \right) \text{III} \quad (3.41) \end{aligned}$$

where $A \equiv A(1>2) + A(2>1)$ stands for the sum of all six A type space-time amplitudes and so on. As before the A, \bar{B} and \bar{C} terms are proportional to $s \ln s$ at most and so are dropped. As above, the $\bar{B}(1>2)$ type terms have no non-zero flow diagrams, so they too are dropped. The $\bar{B}(1>3)$ type terms do have a non-zero flow diagram, shown in Fig. 27, but the s dependence is (using N given in eqn. II.26 of Appendix II)

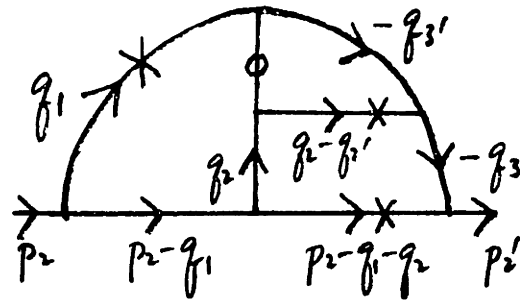


Fig. 27

$$S \int_{p_1}^{p_2} \frac{dq_1}{2\pi} \int_{p_1}^{p_2} \frac{dq_2}{2\pi} \frac{1}{q_1 - q_2} \frac{\left\{ 1 \text{ or } \frac{q_2}{q_1} (\bar{q}_{11}^2 + \lambda^2) \text{ or } \frac{q_1}{q_2} ((\bar{q}_{21} - \bar{q}_{21}')^2 + \lambda^2) \right\}}{(q_2 - \frac{\bar{q}_{11}^2 + \lambda^2}{q_1} + \bar{q}_{21}^2 + \lambda^2) (q_1 - \frac{\bar{q}_{21} - \bar{q}_{21}'}{q_2} + \bar{q}_{31}^2 + \lambda^2)}$$

$$\Rightarrow 0 \text{ (slns) } + \text{divergent terms}$$

(3.42)

so these terms too are dropped. This leaves the $\bar{C}(1>2)$ terms for which (3.38) is replaced by

$$\delta\left(\sum_{i=1}^3 q_{0(i)}\right) \sum_{\sigma} I_{\sigma} \frac{1}{(q_{0(1)} - i\epsilon)(q_{0(1)} + q_{0(1)} - i\epsilon)} = (-2\pi i) \frac{1}{q_{1'} + i\epsilon} \delta(q_{1'} + q_2) \delta(q_{3'}) \quad (3.43)$$

and the contributing flow diagram is shown in Fig. 28. The

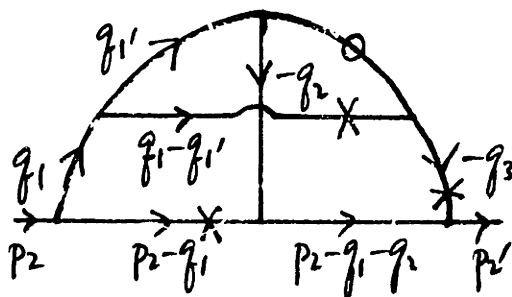


Fig. 28

dominant contribution comes from the region

$p_{2-} \gg q_{1-} \gg q_{1'-} \gg p_{1-}$ and N is given by (3.39) so that (3.41) becomes

$$ig^4 s \left(\frac{g^2 k_{\perp s}}{2\pi} \right)^2 \left(\text{Diagram 1} + \frac{1}{2} \lambda^2 \text{Diagram 2} \right) \mathbb{H}. \quad (3.44)$$

The terms proportional to isospin diagram \mathbb{H} are treated similarly:

$$\begin{aligned} & \left(A_{231} - 2(A_{321}) - 2(A_{312}) - 2(B_{231}) - 2(B_{321}) + B_{312} + C_{123} + C_{231} \right. \\ & \quad \left. + 3(C_{321}) + C_{312} \right) \mathbb{H} \\ = & \left\{ \begin{aligned} & (A_{123} + A_{132} + A_{213}) - 2(A_{321} + A_{312} + B_{123} + B_{132} + C_{213} + C_{231}) \\ & + (B_{123} + B_{132} + C_{231}) + (B_{123} + B_{132} + B_{213}) \\ & - 2(A_{123} + A_{213} + B_{231} + B_{321} + C_{132} + C_{312}) + (A_{123} + A_{213} + C_{312}) \\ & + 2(C_{123} + C_{132} + C_{213} + C_{231} + C_{321} + C_{312}) \\ & + (A_{132} + A_{231} + B_{213} + B_{312} + C_{123} + C_{321}) - 2(A_{132} + B_{213} + C_{123}) \end{aligned} \right\} \\ = & \left(A(1>3) - 2\bar{A} + \bar{A}(2>3) + B(1>3) - 2\bar{B} + \bar{B}(1>2) + 2\bar{C} + \bar{C}(1>3) \right) \mathbb{H}. \quad (3.45) \end{aligned}$$

And, as before, the only contribution comes from the $\bar{C}(1>3)$ terms. The answer is

$$-2ig^4 s \left(\frac{g^2 k_{\perp s}}{2\pi} \right)^2 \left(\text{Diagram 1} + \frac{1}{2} \lambda^2 \text{Diagram 2} \right) \mathbb{H}. \quad (3.46)$$

The eighteen diagrams with scalar propagators are shown in Table VI. (3.37) holds with an extra minus sign (due to the sign difference between the scalar and vector-meson propagators), with M^2 replacing λ^2 in the scalar propagator, and with the numerator $N = \lambda^2$. Then the T^6 terms are

$$-\frac{1}{2} g^6 s \frac{g^2 l m s}{2\pi} \lambda^2 \textcircled{\text{III}} \quad (3.47)$$

The T^4 terms proportional to the isospin diagram H are

$$\begin{aligned} & \left(A(371) + B(371) + C(371) \right) \text{H} \\ & \sim \frac{1}{2} i g^4 s \left(\frac{g^2 l m s}{2\pi} \right)^2 \lambda^2 \textcircled{\text{H}} \quad (3.48) \end{aligned}$$

Finally, the terms proportional to the isospin diagram II are

$$\begin{aligned} & - \left(A_{132} + A_{213} + 2(A_{231}) + 3(A_{321}) + 2(A_{312}) \right. \\ & \quad + B_{132} + B_{213} + 2(B_{231}) + 3(B_{321}) + 2(B_{312}) \\ & \quad \left. + C_{132} + C_{213} + 2(C_{231}) + 3(C_{321}) + 2(C_{312}) \right) \text{II} \\ & = \left(\begin{aligned} & -3A + A(1>2) + A(1>3) + A(2>3) \\ & -3B + B(1>2) + B(1>3) + B(2>3) \\ & -3C + C(1>2) + C(1>3) + C(2>3) \end{aligned} \right) \text{II} \\ & = -\frac{3}{2} i g^4 s \left(\frac{g^2 l m s}{2\pi} \right)^2 \lambda^2 \textcircled{\text{II}} \quad (3.49) \end{aligned}$$

<i>Feynman diagram</i> / <i>isospin diagram</i>				
A123				
A132		-1		
A213		-1		
A231		-2		
A321		-3		
A312		-2		
B123				
B132		-1		
B213		-1		
B231		-2		
B321		-3		
B312		-2		
C123				
C132		-1		
C213		-1		
C231		-2		
C321		-3		
C312		-2		

Table VI

In summary, the total amplitudes from the diagrams in Tables V and VI are: to order T^6 , from (3.34) and (3.47),

$$\begin{aligned}
 & g^6 s \frac{g^2 l n s}{2\pi} \left(\text{⊗} + \frac{1}{2} \lambda^2 \text{⊗} \right) \text{III} \\
 & - \frac{1}{2} g^6 s \frac{g^2 l n s}{2\pi} \lambda^2 \text{⊗} \text{III} \\
 & \sim \frac{1}{3} g^6 s \frac{g^2 l n s}{2\pi} \left(\text{⊗} + \frac{1}{2} \lambda^2 \text{⊗} \right) (\text{III} + \text{III} + \text{III}) \\
 & - \frac{1}{2} g^6 s \frac{g^2 l n s}{2\pi} \lambda^2 \text{⊗} \text{III} \tag{3.50}
 \end{aligned}$$

(since the differences between the isospin diagrams III , III and III are $O(T^4)$); and to order T^4 , from (3.40), (3.44), (3.46), (3.48) and (3.49),

$$\begin{aligned}
 & i g^4 s \left(\frac{g^2 l n s}{2\pi} \right)^2 \text{⊗} (\text{II} - 2 \text{H} + \text{H}) \\
 & - \frac{1}{2} i g^4 s \left(\frac{g^2 l n s}{2\pi} \right)^2 \lambda^2 \text{⊗} (-\text{H} + \text{H} + 2 \text{II} = \text{I}) \\
 & \sim i g^4 s \left(\frac{g^2 l n s}{2\pi} \right)^2 \text{⊗} (\text{II} - 2 \text{H} + \text{H}) \tag{3.51}
 \end{aligned}$$

where the isospin identity of Fig. 20 has been used.

iv) IIII Type Diagrams

The twenty-four four meson exchange diagrams are shown in Table VII along with their isospin decompositions into box isospin factors. The sums of the space-time amplitudes which multiply these box isospin factors are of the form (see Fig. 29)

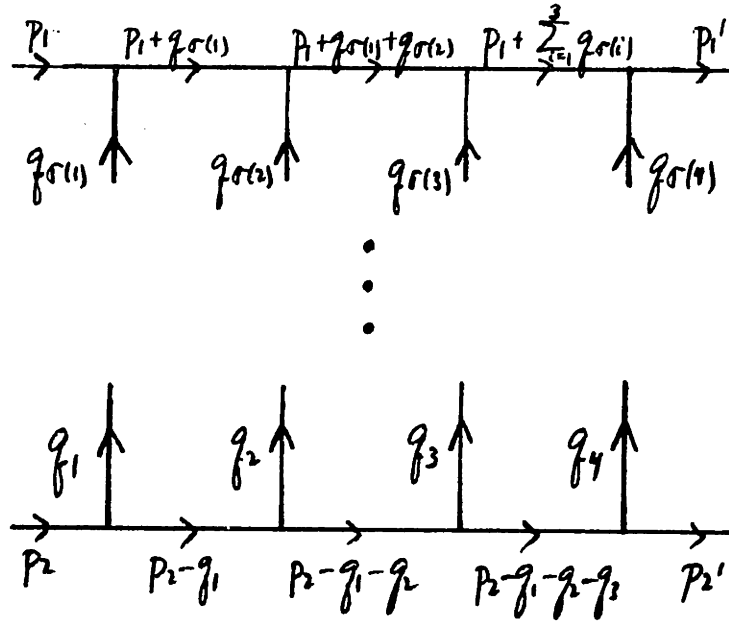


Fig. 29

$$\begin{aligned}
 & (-i)^{1+8+10} g^8 (-2s)^4 \frac{1}{p_1^3 p_2^3} \frac{1}{2^3} \int \prod_{i=1}^3 \frac{d^2 \vec{q}_{i-}}{(2\pi)^2} \int \prod_{i=1}^4 \frac{dq_{it}}{2\pi} (2\pi) \delta\left(\sum_{i=1}^4 q_{it}\right) \\
 & \times \int \prod_{i=1}^4 \frac{dq_{i-}}{2\pi} 2\pi \delta\left(\sum_{i=1}^4 q_{i-}\right) \frac{1}{(-q_{1+} + i\varepsilon)(-q_{1+} - q_{2+} + i\varepsilon)(-q_{1+} - q_{2+} - q_{3+} + i\varepsilon)} \\
 & \times \left(\prod_{i=1}^4 \frac{1}{q_{it} q_{i-} - \vec{q}_{i-}^2 - \lambda^2 + i\varepsilon} \right) \left(\sum_{\sigma} I_{\sigma} \frac{1}{(q_{\sigma(1)} - i\varepsilon)(q_{\sigma(1)} + q_{\sigma(2)} + i\varepsilon)(q_{\sigma(1)} + q_{\sigma(2)} + q_{\sigma(3)} + i\varepsilon)} \right)
 \end{aligned}$$

(3.52)

-60-

Feynman diagram / Isospin diagram									
1234	1								
4321	1	4	-6	-1	-1	1	-4	7	-1
1243	1		-1						
3421	1	4	-5	-1	-1	1	-3	4	
2134	1		-1						
4312	1	4	-5	-1	-1	1	-3	4	
1324	1		-1						
4231	1	4	-5	-1	-1	1	-3	4	
1423	1	1	-2						
3241	1	3	-4	-1	-1			2	
1342	1	1	-2						
2431	1	3	-4	-1	-1			2	
2314	1	1	-2						
4132	1	3	-4	-1	-1			2	
3124	1	1	-2						
4213	1	3	-4	-1	-1			2	
1432	1	1	-3					1	
2341	1	3	-3	-1	-1		1		
3214	1	1	-3					1	
4123	1	3	-3	-1	-1		1		
2143	1		-2					1	
3412	1	4	-4	-1	-1	1	-2	2	
2413	1	2	-3		-1			1	
3142	1	2	-3	-1				1	

Table VII

Diagrams are referenced by numbers which refer to the order in which the exchanged mesons attach to the top line.

where I_{σ} is given in Table VII. For the T^8 terms $I_{\sigma} = 1$ for all twenty-four permutations and, as can be shown using the methods of Appendix IV, (3.52) becomes

$$-\frac{1}{12} i g^8 s \textcircled{\text{I}} \text{IIII} . \quad (3.53)$$

In Appendix IV it is shown that, for the term proportional to the isospin factor III ,

$$\begin{aligned} & \delta\left(\sum_{i=1}^4 q_{i-}\right) \sum_{\sigma} I_{\sigma} \frac{1}{(q_{\sigma(1)-} + i\varepsilon)(q_{\sigma(1)-} + q_{\sigma(2)-} + i\varepsilon) \left(\sum_{i=1}^3 q_{\sigma(i)-} + i\varepsilon\right)} \\ &= (-2\pi i)^2 \left(\frac{1}{q_{4-} + i\varepsilon} \delta(q_{4-} + q_{2-}) \delta(q_{1-}) \delta(q_{3-}) + 2 \frac{1}{q_{4-} + i\varepsilon} \delta(q_{4-} + q_{1-}) \delta(q_{2-}) \delta(q_{3-}) \right. \\ & \quad \left. + \frac{1}{q_{3-} + i\varepsilon} \delta(q_{3-} + q_{1-}) \delta(q_{2-}) \delta(q_{4-}) \right), \quad (3.54) \end{aligned}$$

and that for the term proportional to the isospin factor IIII ,

$$\begin{aligned} & \delta\left(\sum_{i=1}^4 q_{i-}\right) \sum_{\sigma} I_{\sigma} \frac{1}{(q_{\sigma(1)-} + i\varepsilon)(q_{\sigma(1)-} + q_{\sigma(4)-} + i\varepsilon) \left(\sum_{i=1}^3 q_{\sigma(i)-} + i\varepsilon\right)} \\ &= (-2\pi i)^2 \left(\frac{-1}{q_{2-} + i\varepsilon} \delta(q_{2-} + q_{1-}) \delta(q_{3-}) \delta(q_{4-}) + \frac{-1}{q_{3-} + i\varepsilon} \delta(q_{3-} + q_{1-}) \delta(q_{2-}) \delta(q_{4-}) \right. \\ & \quad + \frac{-1}{q_{4-} + i\varepsilon} \delta(q_{4-} + q_{1-}) \delta(q_{2-}) \delta(q_{3-}) + \frac{-1}{q_{3-} + i\varepsilon} \delta(q_{3-} + q_{2-}) \delta(q_{1-}) \delta(q_{4-}) \\ & \quad \left. + \frac{-1}{q_{4-} + i\varepsilon} \delta(q_{4-} + q_{2-}) \delta(q_{1-}) \delta(q_{3-}) + \frac{-1}{q_{4-} + i\varepsilon} \delta(q_{4-} + q_{3-}) \delta(q_{1-}) \delta(q_{2-}) \right). \quad (3.55) \end{aligned}$$

In either case the only non-zero flow diagram exists for the terms proportional to $\delta(q_{1-} + q_{4-})\delta(q_{2-})\delta(q_{3-})$; this flow diagram is shown in Fig. 30. The resulting amplitudes are then

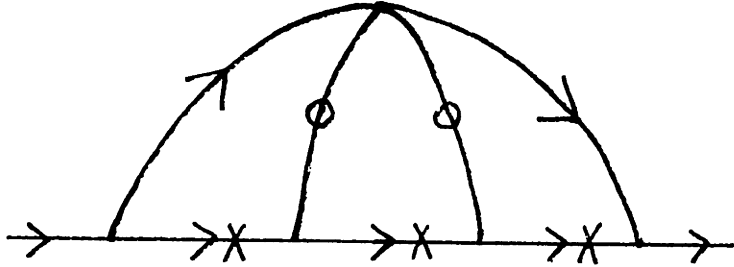


Fig. 30


$$\begin{aligned}
 & -2sg^6 \frac{g^2 lns}{2\pi} \textcircled{0} \text{III} \\
 & \sim -\frac{2}{3} g^6 s \frac{g^2 lns}{2\pi} \textcircled{0} (\text{III} + \text{III} + \text{III}) \quad (3.56)
 \end{aligned}$$

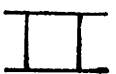
and

$$g^6 s \frac{g^2 lns}{2\pi} \textcircled{0} \text{III} . \quad (3.57)$$

For the term proportional to isospin diagram III , it is shown in Appendix IV that

$$\delta\left(\sum_{i=1}^4 q_{i-}\right) \sum_{\sigma} \frac{I_{\sigma}}{(q_{\sigma(1)-+i\varepsilon})\left(\sum_{i=1}^2 q_{\sigma(i)-+i\varepsilon}\right)\left(\sum_{i=1}^3 q_{\sigma(i)-+i\varepsilon}\right)} = -(-2\pi i)^2 \frac{1}{q_{4-+i\varepsilon}} \delta(q_{4-}+q_{1-})\delta(q_{2-})\delta(q_{3-}) \quad (3.58)$$

so that this amplitude is proportional to $g^2(gT)^4(g^2 \ln s)$ which is too small and is dropped. By symmetry, the terms proportional to isospin diagram  are too small and are dropped.

Now consider the terms proportional to isospin diagram . In Appendix IV it is shown that in this case

$$\begin{aligned}
 & \delta\left(\sum_{i=1}^4 q_{i-}\right) \sum_{\sigma} I_{\sigma} \frac{1}{(q_{\sigma(1)-} + i\varepsilon)(q_{\sigma(2)-} + i\varepsilon)\left(\sum_{i=1}^3 q_{\sigma(i)-} + i\varepsilon\right)} \\
 &= (-2\pi i) \left\{ \frac{1}{(q_{3-} + i\varepsilon)(q_{3-} + q_{2-} + i\varepsilon)} \delta(q_{3-} + q_{2-} + q_{1-}) \delta(q_{4-}) \right. \\
 & \quad - \frac{1}{(q_{3-} + i\varepsilon)(q_{3-} + q_{4-} + i\varepsilon)} \delta(q_{3-} + q_{4-} + q_{1-}) \delta(q_{2-}) - \frac{1}{(q_{4-} + i\varepsilon)(q_{4-} + q_{1-} + i\varepsilon)} \delta(q_{4-} + q_{1-} + q_{3-}) \delta(q_{2-}) \\
 & \quad + \frac{1}{(q_{4-} + i\varepsilon)(q_{4-} + q_{2-} + i\varepsilon)} \delta(q_{4-} + q_{2-} + q_{1-}) \delta(q_{3-}) + \frac{1}{(q_{4-} + i\varepsilon)(q_{4-} + q_{3-} + i\varepsilon)} \delta(q_{4-} + q_{3-} + q_{2-}) \delta(q_{1-}) \\
 & \quad + \frac{1}{q_{2-} + i\varepsilon} \delta(q_{2-} + q_{1-}) \frac{1}{q_{4-} + i\varepsilon} \delta(q_{4-} + q_{3-}) + \frac{1}{q_{3-} + i\varepsilon} \delta(q_{3-} + q_{1-}) \frac{1}{q_{4-} + i\varepsilon} \delta(q_{4-} + q_{2-}) \\
 & \quad \left. + \frac{1}{q_{4-} + i\varepsilon} \delta(q_{4-} + q_{1-}) \frac{1}{q_{2-} + i\varepsilon} \delta(q_{2-} + q_{3-}) + 2 \frac{1}{q_{4-} + i\varepsilon} \delta(q_{4-} + q_{1-}) \frac{1}{q_{3-} + i\varepsilon} \delta(q_{3-} + q_{2-}) \right\} \\
 & \hspace{20em} (3.59)
 \end{aligned}$$

Of the first five terms on the right-hand side of (3.59) only the second and the third (both are proportional to $\delta(q_{1-} + q_{3-} + q_{4-})\delta(q_{2-})$) contribute. They share the same flow diagram, shown in Fig. 31, and they give rise to the space-time amplitudes

$$-ig^4s \left(\frac{g^2 l m s}{2\pi}\right)^2 \textcircled{0} \quad (3.60)$$

and

$$ig^4s \left(\frac{g^2 l m s}{2\pi}\right)^2 \textcircled{0}, \quad (3.61)$$

respectively. Of the last four terms on the right-hand side

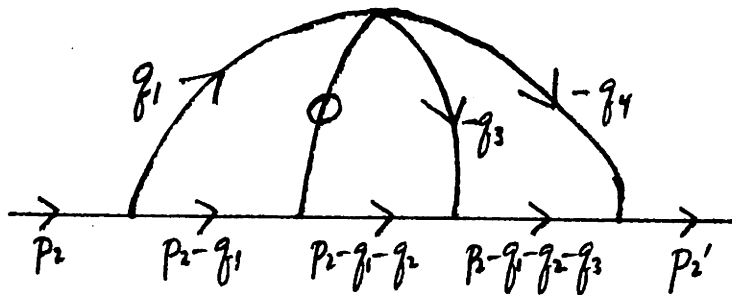


Fig. 31

of (3.59) only the last two contribute; they share the flow diagram shown in Fig. 32, and give rise to the space-time amplitudes

$$-ig^4s \left(\frac{g^2 l m s}{2\pi}\right)^2 \textcircled{0} \quad (3.62)$$

and

$$2ig^4s \left(\frac{g^2 l m s}{2\pi}\right)^2 \textcircled{0} \quad (3.63)$$

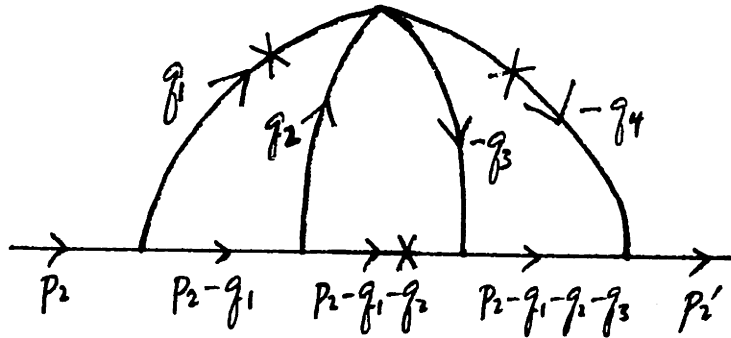


Fig. 32

respectively. Thus the total contribution proportional to isospin diagram II is

$$ig^4 s \left(\frac{g^2 \ln s}{2\pi} \right)^2 \textcircled{\text{O}} \text{II}. \quad (3.64)$$

The amplitudes proportional to the isospin diagrams III and IV cannot be dealt with so simply. The reason is that the sums

$$\delta\left(\sum_{i=1}^4 q_{i-}\right) \sum_{\sigma} I_{\sigma} \frac{1}{(q_{\sigma(1)} - t + i\varepsilon)(q_{\sigma(1)} + q_{\sigma(2)} - t + i\varepsilon) \left(\sum_{i=1}^3 q_{\sigma(i)} - t + i\varepsilon\right)} \quad (3.65)$$

are not proportional to a product of two delta functions. For example, in the III case, neglecting momentarily the $i\varepsilon$ terms in the denominators, we find that (3.65) becomes

$$\delta(q_{1-} + q_{2-} + q_{3-} + q_{4-}) \left(\frac{1}{q_{4-}(q_{4-} + q_{3-})(q_{4-} + q_{3-} + q_{2-})} + \frac{1}{q_{3-}(q_{3-} + q_{4-})(q_{3-} + q_{4-} + q_{2-})} \right)$$

$$\begin{aligned}
 & + \frac{1}{q_4 - (q_4 + q_3 -) (q_4 + q_3 + q_1 -)} + \frac{1}{q_4 - (q_4 + q_2 -) (q_4 + q_2 + q_3 -)} + \frac{1}{q_3 - (q_3 + q_4 -) (q_3 + q_4 + q_1 -)} \\
 & = \delta(q_1 + q_2 + q_3 + q_4) \frac{1}{q_2 - q_3 - (q_1 + q_3 -)} \cdot \quad (3.66)
 \end{aligned}$$

Real terms as large as $s \ln^3 s$ and $s \ln^2 s$ can result! But, as we will show below, when all terms from all flow diagrams are added together, these real terms cancel exactly. We will then calculate the (non-zero) $s \ln^2 s$ contribution from the imaginary terms; these terms come from the vanishing of one of the denominators in (3.65). (Real contributions to (3.65) can also occur if two denominators vanish, but then the amplitude is proportional to $s \ln s$ at most, so is dropped.)

Plugging (3.66) into (3.52) we find that there are three flow diagrams. They are drawn in Fig. 33. (Note the different

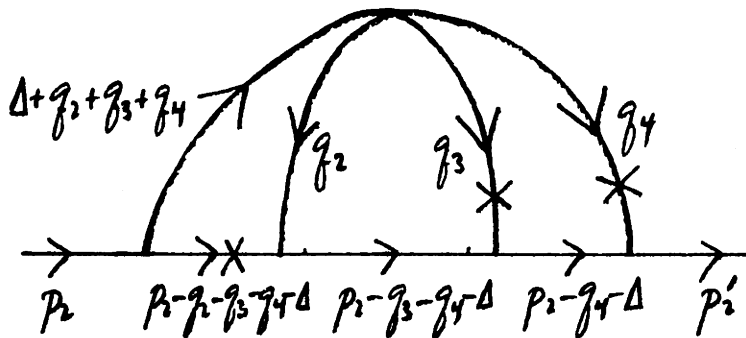


Fig. 33(a)

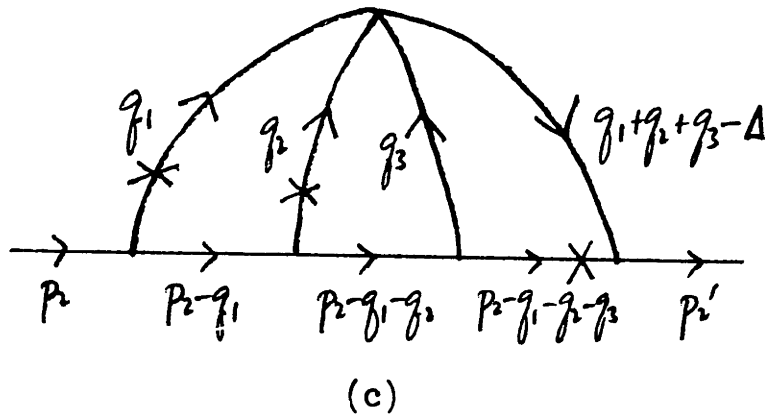
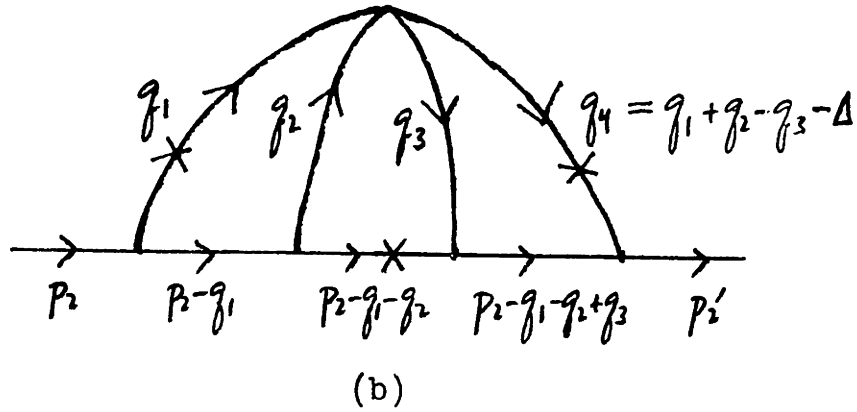


Fig. 33

notation on each diagram; this insures that all the q_i 's are positive.) The contributions corresponding to the flow diagrams in Fig. 33(a), (b) and (c) are respectively

$$-25g^8 \int \prod_{i=2}^4 \frac{d^4 q_{i-}}{(2\pi)^2} \int \prod_{i=2}^4 \frac{d q_{i-}}{2\pi} \frac{1}{(-q_{2-})(-q_{3-})(q_{2-}+q_{4-})} \frac{1}{a_1 a_4 q_{2-} q_{3-} - \left(\frac{a_2}{q_{2-}} + \frac{a_3}{q_{3-}} + \frac{a_4}{q_{4-}}\right) \left(\frac{a_3}{q_{3-}} + \frac{a_4}{q_{4-}}\right)},$$

$q_{2-}, q_{3-}, q_{4-} \gg p_{1-}$

(3.67a)

$$\begin{aligned}
 & -2s g^8 \int \prod_{i=1}^3 \frac{d^2 \vec{q}_{i-}}{(2\pi)^2} \int \prod_{i=1}^4 \frac{dq_{i-}}{2\pi} 2\pi \delta(q_{1-} + q_{2-} - q_{3-} - q_{4-}) \frac{1}{q_{2-}(-q_{3-})(q_{1-} - q_{3-})} \\
 & \quad q_{1-}, q_{2-}, q_{3-}, q_{4-} \gg p_{1-} \\
 & \quad \times \frac{1}{a_1 a_4 q_{2-} q_{3-} \left(\frac{a_1}{q_{1-}} + \frac{a_2}{q_{2-}} \right) \left(\frac{a_3}{q_{3-}} + \frac{a_4}{q_{4-}} \right)} \quad (3.67b)
 \end{aligned}$$

and

$$\begin{aligned}
 & -2s g^8 \int \prod_{i=1}^3 \frac{d^2 \vec{q}_{i+}}{(2\pi)^2} \int \prod_{i=1}^3 \frac{dq_{i-}}{2\pi} \frac{1}{q_{2-} q_{3-} (q_{1-} + q_{3-})} \frac{1}{a_1 a_4 q_{2-} q_{3-} \left(\frac{a_1}{q_{1-}} + \frac{a_2}{q_{2-}} \right) \left(\frac{a_1}{q_{1-}} + \frac{a_2}{q_{2-}} + \frac{a_3}{q_{3-}} \right)}, \\
 & \quad q_{1-}, q_{2-}, q_{3-} \gg p_{1-} \\
 & \quad (3.67c)
 \end{aligned}$$

where

$$a_i \equiv \frac{1}{\vec{q}_{i\pm}^2 + \lambda^2}, \quad i=1,2,3,4. \quad (3.68)$$

It is easy to see that the regions that contribute to the $s \ln^3 s$ term are $q_{4-} \gg q_{3-} \gg q_{2-}$ in (3.67a), $q_{1-} \gg q_{2-}, q_{3-}$ in (3.67b), and $q_{1-} \gg q_{2-} \gg q_{3-}$ in (3.67c) and that these terms cancel.

Under the transformation

$$\begin{aligned}
 \vec{q}_{1\pm} & \leftrightarrow \vec{q}_{4\pm} \\
 \vec{q}_{2\pm} & \leftrightarrow \vec{q}_{3\pm} \\
 q_{1-} & \leftrightarrow q_{4-} \\
 q_{2-} & \leftrightarrow q_{3-}
 \end{aligned} \quad (3.69)$$

and

(3.67a) and (3.67c) are transformed into each other, so the sum of (3.67a), (3.67b) and (3.67c) equals

$$-2sg^8 \int \prod_{i=1}^3 \frac{d^2 \vec{q}_i}{(2\pi)^2} \int \prod_{i=1}^3 \frac{dq_{i-}}{2\pi} \times \frac{I}{a_1 a_4} \quad (3.70a)$$

$q_1, q_2, q_3 \gg p_1$

with

$$I = \frac{1}{q_2^2 q_3^2} \frac{1}{\left(\frac{a_1}{q_1} + \frac{a_2}{q_2}\right)} \left\{ \frac{2}{(q_1 + q_3) \left(\frac{a_1}{q_1} + \frac{a_2}{q_2} + \frac{a_3}{q_3}\right)} \right.$$

$$\left. + \frac{1}{(q_3 - q_1) \left(\frac{a_3}{q_3} + \frac{a_4}{q_1 + q_2 - q_3}\right)} \right\} \quad (3.70b)$$

$q_1 + q_2 > q_3$

In the second term of (3.70b) it is assumed that $q_{1-} + q_{2-} > q_{3-}$.

The strategy now is to divide the q_- space into six regions where the $-$ momenta are ordered and to isolate the divergent terms from each region. In region A, $q_{1-} > q_{2-} > q_{3-}$.

Define

$$x = \frac{q_{2-}}{q_{1-}}, \quad 0 < x < 1 \quad (3.71a)$$

$$y = \frac{q_{3-}}{q_{2-}} = \frac{q_{3-}}{x q_{1-}}, \quad 0 < y < 1 \quad (3.71b)$$

so that

$$\int dq_{1-} dq_{2-} dq_{3-} = \int_{P_{1-}}^{P_{2-}} dq_{1-} \int_0^1 dx \int_0^1 dy x q_{1-}^2, \quad (3.72)$$

and

$$x q_{1-}^2 J = \frac{1}{q_{1-}} \frac{1}{xy(a_1x+a_2)} \left\{ \frac{2}{(1+xy)(xya_1+ya_2+a_3)} - \frac{1}{(1-xy)\left(a_3 + \frac{xy}{1+x-xy} a_4\right)} \right\}. \quad (3.73)$$

The integration over q_{1-} will give a contribution proportional to $\ln s$ which by itself is too small. However, other factors of $\ln s$ can come from the integrations over x and y if these integrations are divergent. This is because in our approximations there are really cutoffs that must be imposed -- for example, $x = \frac{q_{2-}}{q_{1-}} \gg \frac{p_{1-}}{q_{1-}}$. We will show that the divergences over the x and y integrations cancel when the contributions from the six regions are added together. Eqn. (3.73) can lead to divergences when $x \sim 0$ or $y \sim 0$, but there is no divergence coming from the vanishing of the $1 - xy$ term in the denominator.

Next consider region B, where $q_{1-} > q_{3-} > q_{2-}$. Define

$$X = \frac{q_{3-}}{q_{1-}}, \quad 0 < X < 1 \quad (3.74a)$$

$$Y = \frac{q_{2-}}{q_{3-}} = \frac{q_{2-}}{X q_{1-}}, \quad 0 < Y < 1 \quad (3.74b)$$

so that (3.72) holds. Here

$$x q_1^2 I = \frac{1}{q_1 - xy(xya_1 + a_2)} \left\{ \frac{2y}{(1+x)(xya_1 + a_2 + ya_3)} - \frac{1}{(1-x)\left(a_3 + \frac{x}{1+xy-x} a_4\right)} \right\}. \quad (3.75)$$

Divergences come from the regions $x \sim 0$, $y \sim 0$, and $x \sim 1$.

In region C $q_{2-} > q_{1-} > q_{3-}$, so define

$$x = \frac{q_{1-}}{q_{2-}}, \quad 0 < x < 1 \quad (3.76a)$$

and

$$y = \frac{q_{3-}}{q_{1-}} = \frac{q_{3-}}{x q_{2-}}, \quad 0 < y < 1 \quad (3.76b)$$

so that

$$\int dq_{1-} dq_{2-} dq_{3-} = \int_{P_{1-}}^{P_{2-}} dq_{2-} \int_0^1 dx \int_0^1 dy x q_2^2, \quad (3.77)$$

and

$$x q_2^2 I = \frac{1}{q_2 - y(a_1 + xa_2)} \left\{ \frac{2}{(1+y)(ya_1 + xya_2 + a_3)} - \frac{1}{(1-y)\left(a_3 + \frac{xy}{x+1-xy} a_4\right)} \right\}. \quad (3.78)$$

Divergences come from the regions $y \sim 0$ and $y \sim 1$.

In region D, where $q_{2-} > q_{3-} > q_{1-}$, define

$$x = \frac{q_{3-}}{q_{2-}}, \quad 0 < x < 1 \quad (3.79a)$$

and

$$y = \frac{q_{1-}}{q_{3-}} = \frac{q_{1-}}{x q_{2-}}, \quad 0 < y < 1 \quad (3.79b)$$

so that (3.77) holds and

$$x q_{2-}^2 I = \frac{1}{q_{2-}} \frac{y}{a_1 + x y a_2} \left\{ \frac{2y}{(y+1)(a_1 + x y a_2 + y a_3)} + \frac{1}{(1-y)(a_3 + \frac{x}{x y + 1 - x} a_4)} \right\} \quad (3.80)$$

Divergence comes from the second term on the right-hand side of (3.80), from the region $y \sim 1$.

Region E is defined by $q_{3-} > q_{1-} > q_{2-}$. There define

$$x = \frac{q_{1-}}{q_{3-}}, \quad 0 < x < 1 \quad (3.81a)$$

and

$$y = \frac{q_{2-}}{q_{1-}} = \frac{q_{2-}}{x q_{3-}}, \quad 0 < y < 1 \quad (3.81b)$$

so that

$$\int dq_{1-} dq_{2-} dq_{3-} = \int_{R-}^{P_{2-}} dq_{3-} \int_0^1 dx \int_0^1 dy x q_{3-}^2. \quad (3.82)$$

Thus

$$X q_{3-}^2 I = \frac{1}{q_{3-}} \frac{1}{(y a_1 + a_2)} \left\{ \frac{2x}{(1+x)(y a_1 + a_2 + x y a_3)} + \frac{1}{y(1-x) \left(a_3 + \frac{1}{x+xy-1} a_4 \right)} \right\} \quad (3.83)$$

where $x + xy > 1$ in the second term on the right-hand side.

The only divergence comes from this second term on the right-hand side.

Finally, region F is given by $q_{3-} > q_{2-} > q_{1-}$. Define

$$X = \frac{q_{2-}}{q_{3-}}, \quad 0 < X < 1 \quad (3.84a)$$

and

$$y = \frac{q_{1-}}{q_{2-}} = \frac{q_{1-}}{X q_{3-}}, \quad 0 < y < 1 \quad (3.84b)$$

so that (3.82) holds.

$$X q_{3-}^2 I = \frac{1}{q_{3-}} \frac{y}{a_1 + a_2 y} \left\{ \frac{2xy}{(xy+1)(a_1 + y a_2 + xy a_3)} + \frac{1}{(1-xy) \left(a_3 + \frac{a_4}{xy+x-1} \right)} \right\} \quad (3.85)$$

where $xy + x > 1$ in the second term on the right-hand side.

There are no divergences from (3.85).

In region C, when $y \sim 1$,

$$X q_{3-}^2 I_C \sim \frac{-1}{q_{2-} (a_1 + X a_2) (a_3 + X a_4) (1-y)}. \quad (3.86)$$

And in region D, when $y \sim 1$,

$$X q_2^2 I_D \sim \frac{1}{q_2 - (a_1 + X a_2)(a_3 + X a_4)(1-y)}, \quad (3.87)$$

so these two divergences cancel each other. From the second term on the right-hand side of (3.75) (Region B) and the second term on the right-hand side of (3.83) (Region E) we get (suppressing the $\frac{1}{q_-}$ dependence, which, by a change of variable is the same for all these amplitudes)

$$\begin{aligned} & \int_0^1 dx \int_0^1 dy \frac{-1}{X y (X y a_1 + a_2)(1-x)(a_3 + \frac{X}{1+Xy-x} a_4)} + \int_{\frac{1}{2}}^1 dx \int_{\frac{1-x}{X}}^1 dy \frac{1}{(y a_1 + a_2) y (1-x)(a_3 + \frac{1}{X+Xy-1} a_4)} \\ &= \int_0^1 dx \int_0^1 dy \left(\frac{-1}{X y (X y a_1 + a_2)(1-x)(a_3 + \frac{X}{1+Xy-x} a_4)} + \frac{1}{y (y a_1 + a_2)(1-x)(a_3 + \frac{1}{y} a_4)} \right) \\ &+ \int_{\frac{1}{2}}^1 dx \int_{\frac{1-x}{X}}^1 dy \left(\frac{1}{(y a_1 + a_2) y (1-x)(a_3 + \frac{1}{X+Xy-1} a_4)} - \frac{1}{y (y a_1 + a_2)(1-x)(a_3 + \frac{1}{y} a_4)} \right) \\ &\quad - \int_0^1 dy \int_0^{\frac{1+y}{1+y}} dx \frac{1}{y (y a_1 + a_2)(1-x)(a_3 + \frac{1}{y} a_4)} \\ &= - \int_0^1 dx \int_0^1 dy \frac{y^2(x+1)(1+Xy-x)a_1 a_3 + y(1+Xy-x)a_2 a_3 + (X^2 y^2 + X y^2 + y)a_1 a_4 + (1+Xy)a_2 a_4}{X y (X y a_1 + a_2)(y a_1 + a_2)(y a_3 + a_4)((1+Xy-x)a_3 + X a_4)} \\ &+ \int_{\frac{1}{2}}^1 dx \int_{\frac{1-x}{X}}^1 dy \frac{-(1+y)a_4}{y (y a_1 + a_2)(y a_3 + a_4)((X+Xy-1)a_3 + a_4)} - \int_0^1 dy \int_0^{\frac{1+y}{1+y}} dx \frac{1}{(y a_1 + a_2)(1-x)(y a_3 + a_4)}. \end{aligned} \quad (3.88)$$

Both of the last two integrals in (3.88) are convergent, so their contributions can be ignored. The first integral in (3.88) can be divided into parts

$$\begin{aligned}
 & - \int_0^1 dx \int_0^1 dy \frac{a_2 a_4}{x y (x y a_1 + a_2) (y a_1 + a_2) (y a_3 + a_4) ((1+x y-x)a_3 + x a_4)} \\
 & - \int_0^1 dx \int_0^1 dy \frac{y(x+1)(1+x y-x)a_1 a_3 + (1+x y-x)a_2 a_3 + (x^2 y + x y + 1)a_1 a_4 + x a_2 a_4}{x(x y a_1 + a_2) (y a_1 + a_2) (y a_3 + a_4) ((1+x y-x)a_3 + x a_4)} \\
 & = - \int_0^1 dx \int_0^1 dy \frac{a_2 a_4}{x y (x y a_1 + a_2) (y a_1 + a_2) (y a_3 + a_4) ((1+x y-x)a_3 + x a_4)} \\
 & - \int_0^1 dx \int_0^1 dy \frac{y a_1 a_3 + a_2 a_3 + a_1 a_4}{x a_2 (y a_1 + a_2) (y a_3 + a_4) a_3} + \text{convergent terms} \quad (3.89)
 \end{aligned}$$

From the first term on the right-hand side of (3.75) (Region B) we get

$$\begin{aligned}
 & \int_0^1 dx \int_0^1 dy \frac{2}{x(x y a_1 + a_2) (1+x) (x y a_1 + a_2 + y a_3)} \\
 & = \int_0^1 dx \int_0^1 dy \frac{2}{x a_2 (a_2 + y a_3)} + \text{convergent terms} \\
 & = \int_0^1 dx \frac{2}{x a_2 a_3} \ln \left(1 + \frac{a_3}{a_2} \right) + \text{convergent terms} \quad (3.90)
 \end{aligned}$$

The divergent term from the $y \sim 0$ region in (3.78) is

$$\int_0^1 dx \int_0^1 dy \frac{1}{y(a_1 + xa_2)a_3} = \int_0^1 dx \frac{1}{xa_2a_3} \ln\left(1 + \frac{a_2}{a_1}\right). \quad (3.91)$$

Finally, region A gives the contribution (from (3.73))

$$\begin{aligned} & \int_0^1 dx \int_0^1 dy \frac{-xy(1+xy)(1-xy+x)a_1 - y(1+xy)(1+x-xy)a_2 + (1-3xy)(1+x-xy)a_3 + 2xy(1-xy)a_4}{xy(1+xy)(1-xy)(xa_1+a_2)(xya_1+ya_2+a_3)((1+x-xy)a_3+xya_4)} \\ &= \int_0^1 dx \int_0^1 dy \frac{a_3}{xy(1+xy)(1-xy)(xa_1+a_2)(xya_1+ya_2+a_3)((1+x-xy)a_3+xya_4)} \\ &+ \int_0^1 dx \int_0^1 dy \frac{1}{y(xa_1+a_2)(1+x)a_3} - \int_0^1 dx \int_0^1 dy \frac{1}{x(ya_2+a_3)a_3} + \text{convergent terms} \\ &= \int_0^1 dx \int_0^1 dy \frac{a_3}{xy(1+xy)(1-xy)(xa_1+a_2)(xya_1+ya_2+a_3)((1+x-xy)a_3+xya_4)} \\ &+ \int_0^1 dx \frac{1}{xa_3(a_1-a_2)} \left(\ln\left(1 + \frac{a_1}{a_2}\right) - \ln 2 \right) \\ &- \int_0^1 dx \frac{1}{xa_2a_3} \ln\left(1 + \frac{a_2}{a_3}\right) + \text{convergent terms} \quad (3.92) \end{aligned}$$

The sum of (3.89) and the first integral in (3.92) is

$$\begin{aligned} & \int_0^1 dx \int_0^1 dy \frac{a_1a_3a_4 + a_2a_3^2 - a_2^2a_4 + a_1a_3^2y}{xa_2a_3(ya_1+a_2)(ya_2+a_3)(ya_3+a_4)} \\ &+ \int_0^1 dx \int_0^1 dy \frac{a_2a_4 - 2a_2a_3 - a_1a_3 - a_1a_3x}{ya_2a_3(1+x)(xa_1+a_2)(x(a_4-a_3)+a_3)} \end{aligned}$$

$$- \int_0^1 dx \int_0^1 dy \frac{y a_1 a_3 + a_2 a_3 + a_1 a_4}{x a_2 a_3 (y a_1 + a_2)(y a_3 + a_4)} + \text{convergent terms. (3.93)}$$

Decomposing the integrands into partial fractions and dropping the convergent terms, this becomes

$$\begin{aligned} & \int_0^1 dx \int_0^1 dy \left\{ \frac{a_1}{x a_2 (a_1 a_3 - a_2^2)} \left(\frac{a_1}{y a_1 + a_2} - \frac{a_2}{y a_2 + a_3} \right) \right. \\ & + \frac{a_3^2 - a_2 a_4}{x a_3} \left(\frac{a_1}{y a_1 + a_2} \cdot \frac{a_1}{(a_1 a_3 - a_2^2)(a_1 a_4 - a_2 a_3)} + \frac{a_2}{y a_2 + a_3} \cdot \frac{a_2}{(a_3^2 - a_1 a_3)(a_2 a_4 - a_3^2)} \right. \\ & \quad \left. \left. + \frac{a_3}{y a_3 + a_4} \cdot \frac{a_3}{(a_2 a_3 - a_1 a_4)(a_3^2 - a_2 a_4)} \right) \right\} \\ & + \int_0^1 dx \int_0^1 dy \left\{ \frac{-a_1}{x a_2 (a_1 a_3 + a_2 a_3 - a_2 a_4)} \left(\frac{a_1}{y a_1 + a_2} - \frac{a_4 - a_3}{y(a_4 - a_3) + a_3} \right) \right. \\ & + \frac{a_4 - 2a_3}{x a_3} \left(\frac{1}{(1+y)(a_2 - a_1)(2a_3 - a_4)} + \frac{a_1}{y a_1 + a_2} \cdot \frac{a_1}{(a_1 - a_2)(a_1 a_3 + a_2 a_3 - a_2 a_4)} \right. \\ & \quad \left. \left. + \frac{a_4 - a_3}{(a_4 - a_3)y + a_3} \cdot \frac{a_4 - a_3}{(a_2 a_4 - a_2 a_3 - a_1 a_3)(a_4 - 2a_3)} \right) \right\} \\ & - \int_0^1 dx \int_0^1 dy \left\{ \frac{a_3}{x a_2 a_3 (y a_3 + a_4)} + \frac{a_1 a_4}{x a_2 a_3} \frac{1}{(a_1 a_4 - a_2 a_3)} \left(\frac{a_1}{y a_1 + a_2} - \frac{a_3}{y a_3 + a_4} \right) \right\} \end{aligned}$$

$$\begin{aligned}
 &= \int_0^1 dx \left\{ \frac{a_1}{x a_2 (a_1 a_3 - a_2^2)} \left(\ln\left(1 + \frac{a_1}{a_2}\right) - \ln\left(1 + \frac{a_2}{a_3}\right) \right) \right. \\
 &\quad + \frac{a_3^2 - a_2 a_4}{x a_3} \frac{a_1}{(a_1 a_3 - a_2^2)(a_1 a_4 - a_2 a_3)} \ln\left(1 + \frac{a_1}{a_2}\right) - \frac{a_2}{x a_3} \frac{1}{a_2^2 - a_1 a_3} \ln\left(1 + \frac{a_2}{a_3}\right) \\
 &\quad + \frac{1}{x(a_2 a_3 - a_1 a_4)} \ln\left(1 + \frac{a_3}{a_4}\right) - \frac{a_1}{x a_2 (a_1 a_3 + a_2 a_3 - a_2 a_4)} \ln\left(1 + \frac{a_1}{a_2}\right) \\
 &\quad + \frac{a_1}{x a_2 (a_1 a_3 + a_2 a_3 - a_2 a_4)} (\ln a_4 - \ln a_3) + \frac{1}{x a_3 (a_1 - a_2)} \ln 2 \\
 &\quad + \frac{a_1 (a_4 - 2a_3)}{x a_3 (a_1 - a_2) (a_1 a_3 + a_2 a_3 - a_2 a_4)} \ln\left(1 + \frac{a_1}{a_2}\right) + \frac{a_4 - a_3}{x a_3 (a_2 a_4 - a_2 a_3 - a_1 a_3)} (\ln a_4 - \ln a_3) \\
 &\quad - \frac{1}{x a_2 a_3} \ln\left(1 + \frac{a_3}{a_4}\right) - \frac{a_1 a_4}{x a_2 a_3 (a_1 a_4 - a_2 a_3)} \ln\left(1 + \frac{a_1}{a_2}\right) + \frac{a_1 a_4}{x a_2 a_3 (a_1 a_4 - a_2 a_3)} \ln\left(1 + \frac{a_3}{a_4}\right) \\
 &= \int_0^1 dx \left\{ \frac{\ln\left(1 + \frac{a_1}{a_2}\right)}{x} \frac{-a_1}{a_2 a_3 (a_1 - a_2)} + \frac{\ln\left(1 + \frac{a_2}{a_3}\right)}{x} \frac{-1}{a_2 a_3} \right. \\
 &\quad \left. + \frac{\ln a_4 - \ln a_3}{x} \frac{1}{a_2 a_3} + \frac{\ln 2}{x a_3 (a_1 - a_2)} \right\}. \quad (3.94)
 \end{aligned}$$

Thus the sum of all the divergent terms, from (3.90), (3.91), the second and third terms of (3.92), and (3.94) equals

$$\begin{aligned}
 &\int_0^1 dx \frac{1}{x} \left\{ -\frac{\ln\left(1 + \frac{a_1}{a_2}\right)}{a_2 a_3} - 2 \frac{\ln\left(1 + \frac{a_2}{a_3}\right)}{a_2 a_3} + \frac{\ln\left(1 + \frac{a_2}{a_1}\right)}{a_2 a_3} + 2 \frac{\ln\left(1 + \frac{a_3}{a_2}\right)}{a_2 a_3} \right\} \\
 &\quad + \int_0^1 dx \frac{1}{x} \frac{\ln a_4 - \ln a_3}{a_2 a_3}. \quad (3.95)
 \end{aligned}$$

From (3.70a) there is a factor of $\frac{1}{a_1 a_4}$ which multiplies all of the above terms, so they all cancel. Therefore the real terms of the space-time amplitude multiplying the isospin diagram \mathbb{H} are $O(s \ln s)$ and can be dropped.

We will now show that the same holds for the spacetime amplitude multiplying the isospin diagram \mathbb{H} . Denote the isospin coefficients in Table VII for isospin diagram \mathbb{H} by I_σ and for isospin diagram \mathbb{H} by I'_σ . Then

$$\begin{aligned} & \delta(q_{1-} + q_{2-} + q_{3-} + q_{4-}) \sum_{\sigma} (I'_\sigma + 3 I_\sigma) \frac{1}{(q_{\sigma(1)} + i\varepsilon)(q_{\sigma(1)} + q_{\sigma(2)} + i\varepsilon) \left(\sum_{i=1}^3 q_{\sigma(i)} + i\varepsilon \right)} \\ &= \frac{-1}{(q_{4-} + i\varepsilon)(q_{4-} + q_{3-} + i\varepsilon)(q_{4-} + q_{3-} + q_{2-} + i\varepsilon)} + \frac{1}{(q_{2-} + i\varepsilon)(q_{2-} + q_{3-} + i\varepsilon)(q_{2-} + q_{3-} + q_{4-} + i\varepsilon)} \\ &+ \frac{1}{(q_{4-} + i\varepsilon)(q_{4-} + q_{1-} + i\varepsilon)(q_{4-} + q_{1-} + q_{2-} + i\varepsilon)} + \frac{1}{(q_{3-} + i\varepsilon)(q_{3-} + q_{4-} + i\varepsilon)(q_{3-} + q_{4-} + q_{1-} + i\varepsilon)} \end{aligned}$$

and dropping the $i\varepsilon$ terms from the denominator

$$\begin{aligned} & \approx \frac{-1}{q_{4-}(q_{4-} + q_{3-})(q_{4-} + q_{3-} + q_{2-})} + \frac{1}{q_{2-}(q_{2-} + q_{3-})(q_{2-} + q_{3-} + q_{4-})} \\ &+ \frac{1}{q_{4-}(-q_{3-} - q_{2-})(-q_{3-})} + \frac{1}{q_{3-}(q_{3-} + q_{4-})(-q_{2-})} = 0, \end{aligned} \tag{3.96}$$

and we are done.

Now we shall calculate the isln^2 's contributions. First consider the \mathbb{H} isospin diagram contribution. Since

$$\frac{1}{q_- + i\varepsilon} = P \frac{1}{q_-} - i\pi \delta(q_-) \quad (3.97)$$

the leading imaginary term coming from the diagram (4321) (see Table VII for the notation) comes from

$$\begin{aligned} \frac{1}{(q_4 + i\varepsilon)(q_4 + q_3 + i\varepsilon)(q_4 + q_3 + q_2 + i\varepsilon)} &\Rightarrow -i\pi \left(\frac{\delta(q_4)}{(q_4 + q_3)(q_4 + q_3 + q_2)} \right. \\ &\left. + \frac{\delta(q_4 + q_3)}{q_4 (q_4 + q_3 + q_2)} + \frac{\delta(q_4 + q_3 + q_2)}{q_4 (q_4 + q_3)} \right). \quad (3.98) \end{aligned}$$

However, none of the terms in (3.98) has a non-zero flow diagram. Similarly, there is no contribution from diagrams (3421), (4312), or (4231). For diagram (3412),

$$\begin{aligned} \frac{1}{(q_3 + i\varepsilon)(q_3 + q_4 + i\varepsilon)(q_3 + q_4 + q_1 + i\varepsilon)} &\Rightarrow -i\pi \left(\frac{\delta(q_3)}{(q_3 + q_4)(q_3 + q_4 + q_1)} \right. \\ &\left. + \frac{\delta(q_3 + q_4)}{q_3 (q_3 + q_4 + q_1)} + \frac{\delta(q_3 + q_4 + q_1)}{q_3 (q_3 + q_4)} \right). \quad (3.99) \end{aligned}$$

The first and third terms on the right-hand side of (3.99) have non-zero flow diagrams which are shown in Fig. 34(a,b). Each leads to a contribution equal to

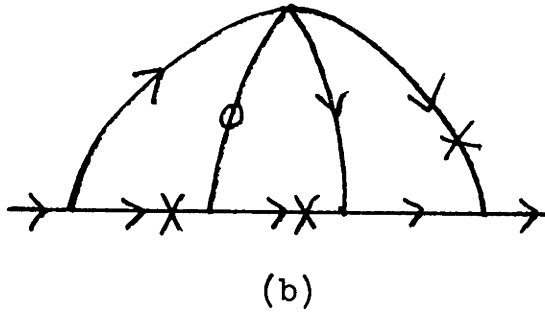
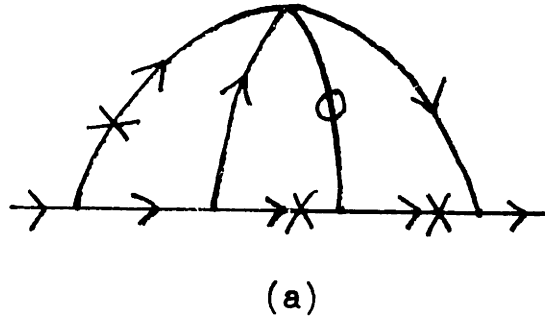


Fig. 34

$$\frac{1}{2} ig^4 s \left(\frac{g^2 lms}{2\pi} \right)^2 \textcircled{0}, \quad (3.100)$$

so that the total amplitude proportional to the isospin diagram \mathbb{H} is

$$ig^4 s \left(\frac{g^2 lms}{2\pi} \right)^2 \textcircled{0} \mathbb{H}. \quad (3.101)$$

For the \mathbb{H} isospin diagram contributions, by the above, the (3412) diagram gives a contribution equal to

$$-2ig^4 s \left(\frac{g^2 lms}{2\pi} \right) \textcircled{0}. \quad (3.102)$$

For diagram (2341), there are two contributing flow diagrams, one shown in Fig. 34(b) and the other shown in Fig. 35. They

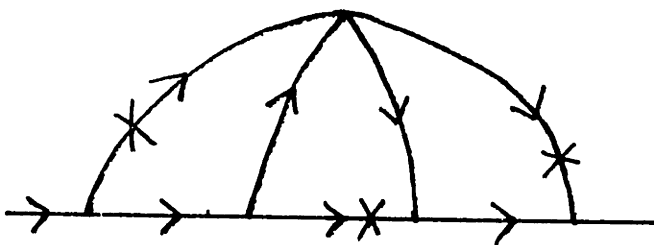


Fig. 35

give the contributions

$$\frac{1}{2} ig^4 s \left(\frac{g^2 lns}{2\pi} \right)^2 \textcircled{0} \quad (3.103)$$

and

$$-\frac{1}{2} ig^4 s \left(\frac{g^2 lns}{2\pi} \right)^2 \textcircled{0} \quad (3.104)$$

respectively. And for diagram (4123) there are again two non-zero flow diagrams, one shown in Fig. 34(a) with a contribution given by (3.103), and the other shown in Fig. 35 with a contribution given by (3.104). Thus the total amplitude proportional to the isospin diagram H is

$$-2ig^4 s \left(\frac{g^2 lns}{2\pi} \right)^2 \textcircled{0} \text{H}. \quad (3.105)$$

To summarize, the total contribution coming from the eighth order multi-meson exchange diagrams is, from (3.53), (3.56), (3.57), (3.64), (3.101) and (3.105),

$$\begin{aligned} & -\frac{1}{12} ig^8 s \textcircled{0} \text{IIII} - \frac{2}{3} g^6 s \frac{g^2 lns}{2\pi} \textcircled{0} (\text{HII} + \text{HII} + \text{III}) \\ & + g^6 s \frac{g^2 lns}{2\pi} \textcircled{0} \text{III} + ig^4 s \left(\frac{g^2 lns}{2\pi} \right)^2 \textcircled{0} \text{II} \end{aligned}$$

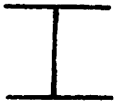
$$+ ig^4 s \left(\frac{g^2 l m s}{2\pi} \right)^2 \text{Diagram 1} - 2 ig^4 s \left(\frac{g^2 l m s}{2\pi} \right)^2 \text{Diagram 2}. \quad (3.106)$$

This ends the calculation by Feynman diagrams of the scattering amplitude through the eighth order in the coupling constant.

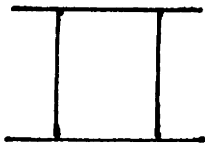
IV. The Feynman Diagram Calculation. Summary

Prototype Feynman Diagram

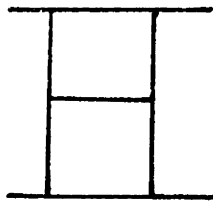
Scattering Amplitude \mathcal{M}



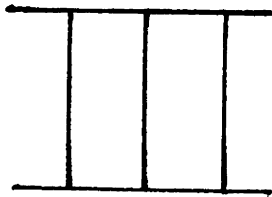
$$2g^2s \frac{1}{\Delta_i^2 + \lambda^2} \text{ I}$$



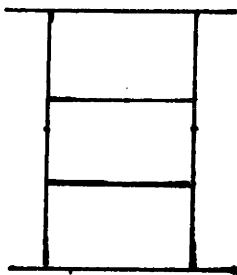
$$ig^4s \text{ (circle) II} - 2g^2s \left(\frac{g^2\ln s}{2\pi}\right) \text{ (circle) I}$$



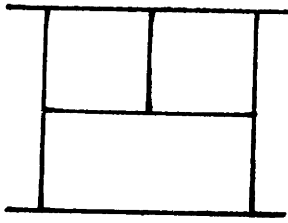
$$-ig^4s \left(\frac{g^2\ln s}{2\pi}\right) \left(\text{circle} + \frac{1}{2}\lambda^2 \text{ circle}\right) \text{ III} \\ + \frac{1}{2}ig^4s \left(\frac{g^2\ln s}{2\pi}\right) \lambda^2 \text{ circle II} + g^2s \left(\frac{g^2\ln s}{2\pi}\right)^2 \text{ circle I}$$



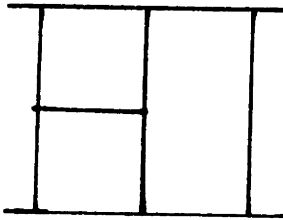
$$-\frac{1}{3}g^6s \text{ (circle) III} \\ + 2ig^4s \left(\frac{g^2\ln s}{2\pi}\right) \text{ (circle) (III - II)}$$



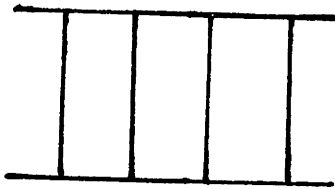
$$\frac{1}{8}ig^4s \left(\frac{g^2\ln s}{2\pi}\right)^2 \left(4 \text{ circle} + 4\lambda^2 \text{ circle} + \lambda^4 \text{ circle}\right) \text{ III} \\ - \frac{1}{4}ig^4s \left(\frac{g^2\ln s}{2\pi}\right)^2 \left(2\lambda^2 \text{ circle} + \lambda^4 \text{ circle}\right) \text{ III} \\ + \frac{1}{8}ig^4s \left(\frac{g^2\ln s}{2\pi}\right)^2 \lambda^4 \text{ circle II} \\ - \frac{1}{3}g^2s \left(\frac{g^2\ln s}{2\pi}\right)^3 \text{ circle I}$$



$$\begin{aligned}
 & -ig^4s \left(\frac{g^2 lns}{2\pi}\right)^2 \left(2 \textcircled{\circ} + \lambda^2 \textcircled{\circ}\right) \text{III} \\
 & + 2ig^4s \left(\frac{g^2 lns}{2\pi}\right)^2 \left(\textcircled{\circ} + \lambda^2 \textcircled{\circ}\right) \text{III} \\
 & -ig^4s \left(\frac{g^2 lns}{2\pi}\right)^2 \lambda^2 \textcircled{\circ} \text{II}
 \end{aligned}$$



$$\begin{aligned}
 & \frac{1}{3} g^6s \left(\frac{g^2 lns}{2\pi}\right) \left(\textcircled{\circ} + \frac{1}{2} \lambda^2 \textcircled{\circ}\right) \left(\text{III} + \text{III} + \text{III}\right) \\
 & - \frac{1}{2} g^6s \left(\frac{g^2 lns}{2\pi}\right) \lambda^2 \textcircled{\circ} \text{III} \\
 & + ig^4s \left(\frac{g^2 lns}{2\pi}\right)^2 \textcircled{\circ} \left(\text{II} - 2 \text{III} + \text{III}\right)
 \end{aligned}$$



$$\begin{aligned}
 & -\frac{1}{12} ig^8s \textcircled{\circ} \text{III} \\
 & -\frac{2}{3} g^6s \left(\frac{g^2 lns}{2\pi}\right) \textcircled{\circ} \left(\text{III} + \text{III} + \text{III}\right) \\
 & + g^6s \left(\frac{g^2 lns}{2\pi}\right) \textcircled{\circ} \text{III} \\
 & ig^4s \left(\frac{g^2 lns}{2\pi}\right)^2 \textcircled{\circ} \left(\text{III} - 2 \text{III} + \text{II}\right)
 \end{aligned}$$

Table VIII

The amplitudes in the right-hand column come from the prototype Feynman diagram and all others related to it by up-down inversion, by replacing a vector-meson by a scalar or by a four-vertex, or by any combination of these processes.

V. The Calculation from Exponentiation

The high-energy scattering amplitude \mathcal{M} , calculated through the eighth order in the previous section, is the sum of infinitely many terms coming from infinitely many Feynman diagrams. We believe that this summation can be performed and the result expressed in closed form; that is, \mathcal{M} can be simply expressed in terms of the operator exponential formula

$$(2\pi)^4 \delta^{(4)}(P_i - P_f) \mathcal{M} = i \sqrt{\frac{\pi}{n}} \left(1 - e^{iV} \right) \quad (5.1)$$

where V is given by (1.7). (For the elastic scattering of bosons, $\sqrt{\frac{\pi}{n}} = 5$.) To demonstrate that this is so, we will expand (5.1) as a power series in g and show that it agrees term by term (through the eighth order) with the Feynman diagram calculation.

As an illustration of the techniques involved we will calculate the $(gT)^6 (g^2 \ln s)$ term from (5.1). Because there is a factor of T^2 from each V , only the $\frac{(iV)^3}{3!}$ term from the power series expansion of e^{iV} contributes. Besides the g^6 factor associated with the T^6 factor there is an extra g^2 factor which can come either from the Reggeization of one of the exchanged vector-mesons or from the creation and subsequent annihilation of a W -meson or Z -scalar.

Suppose first that one of the exchanged mesons Reggeizes; the isospin factor for this process is III , and the space-time amplitude is (see Fig. 36)

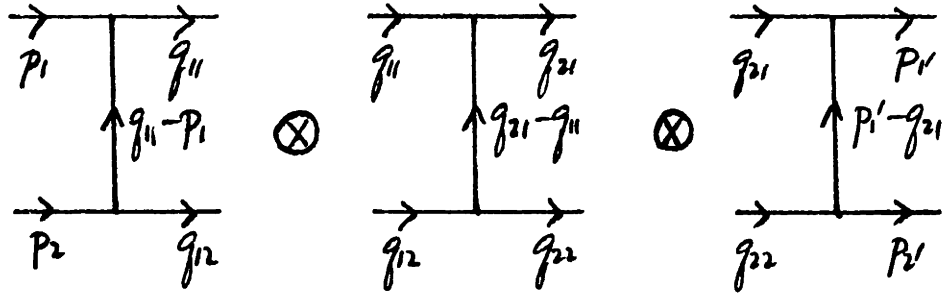


Fig. 36

$$\begin{aligned}
 & -iS \frac{i^3}{3!} \int \frac{d^3 \vec{q}_{11}}{(2\pi)^3} \frac{d^3 \vec{q}_{12}}{(2\pi)^3} \frac{d^3 \vec{q}_{21}}{(2\pi)^3} \frac{d^3 \vec{q}_{22}}{(2\pi)^3} \langle \vec{p}'_1, \vec{p}'_2 | V | \vec{q}_{21}, \vec{q}_{22} \rangle \\
 & \quad \times \langle \vec{q}_{21}, \vec{q}_{22} | V | \vec{q}_{11}, \vec{q}_{12} \rangle \langle \vec{q}_{11}, \vec{q}_{12} | V | \vec{p}_1, \vec{p}_2 \rangle \\
 & = - \frac{S}{3!} \int \frac{d^3 \vec{q}_{11}}{(2\pi)^3} \frac{d^3 \vec{q}_{12}}{(2\pi)^3} \frac{d^3 \vec{q}_{21}}{(2\pi)^3} \frac{d^3 \vec{q}_{22}}{(2\pi)^3} (2\pi)^4 \delta^{(4)}(p'_1 + p'_2 - q_{21} - q_{22}) \\
 & \quad \times \frac{2g^2}{(\vec{p}'_1 - \vec{q}_{21})^2 + \lambda^2} \left(1 - \alpha(\vec{p}'_1 - \vec{q}_{21}) \ln s + \dots \right) \\
 & \quad \times (2\pi)^4 \delta^{(4)}(q_{21} + q_{22} - q_{11} - q_{12}) \frac{2g^2}{(\vec{q}_{21} - \vec{q}_{11})^2 + \lambda^2} \left(1 - \alpha(\vec{q}_{21} - \vec{q}_{11}) \ln s + \dots \right) \\
 & \quad \times (2\pi)^4 \delta^{(4)}(q_{11} + q_{12} - p_1 - p_2) \frac{2g^2}{(\vec{q}_{11} - \vec{p}_1)^2 + \lambda^2} \left(1 - \alpha(\vec{q}_{11} - \vec{p}_1) \ln s + \dots \right) \\
 & \sim - \frac{S}{3!} (2\pi)^4 \delta^{(4)}(p_1 + p_2 - p'_1 - p'_2) (2g^2)^3 \frac{1}{2^2} \int \frac{d^2 \vec{q}_{1\perp}}{(2\pi)^2} \frac{d^2 \vec{q}_{2\perp}}{(2\pi)^2} \\
 & \quad \frac{1}{[(\vec{p}'_1 - \vec{q}_{21})^2 + \lambda^2][(\vec{q}_{21} - \vec{q}_{11})^2 + \lambda^2][(\vec{q}_{11} - \vec{p}_1)^2 + \lambda^2]} \left(1 - (\alpha(\vec{p}'_1 - \vec{q}_{21}) + \alpha(\vec{q}_{21} - \vec{q}_{11}) \right. \\
 & \quad \left. + \alpha(\vec{q}_{11} - \vec{p}_1)) \ln s + \dots \right)
 \end{aligned}$$

where we have used

$$\int dq_3 \delta\left(\sqrt{\vec{p}_1^2 + \lambda^2} + \sqrt{\vec{p}_2^2 + \lambda^2} - \sqrt{\vec{q}_3^2 + \vec{q}_1^2 + \lambda^2} - \sqrt{(\vec{p}_1 + \vec{p}_2 - \vec{q})^2 + \lambda^2}\right) \sim \frac{1}{2} \quad (5.3)$$

Keeping only the g^8 terms in (5.2), we get, with $\Delta = p_1 - p_1'$,

$$\begin{aligned} & \frac{3s}{3!} (2\pi)^4 \delta^{(4)}(p_1 + p_2 - p_1' - p_2') (2g^2)^3 \frac{1}{2^2} \frac{g^2 \ln s}{2\pi} \int \frac{d^2 \vec{k}_{14}}{(2\pi)^2} \frac{d^2 \vec{k}_{24}}{(2\pi)^2} \\ & \frac{1}{(\vec{k}_{14}^2 + \lambda^2)(\vec{k}_{24}^2 + \lambda^2)((\vec{\Delta}_1 - \vec{k}_{14} - \vec{k}_{24})^2 + \lambda^2)} \int \frac{d^2 \vec{k}_{34}}{(2\pi)^2} \frac{1}{(\vec{k}_{34}^2 + \lambda^2)((\vec{\Delta}_1 - \vec{k}_{14} - \vec{k}_{24} - \vec{k}_{34})^2 + \lambda^2)} \\ & = (2\pi)^4 \delta^{(4)}(p_1 + p_2 - p_1' - p_2') g^6 s \left(\frac{g^2 \ln s}{2\pi}\right) \textcircled{0} \quad (5.4) \end{aligned}$$

Notice that we started with a three-Reggion exchange term (i.e. V^3) and generated a four-meson exchange term by expanding the Reggeized vector-meson propagator. This series expansion

$$\frac{S^{-\alpha(\Delta_1)}}{\Delta_1^2 + \lambda^2} = \frac{1}{\Delta_1^2 + \lambda^2} - \frac{g^2 \ln s}{2\pi} \int \frac{d^2 \vec{q}_1}{(2\pi)^2} \frac{1}{(\vec{q}_1^2 + \lambda^2)((\vec{\Delta}_1 - \vec{q}_1)^2 + \lambda^2)} + \dots \quad (5.5)$$

may be expressed diagrammatically in terms of transverse-momentum diagrams, as shown in Fig. 37(a). The elastic part of the three-Reggion exchange can then be represented as an infinite sum of transverse-momentum diagrams as shown in Fig. 37(b).

$$\text{Diagram (a)} = \int \left[- \frac{g^2 \ln s}{2\pi} \text{Diagram 1} + \frac{1}{2!} \left(\frac{g^2 \ln s}{2\pi} \right)^2 \text{Diagram 2} - \frac{1}{3!} \left(\frac{g^2 \ln s}{2\pi} \right)^3 \text{Diagram 3} + \dots \right]$$

(a)

$$\text{Diagram (b)} = \text{Diagram 1} - 3 \frac{g^2 \ln s}{2\pi} \text{Diagram 2} + 3 \left(\frac{g^2 \ln s}{2\pi} \right)^2 \text{Diagram 3}$$

$$+ \frac{3}{2} \left(\frac{g^2 \ln s}{2\pi} \right)^2 \text{Diagram 4} - \frac{1}{2} \left(\frac{g^2 \ln s}{2\pi} \right)^3 \text{Diagram 5} + \dots$$

(b)

Fig. 37

Suppose now that a vector-meson or scalar is created and then annihilated. There are three ways this can happen, as illustrated in Fig. 38. The amplitude for the process shown in Fig. 38(a) is

$$-i s \frac{i^3}{3!} \sum_{spin} \int \frac{d^3 \vec{q}_1}{(2\pi)^3} \frac{d^3 k}{(2\pi)^3} \frac{d^3 \vec{q}_2}{(2\pi)^3} \frac{d^3 \vec{q}_3}{(2\pi)^3} \frac{d^3 \vec{q}_4}{(2\pi)^3}$$

$$\times \langle \vec{p}_1, \vec{p}_2 | V | \vec{q}_1, \vec{q}_2 \rangle \langle \vec{q}_1, \vec{q}_2 | V | \vec{q}_3, \vec{q}_4, \vec{k} \rangle \langle \vec{q}_3, \vec{q}_4, \vec{k} | V | \vec{p}_1, \vec{p}_2 \rangle$$

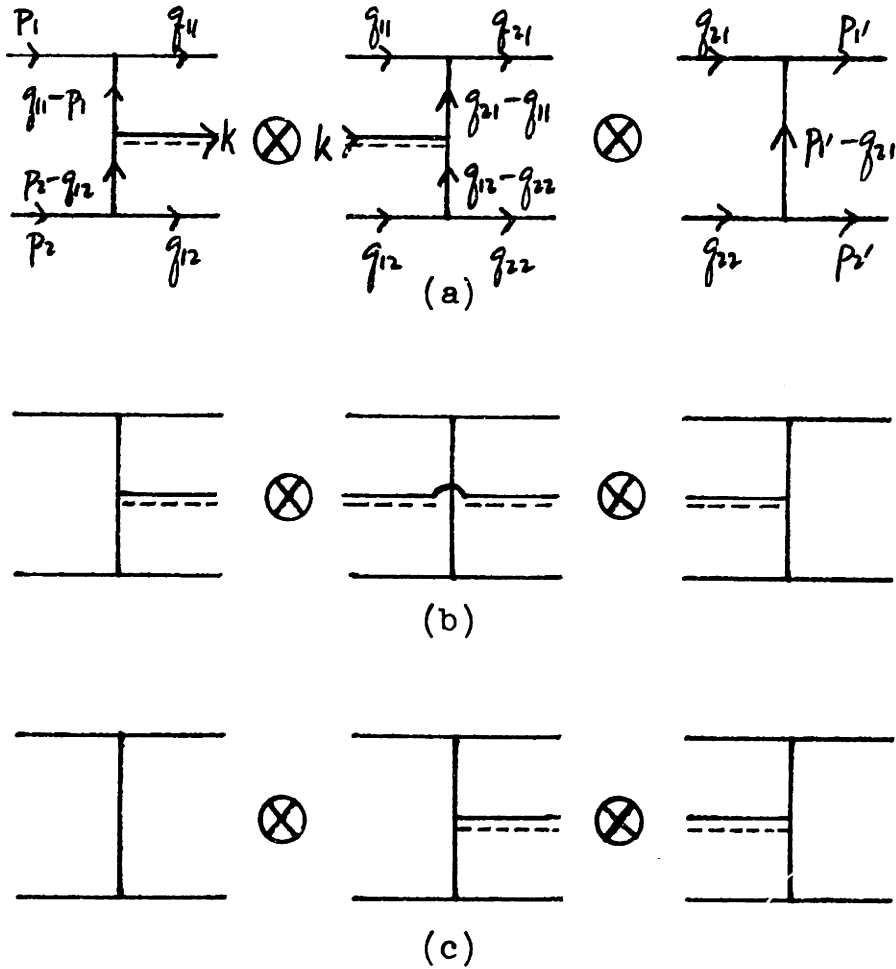


Fig. 38

The double line stands for either a vector-meson or a scalar.

$$\begin{aligned}
 &= -\frac{5}{3!} (2\pi)^4 \delta^{(4)}(p_1 + p_2 - p_1' - p_2') \frac{1}{2^2} \int \frac{d^3 \vec{q}_{11}}{(2\pi)^2} \frac{d^3 \vec{q}_{21}}{(2\pi)^2} \frac{d^3 \vec{k}_1}{(2\pi)^2} \int_{-\omega}^{\omega} \frac{dk_3}{2\pi} \left(\frac{2g^3}{\sqrt{2E}} \right)^2 2g^2 \\
 &\times \frac{1}{\left((\vec{p}_{12} - \vec{q}_{11})^2 + \lambda^2 \right) \left((\vec{q}_{12} - \vec{p}_{21})^2 + \lambda^2 \right) \left((\vec{q}_{11} - \vec{q}_{21})^2 + \lambda^2 \right) \left((\vec{q}_{21} - \vec{q}_{12})^2 + \lambda^2 \right) \left((\vec{p}'_{12} - \vec{q}_{11})^2 + \lambda^2 \right)} \\
 &\times \left(\sum_{i=1}^3 \Gamma(q_{11} - p_1, p_2 - q_{12}) \cdot \varepsilon^i(k) \Gamma(q_{21} - q_{11}, q_{12} - q_{22}) \cdot \varepsilon^i(k) \text{II} + \lambda^2 \text{III} \right) \quad (5.6)
 \end{aligned}$$

where $E = \sqrt{k_3^2 + \vec{k}_\perp^2 + \lambda^2}$, where the sum in i ($i=1,2,3$) is over the three independent polarization vectors $\epsilon^i(k)$, and where only the g^8 term has been kept (so that $s_i^{-\alpha}(\vec{\Delta}_{i\perp})$ has been set equal to unity).

We make an aside to calculate the product of the vertex factors for the W-mesons (see Fig. 39),

$$\begin{aligned} \sum_{i=1}^3 \Gamma_i(\Delta_1, \Delta_2) \cdot \epsilon^i(k) \Gamma_2(\Delta'_1, \Delta'_2) \cdot \epsilon^i(k) &= \sum_{i=1}^3 \Gamma_{1\mu} \Gamma_{2\nu} \epsilon_\mu^i \epsilon_\nu^i \\ &= \Gamma_{1\mu} \Gamma_{2\nu} \left(-g_{\mu\nu} + \frac{k_\mu k_\nu}{\lambda^2} \right) = -\Gamma_1 \cdot \Gamma_2 = -\frac{1}{2} \Gamma_{1+} \Gamma_{2-} - \frac{1}{2} \Gamma_{1-} \Gamma_{2+} + \vec{\Gamma}_{1\perp} \cdot \vec{\Gamma}_{2\perp} \end{aligned} \quad (5.7)$$

where we have used the gauge invariant property of the vertex function, $\Gamma \cdot k = 0$. This equals

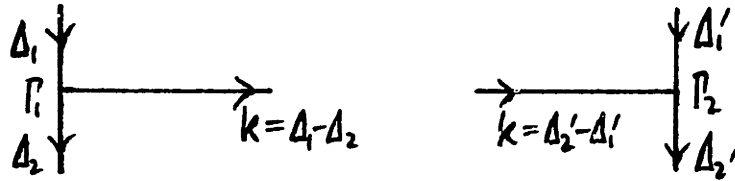


Fig. 39

$$\begin{aligned} & -\frac{1}{2} (2k_+) \left(\frac{1}{2} - \frac{\vec{\Delta}_{1\perp}^2 + \lambda^2}{k_1^2 + \lambda^2} \right) (-2k_-) \left(\frac{1}{2} - \frac{\vec{\Delta}'_{2\perp}^2 + \lambda^2}{k_1^2 + \lambda^2} \right) \\ & -\frac{1}{2} (-2k_-) \left(\frac{1}{2} - \frac{\vec{\Delta}'_{2\perp}^2 + \lambda^2}{k_1^2 + \lambda^2} \right) (2k_+) \left(\frac{1}{2} - \frac{\vec{\Delta}_{1\perp}^2 + \lambda^2}{k_1^2 + \lambda^2} \right) - (\vec{\Delta}_1 + \vec{\Delta}_{2\perp}) \cdot (\vec{\Delta}'_1 + \vec{\Delta}'_{2\perp}) \\ & = 2(k_1^2 + \lambda^2) \left[\left(\frac{1}{2} - \frac{\vec{\Delta}_{1\perp}^2 + \lambda^2}{k_1^2 + \lambda^2} \right) \left(\frac{1}{2} - \frac{\vec{\Delta}'_{2\perp}^2 + \lambda^2}{k_1^2 + \lambda^2} \right) + \left(\frac{1}{2} - \frac{\vec{\Delta}'_{1\perp}^2 + \lambda^2}{k_1^2 + \lambda^2} \right) \left(\frac{1}{2} - \frac{\vec{\Delta}_{2\perp}^2 + \lambda^2}{k_1^2 + \lambda^2} \right) \right] \\ & + (\vec{\Delta}'_1^2 + \lambda^2) + (\vec{\Delta}'_{2\perp}^2 + \lambda^2) + (\vec{\Delta}_1^2 + \lambda^2) + (\vec{\Delta}_{2\perp}^2 + \lambda^2) - (k_1^2 + \lambda^2) - 2((\vec{\Delta}_1 + \vec{\Delta}_{2\perp})^2 + \lambda^2) - \lambda^2 \end{aligned}$$

$$= 2 \frac{(\vec{\Delta}_{1\perp}^2 + \lambda^2)(\vec{\Delta}_{2\perp}'^2 + \lambda^2) + (\vec{\Delta}_{1\perp}'^2 + \lambda^2)(\vec{\Delta}_{2\perp}^2 + \lambda^2)}{\vec{k}_{\perp}^2 + \lambda^2} - 2 \left[(\vec{\Delta}_{1\perp} + \vec{\Delta}_{1\perp}')^2 + \lambda^2 \right] - \lambda^2 \quad (5.8)$$

The only dependence on the longitudinal momentum k_3 in (5.6) is therefore through E , and

$$\int_{-w}^w \frac{dk_3}{2\pi} \frac{1}{2E} \sim \int_{\frac{1}{2w}}^{2w} \frac{dk_-}{2\pi} \frac{1}{2k_-} = \frac{1}{2} \frac{\ln s}{2\pi} \quad (5.9)$$

Therefore, the amplitude in (5.6) becomes, with $\Delta = p_1 - p_1'$,

$$\begin{aligned} & - \frac{5}{3!} (2\pi)^4 \delta^{(4)}(p_1 + p_2 - p_1' - p_2') \frac{2^3 g^8}{2^2} \frac{\ln s}{2(2\pi)} \int \prod_{i=1}^3 \frac{d^2 \vec{k}_{i\perp}}{(2\pi)^2} \frac{1}{(\vec{k}_{i\perp}^2 + \lambda^2)} \\ & \times \frac{1}{\left((\vec{k}_{2\perp} - \vec{k}_{1\perp})^2 + \lambda^2 \right) \left(\vec{k}_{3\perp}^2 + \lambda^2 \right) \left((\vec{k}_{2\perp} - \vec{k}_{3\perp})^2 + \lambda^2 \right) \left((\vec{\Delta}_{\perp} - \vec{k}_{2\perp})^2 + \lambda^2 \right)} \\ & \times \left\{ \left(2 \frac{(\vec{k}_{1\perp}^2 + \lambda^2) \left((\vec{k}_{2\perp} - \vec{k}_{3\perp})^2 + \lambda^2 \right) + \left((\vec{k}_{2\perp} - \vec{k}_{1\perp})^2 + \lambda^2 \right) \left(\vec{k}_{3\perp}^2 + \lambda^2 \right)}{(\vec{k}_{1\perp} - \vec{k}_{3\perp})^2 + \lambda^2} \right. \right. \\ & \quad \left. \left. - 2 (\vec{k}_{2\perp}^2 + \lambda^2) - \lambda^2 \right) \text{II} + \lambda^2 \text{III} \right\} \\ & = (2\pi)^4 \delta^{(4)}(p_1 + p_2 - p_1' - p_2') \frac{1}{6} g^6 s \frac{g^2 \ln s}{2\pi} \left\{ \left(2 \text{I} + 2 \text{II} \right. \right. \\ & \quad \left. \left. - 2 \text{III} - \lambda^2 \text{IV} \right) \text{II} + \lambda^2 \text{V} \text{III} \right\}. \quad (5.10) \end{aligned}$$

The amplitudes for the processes shown in Fig. 38(b,c) are also given by (5.10), with the isospin factors appropriately adjusted.

Eqn. (5.8) which represents the product of two vertex functions can formally be represented in terms of transverse-momentum diagrams as illustrated in Fig. 40. In that figure, slashes on a line mean that the corresponding propagator is absent and the two vertices at either end of the line are to be fused together into one. An example is given in Fig. 41.

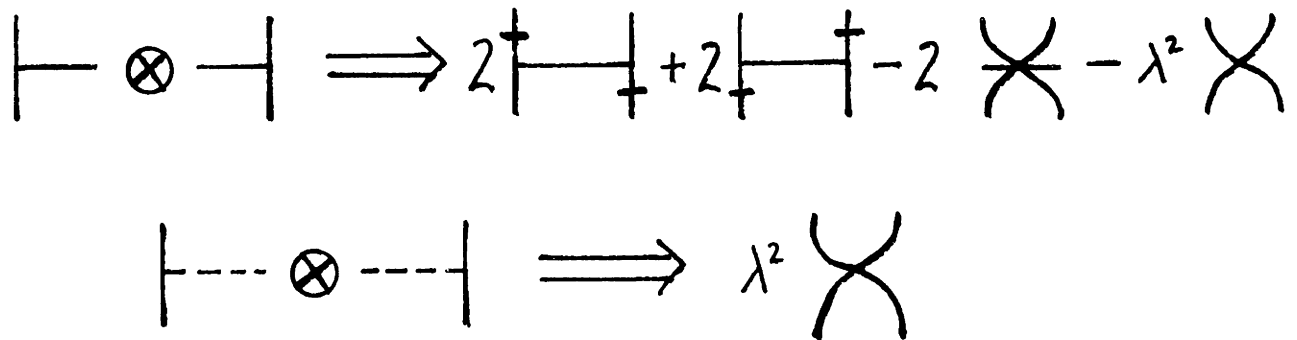


Fig. 40

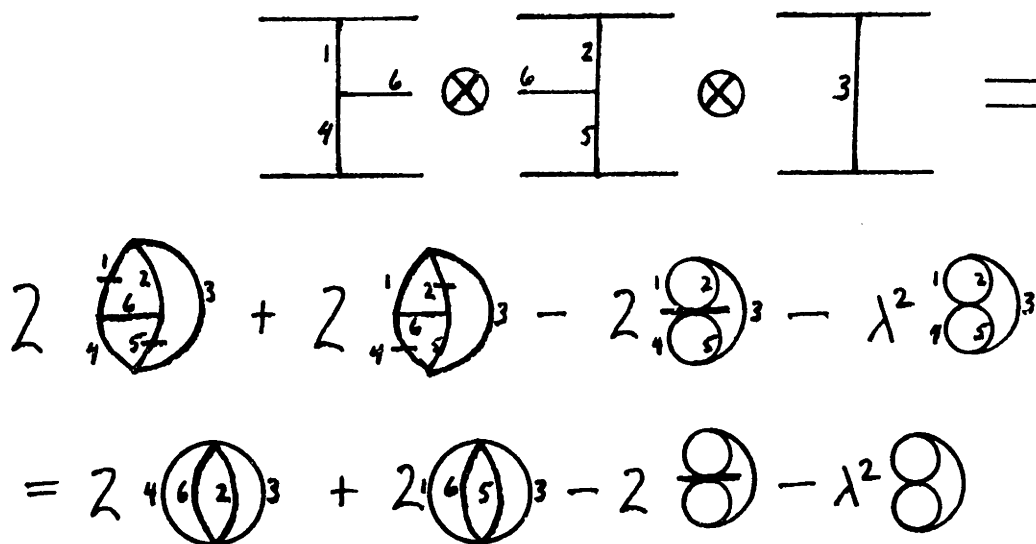


Fig. 41

From the above example, it should be clear that the following rules apply when calculating the terms proportional to T^{2n} in (5.1) via exponentiation:

i) There is an overall delta function which expresses energy-momentum conservation: $(2\pi)^4 \delta^{(4)}(P_i - P_f)$;

ii) There is an overall factor of $\frac{i^{n-1}}{n!}$;

iii) There is a single factor of $\sqrt{\prod_m f_m}$ from (5.1) and n factors of $\frac{1}{\sqrt{\prod_m f_m}}$ from (1.7), where the products

are over the incoming and outgoing particles in the appropriate initial, final or intermediate states;

there is a factor of $2s$ from each of the n potentials;

and there is a factor of $1/2$ from each of the $n-1$

integrations over the delta functions in the energies

(see eqn. (5.3)). The net result is a factor of

$2s \frac{1}{\prod_i (2E_i)}$ where the product is over all intermediate

state particles which are created and then destroyed;

iv) These energy factors are integrated over the

longitudinal momenta to give a factor of

$$g^2 \int_{-\omega}^{\omega} \frac{dk_3}{2\pi} \frac{1}{2E} \sim g^2 \int_{\frac{1}{2\omega}}^{2\omega} \frac{dk_-}{(2\pi)(2k_-)} = \frac{1}{2} \left(\frac{g^2 \ln s}{2\pi} \right).$$

(If the $-$ momenta are ordered there will be additional

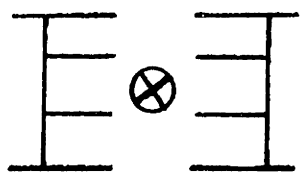
factors, as the $\frac{1}{2!}$ in

$$g^2 \int_{\frac{1}{2\omega}}^{2\omega} \frac{dk_{1-}}{2\pi} \frac{1}{2k_{1-}} g^2 \int_{\frac{1}{2\omega}}^{k_{1-}} \frac{dk_{2-}}{2\pi} \frac{1}{2k_{2-}} = \frac{1}{2!} \left(\frac{g^2 \ln s}{2(2\pi)} \right)^2 ;$$

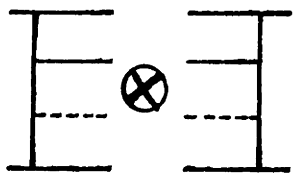
- v) There is a factor of $\frac{1}{\vec{k}_\perp^2 + \lambda^2}$ for each of the exchanged mesons in a potential V , and an integration $\int \frac{d^2\vec{k}_\perp}{(2\pi)^2}$ over the transverse-momenta of each closed loop;
- vi) From the Reggeization of a vector-meson there are factors of $-\frac{g^2 \ln s}{2\pi}$ times the appropriate transverse-momentum integration (see Fig. 37);
- vii) The squares of the vertex factors are given in Fig. 40.

The results of the calculation from exponentiation through the eighth order are given in Table IX. They agree with the results of the Feynman diagram calculation as claimed.

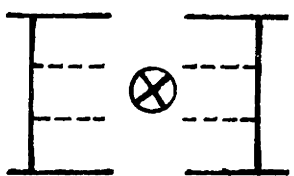
Potential	Scattering Amplitude M
	$2g^2s \frac{1}{\Delta_1^2 + \lambda^2} \text{I}$
	$-2g^2s \frac{g^2bms}{\mathcal{J}2\pi} \text{I}$
	$g^2s \left(\frac{g^2bms}{\mathcal{J}2\pi}\right)^2 \text{II}$
	$-\frac{1}{3}g^2s \left(\frac{g^2bms}{\mathcal{J}2\pi}\right)^3 \text{II}$
	$ig^4s \text{II}$
	$-2ig^4s \frac{g^2bms}{\mathcal{J}2\pi} \text{II}$
	$ig^4s \left(\frac{g^2bms}{\mathcal{J}2\pi}\right)^2 \text{II}$
	$ig^4s \left(\frac{g^2bms}{\mathcal{J}2\pi}\right)^2 \text{II}$
	$-ig^4s \frac{g^2bms}{\mathcal{J}2\pi} \left(\text{II} + \frac{1}{2}\lambda^2 \text{II} - 2\text{II}\right) \text{III}$
	$\frac{1}{2}ig^4s \frac{g^2bms}{\mathcal{J}2\pi} \lambda^2 \text{II}$
	$ig^4s \left(\frac{g^2bms}{\mathcal{J}2\pi}\right)^2 \left(2\text{II} + \lambda^2 \text{II} - 2\text{II} - 2\text{II}\right) \text{III}$
	$-ig^4s \left(\frac{g^2bms}{\mathcal{J}2\pi}\right)^2 \lambda^2 \text{II}$



$$ig^4s \left(\frac{g^2bns}{2\pi}\right)^2 \left(\frac{1}{2} \text{⊗} + \frac{1}{2} \lambda^2 \text{⊗} + \frac{1}{8} \lambda^4 \text{⊗} \right. \\ \left. - 2 \text{⊗} - \lambda^2 \text{⊗} + \text{⊗} + \text{⊗} \right) \text{H}$$



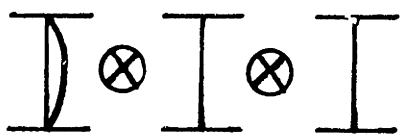
$$-\frac{1}{4} ig^4s \left(\frac{g^2bns}{2\pi}\right)^2 \left(2\lambda^2 \text{⊗} - 4\lambda^2 \text{⊗} + \lambda^4 \text{⊗} \right) \text{H}$$



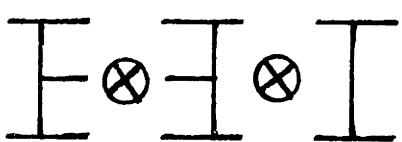
$$\frac{1}{8} ig^4s \left(\frac{g^2bns}{2\pi}\right)^2 \lambda^4 \text{⊗} \text{II}$$



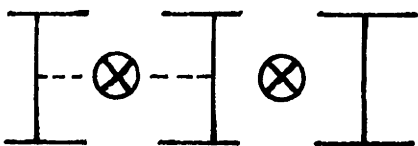
$$-\frac{1}{3} g^6s \text{⊗} \text{III}$$



$$g^6s \frac{g^2bns}{2\pi} \text{⊗} \text{III}$$



$$-\frac{1}{6} g^6s \frac{g^2bns}{2\pi} \left(4 \text{⊗} - 2 \text{⊗} - \lambda^2 \text{⊗} \right) \\ \times \left(\text{H} + \text{H} + \text{H} \right)$$



$$-\frac{1}{2} g^6s \frac{g^2bns}{2\pi} \lambda^2 \text{⊗} \text{III}$$



$$-\frac{1}{12} ig^8s \text{⊗} \text{IIII}$$

Table IX

Reggeization in the potential is indicated by multiple lines.

VI. The Eikonal Form in Impact-Distance Space

The potential V as given by (1.7) and (1.8) - (1.12) may be written

$$\begin{aligned}
 V = & (2\pi)^4 \delta^{(4)}(P_i - P_f) \left(-T_i^{(1)} T_j^{(2)} \right) \left\{ \int \frac{d^3 \vec{\Delta}_\perp}{(2\pi)^2} \frac{2g^2}{\Delta_\perp^2 + \lambda^2} S^{-\alpha(\vec{\Delta}_\perp)} \delta_{ij} A(\vec{\Delta}_\perp) \right. \\
 & + \int \frac{d^2 \vec{\Delta}_{1\perp}}{(2\pi)^2} \frac{d^2 \vec{\Delta}_{2\perp}}{(2\pi)^2} \frac{d^3 k}{(2\pi)^3} \frac{1}{\sqrt{2E}} (2\pi)^2 \delta^{(2)}(\vec{\Delta}_{1\perp} - \vec{k}_\perp - \vec{\Delta}_{2\perp}) \frac{2g^3}{(\Delta_{1\perp}^2 + \lambda^2)(\Delta_{2\perp}^2 + \lambda^2)} S_1^{-\alpha(\vec{\Delta}_{1\perp})} S_2^{-\alpha(\vec{\Delta}_{2\perp})} \\
 & \times \left(\sum_{\alpha=1}^3 \left[\vec{\Sigma}_\perp^\alpha \cdot (\vec{\Delta}_{1\perp} + \vec{\Delta}_{2\perp}) - \Sigma_+^\alpha k_- \left(\frac{1}{2} - \frac{\Delta_{2\perp}^2 + \lambda^2}{k_\perp^2 + \lambda^2} \right) + \Sigma_-^\alpha k_+ \left(\frac{1}{2} - \frac{\Delta_{1\perp}^2 + \lambda^2}{k_\perp^2 + \lambda^2} \right) \right] \sum_{\ell=1}^3 a_{\alpha\ell}^+(\vec{k}) i \varepsilon_{ij\ell} \right. \\
 & \quad \left. - \lambda b^+(\vec{k}) \delta_{ij} \right) A(\vec{\Delta}_\perp) \\
 & + \int \frac{d^2 \vec{\Delta}_{1\perp}}{(2\pi)^2} \frac{d^2 \vec{\Delta}_{2\perp}}{(2\pi)^2} \frac{d^3 k}{(2\pi)^3} \frac{1}{\sqrt{2E}} (2\pi)^2 \delta^{(2)}(\vec{\Delta}_{1\perp} + \vec{k}_\perp - \vec{\Delta}_{2\perp}) \frac{2g^3}{(\Delta_{1\perp}^2 + \lambda^2)(\Delta_{2\perp}^2 + \lambda^2)} S_1^{-\alpha(\vec{\Delta}_{1\perp})} S_2^{-\alpha(\vec{\Delta}_{2\perp})} \\
 & \times \left(\sum_{\alpha=1}^3 \left[-\vec{\Sigma}_\perp^\alpha \cdot (\vec{\Delta}_{1\perp} + \vec{\Delta}_{2\perp}) - \Sigma_+^\alpha k_- \left(\frac{1}{2} - \frac{\Delta_{2\perp}^2 + \lambda^2}{k_\perp^2 + \lambda^2} \right) + \Sigma_-^\alpha k_+ \left(\frac{1}{2} - \frac{\Delta_{1\perp}^2 + \lambda^2}{k_\perp^2 + \lambda^2} \right) \right] \sum_{\ell=1}^3 a_{\alpha\ell}(\vec{k}) i \varepsilon_{ij\ell} \right. \\
 & \quad \left. - \lambda b(\vec{k}) \delta_{ij} \right) A(\vec{\Delta}_\perp) + \dots \left. \right\} \quad (6.1)
 \end{aligned}$$

In (6.1) $E = k_0 = \sqrt{\vec{k}^2 + \lambda^2}$ is the energy of the created or

destroyed particle; $A(\vec{\Delta}_{1\perp})$ is an operator which changes the transverse momentum of the large + momentum particle by the amount $\vec{\Delta}_{1\perp}$:

$$A(\vec{\Delta}_{1\perp}) |\vec{\Delta}_1\rangle = |\vec{\Delta}_1 + \vec{\Delta}_{1\perp}\rangle; \quad (6.2)$$

$a_{\alpha l}^\dagger(\vec{k})$ ($a_{\alpha l}(\vec{k})$) creates (destroys) a vector-meson with momentum \vec{k} , polarization α and isospin l

$$a_{\alpha l}^\dagger(\vec{k}) |0\rangle = |\vec{k}, \alpha, l\rangle, \quad (6.3a)$$

$$a_{\alpha l}(\vec{k}) |0\rangle = 0; \quad (6.3b)$$

and $b^\dagger(\vec{k})$ ($b(\vec{k})$) creates (destroys) a scalar Z with momentum \vec{k}

$$b^\dagger(\vec{k}) |0\rangle = |\vec{k}\rangle, \quad (6.4a)$$

$$b(\vec{k}) |0\rangle = 0. \quad (6.4b)$$

$|0\rangle$ is the state with no intermediate energy particles (i.e. only extremely energetic particles) and the states are normalized so that

$$\langle \vec{\Delta}_1 | \vec{\Delta}_1' \rangle = (2\pi)^2 \delta^{(2)}(\vec{\Delta}_1 - \vec{\Delta}_1'), \quad (6.5)$$

$$\langle \vec{k}, \alpha, l | \vec{k}', \alpha', l' \rangle = \delta_{\alpha\alpha'} \delta_{ll'} (2\pi)^3 \delta^{(3)}(\vec{k} - \vec{k}'), \quad (6.6)$$

etc.

If we define $U(\vec{b}_L, s)$ by

$$\begin{aligned} & \langle \vec{p}'_1, \vec{p}'_2, \vec{k}'_1, \dots, \vec{k}'_n \mid V \mid \vec{p}_1, \vec{p}_2, \vec{k}_1, \dots, \vec{k}_m \rangle \\ &= (2\pi)^4 \delta^{(4)}(P_i - P_f) 2 \int d^2 \vec{b}_L e^{i \vec{\Delta}_L \cdot \vec{b}_L} \langle \vec{k}'_1, \dots, \vec{k}'_n \mid U(\vec{b}_L, s) \mid \vec{k}_1, \dots, \vec{k}_m \rangle \end{aligned} \quad (6.7)$$

where $\vec{\Delta}_L = \vec{p}_{1\perp} - \vec{p}_{1'\perp}$, then

$$\begin{aligned} U(\vec{b}_L, s) = & \int \frac{d^2 \vec{\Delta}_{1\perp}}{(2\pi)^2} e^{-i \vec{\Delta}_{1\perp} \cdot \vec{b}_L} \left(-T_i^{(1)} T_j^{(2)} \right) \left\{ g^2 \frac{\ell^{-\tau_0} \alpha(\vec{\Delta}_{1\perp})}{\vec{\Delta}_{1\perp}^2 + \lambda^2} \delta_{ij} \right. \\ & + g^3 \int \frac{d^2 \vec{\Delta}_{2\perp}}{(2\pi)^2} \frac{d^2 \vec{k}_\perp}{(2\pi)^2} (2\pi)^2 \delta^{(2)}(\vec{\Delta}_{1\perp} - \vec{k}_\perp - \vec{\Delta}_{2\perp}) \int_{-\frac{1}{2}\tau_0}^{\frac{1}{2}\tau_0} \frac{d\tau}{2\pi} \frac{\ell^{-(\frac{1}{2}\tau_0 - \tau) \alpha(\vec{\Delta}_{1\perp})}}{\vec{\Delta}_{1\perp}^2 + \lambda^2} \\ & \times \frac{\ell^{-\frac{1}{2}(\tau_0 + \tau) \alpha(\vec{\Delta}_{2\perp})}}{\vec{\Delta}_{2\perp}^2 + \lambda^2} \left(\sum_{\alpha=1}^3 \left[\vec{\Sigma}_\perp^\alpha \cdot (\vec{\Delta}_{1\perp} + \vec{\Delta}_{2\perp}) - \Sigma_+^\alpha \ell^{-\tau} \sqrt{\vec{k}_\perp^2 + \lambda^2} \left(\frac{1}{2} - \frac{\vec{\Delta}_{2\perp}^2 + \lambda^2}{\vec{k}_\perp^2 + \lambda^2} \right) \right. \right. \\ & \left. \left. + \Sigma_-^\alpha \ell^{\tau} \sqrt{\vec{k}_\perp^2 + \lambda^2} \left(\frac{1}{2} - \frac{\vec{\Delta}_{1\perp}^2 + \lambda^2}{\vec{k}_\perp^2 + \lambda^2} \right) \right] \sum_{l=1}^3 \frac{(a_{\alpha l}^+(\vec{k}_\perp, \tau) - a_{\alpha l}(-\vec{k}_\perp, \tau))}{\sqrt{2}} i \varepsilon_{ijl} \right. \\ & \left. - \lambda \frac{b^+(\vec{k}_\perp, \tau) + b(-\vec{k}_\perp, \tau)}{\sqrt{2}} \delta_{ij} \right) + \dots \left. \right\} \end{aligned} \quad (6.8)$$

where

$$\tau_0 = \ln s, \quad (6.9)$$

$$\tau = \frac{1}{2} \ln \frac{k_+}{k_-}, \quad (6.10a)$$

$$k_+ = e^\tau \sqrt{\vec{k}_\perp^2 + \lambda^2}, \quad (6.10b)$$

$$k_- = e^{-\tau} \sqrt{\vec{k}_\perp^2 + \lambda^2}, \quad (6.10c)$$

and where the creation or annihilation operators $a_{\alpha\ell}^\dagger(\vec{k}_\perp, \tau)$, $a_{\alpha\ell}(\vec{k}_\perp, \tau)$, $b^\dagger(\vec{k}_\perp, \tau)$ and $b(\vec{k}_\perp, \tau)$ create or annihilate a vector-meson (polarization α , isospin ℓ) or a scalar Z with transverse momentum \vec{k}_\perp and rapidity τ . Note that

$$\int_{-W}^W \frac{dk_3}{E} \approx \int_{-\frac{1}{2}\tau_0}^{\frac{1}{2}\tau_0} d\tau, \quad (6.11)$$

$$a_{\alpha\ell}^\dagger(\vec{k}) = \frac{1}{\sqrt{E}} a_{\alpha\ell}^\dagger(\vec{k}_\perp, \tau), \quad (6.12)$$

etc., and the states are normalized so that

$$\langle \vec{k}'_\perp, \tau' | \vec{k}_\perp, \tau \rangle = (2\pi)^3 \delta^{(2)}(\vec{k}_\perp - \vec{k}'_\perp) \delta(\tau - \tau'). \quad (6.13)$$

In the higher order terms in (6.8) the rapidities of the created and annihilated particles are ordered. $U(\vec{b}_\perp, s)$ is explicitly hermitian.

From (6.7) it follows that

$$\begin{aligned} & \langle \vec{p}'_1, \vec{p}'_2, n | e^{iV} | \vec{p}_1, \vec{p}_2, m \rangle \\ &= (2\pi)^4 \delta^{(4)}(p_i - p_f) 2 \int d^2 \vec{b}_1 e^{i \vec{A}_1 \cdot \vec{b}_1} \langle n | e^{iU(\vec{b}_1, s)} | m \rangle \end{aligned} \quad (6.14)$$

and (1.1) follows easily.

VII. Conclusion

There are important differences between the eikonal forms in QED and Yang-Mills theory. In QED, the potential U may be thought of as a generalized static field (elastic and inelastic) due to the target electron, so that e^{iU} is then the amplitude for the scattering of the projectile electron from this potential. Such an interpretation is possible because the target electron remains an electron after the emission of any number of photons. In Yang-Mills theory, however, the W -meson carries isospin and its charge state changes as it interacts with the scattered meson. Thus the concept of a static field no longer applies.

In QED the potential consists of the lowest order diagrams for each process. In particular the elastic part of the potential represents the exchange of a photon and is related to the Coulomb (or Yukawa) potential between the two high-energy electrons. The counterpart of this term in the Yang-Mills potential is not the exchange of a W -meson, but rather of a Regge-pole on which the W -meson lies. Thus the potential U (see eqn. (6.8)) is a function of the energy of the projectile.

In the diagrammatic calculation in Yang-Mills theory, it is possible to identify those terms which have counterparts in QED. These are the ones in which the order of T is

correctly given by counting the number of vertices on the high-energy lines. The QED counterpart of the Yang-Mills isospin T is the charge Z of the incident electrons. In diagrammatic calculations in QED, the power of Z is always equal to the number of vertices on the high-energy electron lines. But in Yang-Mills theory the non-abelian nature of the isospin means that there are many more terms present (see Table VIII). (For example, the T^2 terms come from not only the one meson exchange diagram but from the tower diagrams as well.) Physically, these terms represent the effect, mentioned above, of the changing charge state of the target particle.

There are two major advantages of the eikonal form. First, it is explicitly unitary. Second, it is in closed form -- that is, it is not an infinite (and possibly divergent) series. For example, if we were to expand $i(1 - e^{iU})$ in a power series the result would still be unitary, but such an expansion is not useful because successive terms become larger and larger.

The major criticism of our calculational procedure is that we have ignored terms which, individually, are larger than the sum of the terms kept. From each set of diagrams we kept only the most divergent terms and dropped the non-leading terms. In order to preserve the Froissart bound there must be extensive cancellations among these non-leading terms, but we can only hope that their sum represents a small modification

of our result, at least in some energy region. Physically, the terms we have dropped account for the structure of the particles and for the interactions between pionization products.

The generalization from boson-boson scattering to fermion-boson or fermion-fermion scattering is trivial. For each fermion replacing a W-meson the space-time factor is multiplied by a factor of $\frac{1}{2m}$, where m is the fermion mass. This is because the numerator factor associated with the large + momentum line, for example, is

$$\bar{u}(p) \frac{\gamma_+}{\sqrt{2}} (\not{p}+m) \frac{\gamma_+}{\sqrt{2}} (\not{p}+m) \cdots \frac{\gamma_+}{\sqrt{2}} u(p) \sim \left(\frac{2p_+}{\sqrt{2}} \right)^{n-1} \frac{p_+}{\sqrt{2} m} \quad (7.1)$$

where n is the number of fermion-fermion-W vertices, whereas the corresponding numerator factor for W-W scattering is $\left(\frac{2p_+}{\sqrt{2}} \right)^n$.

The generalization to groups other than SU(2) is also presumably simple, since the majority of the isospin manipulations involved only the Jacobi identity.

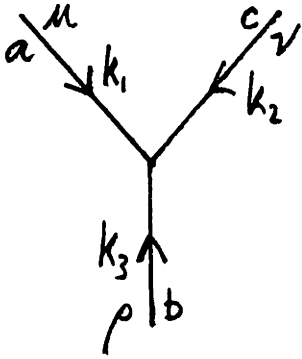
In conclusion, it is our hope that by studying the consequences of eikonalization we can get a realistic idea of the actual high-energy behavior of field theories.

Appendix I. Feynman Rules

The relevant Feynman rules¹⁰ for the SU(2) Yang-Mills theory with an isodoublet of Higgs bosons are:

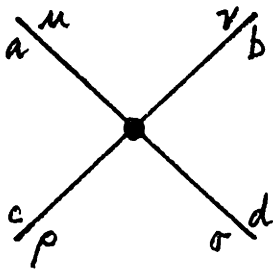
- i) an overall factor of $-i$;
- ii) a factor of $-i$ for each vertex;
- iii) $-i\delta_{ab}g_{\mu\nu}/(k^2 - \lambda^2 + i\epsilon)$ for the vector-meson propagator (here a and b are the isospin indices and μ and ν are the space-time indices);
- iv) $i/(k^2 - M^2 + i\epsilon)$ for the scalar propagator;
- v) $g(i\epsilon_{abc})((k_1 - k_2)_\rho g_{\mu\nu} + (k_2 - k_3)_\mu g_{\nu\rho} + (k_3 - k_1)_\nu g_{\rho\mu})$ for a three-vertex;
- vi) $-g^2\{(i\epsilon_{eac})(i\epsilon_{edb})(g_{\mu\sigma}g_{\rho\nu} - g_{\mu\nu}g_{\rho\sigma}) + (i\epsilon_{ead})(i\epsilon_{ecb})(g_{\mu\rho}g_{\nu\sigma} - g_{\mu\nu}g_{\rho\sigma}) + (i\epsilon_{eba})(i\epsilon_{ecd})(g_{\mu\sigma}g_{\rho\nu} - g_{\mu\rho}g_{\nu\sigma})\}$ for a four-vertex; and
- vii) $-g\lambda\delta_{ab}g_{\mu\nu}$ for a scalar-vector vertex.

The vertex factors are illustrated in Fig. 42. Note that the four-vector vertex consists of three terms, corresponding to the three ways it can be "unfused" to make two three-vector vertices.



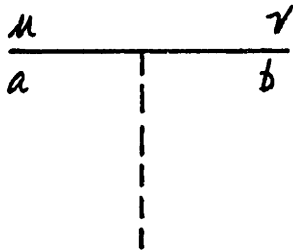
$$g (i\zeta abc) \left[(k_1 - k_2)_\rho g_{\mu\nu} + (k_2 - k_3)_\mu g_{\nu\rho} + (k_3 - k_1)_\nu g_{\rho\mu} \right]$$

(a)



$$-g^2 \left[\begin{array}{l} \text{Diagram 1: } \begin{array}{c} a \quad b \\ \diagdown \quad \diagup \\ c \quad d \end{array} (g_{\mu\sigma} g_{\rho\nu} - g_{\mu\nu} g_{\rho\sigma}) \\ + \text{Diagram 2: } \begin{array}{c} a \quad b \\ \diagup \quad \diagdown \\ c \quad d \end{array} (g_{\mu\rho} g_{\nu\sigma} - g_{\mu\nu} g_{\rho\sigma}) \\ + \text{Diagram 3: } \begin{array}{c} a \quad b \\ \diagdown \quad \diagup \\ c \quad d \end{array} (g_{\mu\sigma} g_{\rho\nu} - g_{\mu\rho} g_{\nu\sigma}) \end{array} \right]$$

(b)



$$-g\lambda \delta_{ab} g_{\mu\nu}$$

(c)

Fig. 42

(a) Three-vector vertex. (b) Four-vector vertex. (c) Scalar-vector vertex. The solid lines are vector-mesons and the dashed line is the scalar. For the four-vertex, the isospin factors are given diagrammatically.

Appendix II. On the Infinite-Momentum Space Technique
and Momentum-Flow Diagrams

When the Feynman rules are applied to calculate the amplitudes of diagrams, multiple integrals appear. The standard way to evaluate these integrals is to introduce a Feynman parameter and then take the high-energy limit ($s \rightarrow \infty$, t fixed). However, this technique becomes very cumbersome, if not impossible, for diagrams with six or more vertices. In order to evaluate higher order diagrams it is necessary to use the infinite-momentum space technique¹¹ and momentum-flow diagrams.¹² The basic idea of the infinite-momentum space technique is to make the high-energy approximations in the integrand and then evaluate the integrals over the longitudinal momenta by contour integration in the complex planes of the + or - momenta. Momentum-flow diagrams are used to keep track of which poles are enclosed by the contours. Several examples will now be given to illustrate how to use these techniques.

First we give some general high-energy approximations and notation. Let p_1 and p_2 be the four-momenta of the incoming particles and $p_1 + \Delta$, $p_2 - \Delta$ be the four-momenta of the outgoing particles. The kinematic region under consideration is

$$s \gg |\Delta^2|, \lambda^2, M^2 \quad (\text{II.1})$$

where $s = (p_1 + p_2)^2$ is the square of the center-of-mass energy

of the incoming particles, λ is the vector-meson mass and M is the scalar mass. For an arbitrary four-vector p define $p_{\pm} = p_0 \pm p_3$. Then

$$p \cdot q = \frac{1}{2} p_+ q_- + \frac{1}{2} p_- q_+ - \vec{p}_{\perp} \cdot \vec{q}_{\perp} \quad (\text{II.2a})$$

and

$$d^4 p = \frac{1}{2} dp_+ dp_- d\vec{p}_{\perp}. \quad (\text{II.2b})$$

(The metric is such that $p^2 = p_0^2 - \vec{p}^2$.) If $p = (p_+, p_-, \vec{p}_{\perp})$ then in the CM system with the momenta of the incoming particles in the z direction,

$$p_1 = \left(p_{1+}, \frac{\lambda^2}{p_{1+}}, 0 \right), \quad (\text{II.3a})$$

$$p_2 = \left(\frac{\lambda^2}{p_{2-}}, p_{2-}, 0 \right) \quad (\text{II.3b})$$

where

$$p_{1+} = p_{2-} \sim \sqrt{s}. \quad (\text{II.3c})$$

It follows that

$$2 p_1 \cdot p_2 \sim s \quad (\text{II.4a})$$

and

$$-\Delta_+ = \Delta_- \sim \frac{\lambda^2}{p_{1+}}. \quad (\text{II.4b})$$

Now consider the second order elastic amplitude. When the external particles are transversely polarized only one diagram contributes. It is shown in Fig. 43. Its amplitude is $\mathcal{M} = M \cdot I$ where M is the space-time factor and I is the isospin factor. Here we will calculate M only. From the Feynman rules (Appendix I)

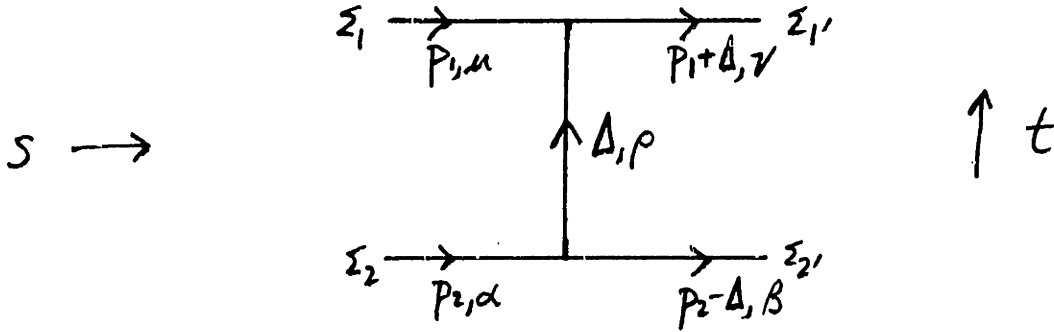


Fig. 43

$$\begin{aligned}
 M = & (-i)^{1+2+1} g^2 \Sigma_{1\mu} \Sigma_{1'\nu} \Sigma_{2\alpha} \Sigma_{2'\beta} \frac{1}{\Delta_+ \Delta_- - \vec{\Delta}_\perp^2 - \lambda^2 + i\epsilon} \\
 & \times \left((2p_1 + \Delta)_\rho g_{\mu\nu} + (-p_1 - 2\Delta)_\mu g_{\nu\rho} + (\Delta - p_1)_\nu g_{\mu\rho} \right) \\
 & \times \left((p_2 + \Delta)_\beta g_{\alpha\rho} + (p_2 - 2\Delta)_\alpha g_{\rho\beta} + (-2p_2 + \Delta)_\rho g_{\alpha\beta} \right). \quad (\text{II.5})
 \end{aligned}$$

M will turn out to be proportional to s, with a factor of \sqrt{s} coming from each vertex. Since $\epsilon_1 \cdot p_1 = \epsilon_{1'} \cdot (p_1 + \Delta) = 0$, it follows that $\epsilon_{1\mu} (-p_1 - 2\Delta)_\mu = -\epsilon_1 \cdot \Delta$ and that $\epsilon_{1'\nu} (\Delta - p_1)_\nu = 2\epsilon_{1'} \cdot \Delta$. Because neither of these last two terms is proportional to \sqrt{s} , they will be dropped. Likewise the $(p_2 + \Delta)_\beta$ and $(p_2 - 2\Delta)_\alpha$ terms from the other vertex factor do not contribute to the leading order and will be dropped. Finally, $\epsilon_1 = (0, 0, \vec{\epsilon}_{1\perp})$, etc., so that $\epsilon_1 \cdot \epsilon_{1'} = -\vec{\epsilon}_{1\perp} \cdot \vec{\epsilon}_{1'\perp}$, etc. Thus, using (II.3) and (II.4),

$$M \sim 2g^2 s \frac{1}{\Delta_{\perp}^2 + \lambda^2} (\vec{\Sigma}_{1\perp} \cdot \vec{\Sigma}_{1'\perp}) (\vec{\Sigma}_{2\perp} \cdot \vec{\Sigma}_{2'\perp}). \quad (\text{II.6})$$

(Since the polarization factors $(\vec{\epsilon}_{1\perp} \cdot \vec{\epsilon}_{1'\perp}) (\vec{\epsilon}_{2\perp} \cdot \vec{\epsilon}_{2'\perp})$ are common to all the amplitudes calculated in this paper, they will hereafter be suppressed.)

It is simpler to calculate this and all other diagrams using the $(+,-,\perp)$ notation throughout. In the product $p_{\mu} q_{\mu}$ the sum over the four space-time indices can be replaced by the sum of the three terms on the right-hand side of (II.2a). This is represented diagrammatically by notating each line of a Feynman diagram with one of the pairs $(+,-)$, $(-,+)$ or (\perp,\perp) , with one sign near each of the two endpoints of the line, as shown in Fig. 44. Each line can have any of these

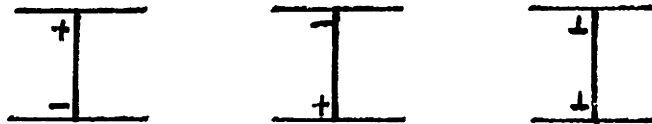


Fig. 44

three polarizations, and all possibilities for all internal lines are summed over. Each three-point vertex then has three signs associated with it, one corresponding to each line. Since a $+$ component always multiplies a $-$ component and a \perp component always multiplies a \perp component,

$$g_{++} = g_{--} = g_{\perp\perp} = g_{+\perp} = g_{\perp+} = g_{-\perp} = g_{\perp-} = 0. \quad (\text{II.7})$$

With the convention that a longitudinal (i.e. + or -) component is always multiplied by an extra factor of $\frac{1}{\sqrt{2}}$,

$$g_{+-} = g_{-+} = 1 \text{ and } g_{\perp\perp} = -1, \quad (\text{II.8})$$

so that the product of two longitudinal components will reproduce the factor of 1/2 in (II.2a) and the product of two transverse components will reproduce the factor of -1 in (II.2a). The advantage of this notation is that all lines emerging from the lines representing the extremely energetic particles are longitudinally polarized; in particular, if the line emerges from a large + (-) momentum line, then the sign on the emerging line associated with that vertex is + (-). This is equivalent to the approximation of dropping all those terms in a vertex on a high-energy line which do not give a contribution proportional to that energy. This was illustrated above in dropping the $(-p_1 - 2\Delta)_\mu$ and $(\Delta - p_1)_\nu$ terms from (II.5). Using this method, the two vertex factors in (II.5) become $\frac{2p_{1+}}{\sqrt{2}}$ and $-\frac{2p_{2-}}{\sqrt{2}}$, so that their product is approximately $-2s$, as above.

As the next example, consider the fourth order diagram in Fig. 45. (The polarization of the particles is shown.) Its space-time amplitude is

$$M \sim (-i)^{1+4+4} g^4 (-2s)^2 \frac{1}{2} \int \frac{d^4q_+}{2\pi^4} \frac{d^4q_-}{2\pi^4} \frac{d^4\vec{q}_\perp}{(2\pi)^2} \frac{1}{(p_{1+} + q_+)(p_{1-} + q_-) - \vec{q}_\perp^2 - \lambda^2 + i\epsilon}$$

$$\times \frac{1}{(p_{2+} - q_+)(p_{2-} - q_-) - (\vec{p}_{2\perp} - \vec{q}_\perp)^2 - \lambda^2 + i\epsilon} \frac{1}{(q_+ q_- - \vec{q}_\perp^2 - \lambda^2 + i\epsilon) (q_+ - \Delta_+)(q_- - \Delta_-) - (\vec{q}_\perp - \vec{d}_\perp)^2 - \lambda^2 + i\epsilon} \quad (\text{II.9})$$

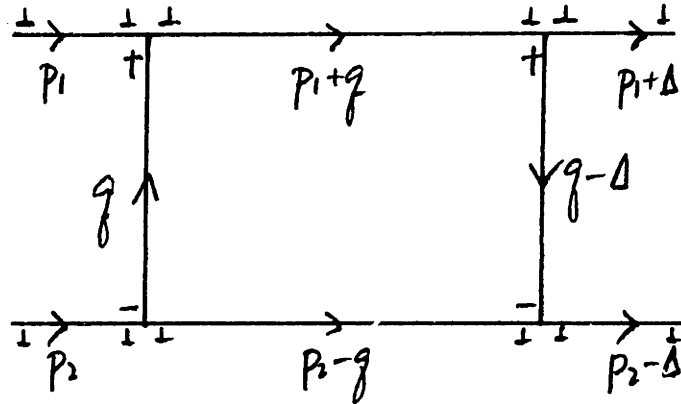


Fig. 45

(Note the factor of $1/2$ coming from (II.2b).) The numerator factors have already been approximated in the high-energy limit. The q_+ integration will be performed by contour integration. To simplify matters, set $\Delta = 0$. Then the poles in the complex q_+ plane occur at

$$q_+ = -p_{1+} + \frac{\vec{q}_+^2 + \lambda^2 - i\epsilon}{p_{1-} + q_-}, \quad (\text{II.10a})$$

$$q_+ = p_{2+} - \frac{\vec{q}_+^2 + \lambda^2 - i\epsilon}{p_{2-} - q_-}, \quad (\text{II.10b})$$

and

$$q_+ = \frac{\vec{q}_+^2 + \lambda^2 - i\epsilon}{q_-} \quad (\text{twice}). \quad (\text{II.10c})$$

If $q_- < -p_{1-}$ then all the poles are in the upper-half-plane and the contour can be closed in the lower-half-plane to give zero. Likewise, if $q_- > p_{2-}$ all the poles are in the lower-

half-plane and the contour can be closed in the upper-half-plane to give zero. A non-zero answer can occur only if either

$$-p_1 < q_- < 0 \quad (\text{II.11a})$$

or

$$0 < q_- < p_2. \quad (\text{II.11b})$$

If (II.11a) holds, the region of integration is of width $\frac{\lambda^2}{p_{1+}}$ and can be shown to be too small to contribute to the leading term. If (II.11b) holds, the contour can be closed in the upper-half-plane to enclose the pole given by (II.10b).

Then (II.9) becomes

$$M \sim -2g^4 s^2 \int \frac{d^2 \vec{q}_\perp}{(2\pi)^2} \int_0^{p_2} \frac{dq_-}{2\pi} \frac{1}{(p_2 - q_-)} \frac{1}{(p_{1+} + p_{2+} - \frac{\vec{q}_\perp^2 + \lambda^2}{p_2 - q_-})(p_1 + q_- - \vec{q}_\perp^2 - \lambda^2 + i\epsilon)}$$

$$\times \frac{1}{\left[\left(p_{2+} - \frac{\vec{q}_\perp^2 + \lambda^2}{p_2 - q_-} \right) q_- - \vec{q}_\perp^2 - \lambda^2 + i\epsilon \right]^2} \quad (\text{II.12})$$

The dominant contribution to the q_- integration comes from the region where

$$0 < q_- \ll p_2, \quad (\text{II.13})$$

so that (II.12) becomes

$$M \sim -\frac{2g^4 s^2}{p_2} \int \frac{d^2 \vec{q}_\perp}{(2\pi)^2} \frac{1}{(\vec{q}_\perp^2 + \lambda^2)^2} \int_0^{p_2} \frac{dq_-}{2\pi} \frac{1}{p_{1+}(p_1 + q_- - \vec{q}_\perp^2 - \lambda^2 + i\epsilon)}. \quad (\text{II.14})$$

The q_- integration in (II.14) is

$$\int_0^{P_2} \frac{dq_-}{2\pi} \frac{1}{P_1 + q_- - \vec{q}_\perp^2 + i\epsilon} = \frac{1}{2\pi P_1} \ln(P_1 + q_- - \vec{q}_\perp^2 + i\epsilon) \Big|_0^{P_2}$$

$$\sim \frac{1}{2\pi P_1} (\ln s - i\pi) \quad (\text{II.15})$$

where the leading real and leading imaginary terms have been kept. This answer is consistent with (II.13) because the upper limit of integration in (II.15) could be replaced by cp_2 for any c of order one and only non-leading terms would be affected. Now

$$M \sim -2g^4 s \frac{\ln s - i\pi}{2\pi} \int \frac{d^2 \vec{q}_\perp}{(2\pi)^2} \frac{1}{(\vec{q}_\perp^2 + \lambda^2)^2} \cdot \quad (\text{II.16})$$

If $\Delta \neq 0$, then the integration over the transverse momentum is replaced by K (see (2.9)).

When calculating the crossed diagram given in Fig.46,

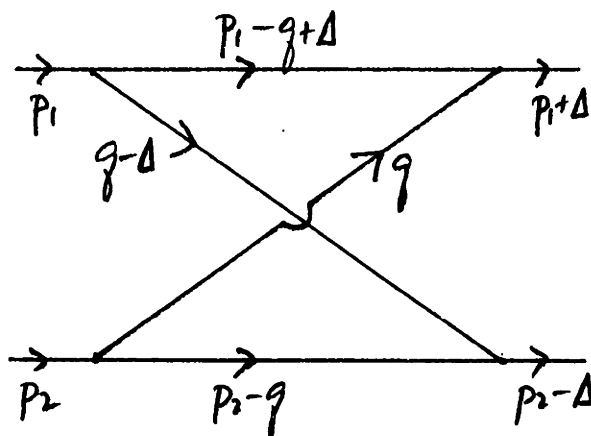


Fig. 46

the only difference is due to the propagator on the top line; and so (II.15) is replaced by

$$\int_0^{P_2^-} \frac{dq_-}{2\pi} \frac{1}{-P_+ q_- - \vec{q}_\perp^2} \sim -\frac{1}{2\pi P_+} \ln s. \quad (\text{II.17})$$

Notice that there is no imaginary amplitude, which is as it should be since there is no unitarity cut.

In order to streamline the calculation in higher orders, all q_+ integrations will be implicit. They will be done by contour integration, with momentum-flow diagrams used to indicate which poles in the complex q_+ plane are enclosed by the contour. Momentum-flow diagrams are similar to Feynman diagrams, except that the arrow associated with the momentum of each line has a special meaning. For a line carrying four-momentum q , the arrow points in the direction of positive q_+ . There may be several momentum-flow diagrams corresponding to each Feynman diagram. For each closed loop, if all the arrows point in the same direction of flow, whether clockwise or counterclockwise, the q_+ integration is zero. If arrows of a given loop point in both directions, then specify one direction; contributions from all the poles corresponding to lines with arrows pointing in that direction must be added together. The two choices of direction correspond to closing the contour in the upper or the lower half of the q_+ plane. If there is only one pole, the line corresponding to it in the flow diagram will be marked with a cross (x). If there are two or more poles, the corresponding lines will

be marked with double slashes (//). Each integration over a pole of the form $\frac{1}{Aq_+ + B + i\epsilon}$ introduces a factor of $\frac{-2\pi i}{|A|}$.

For example, if $\Delta = 0$, there are two (non-zero) flow diagrams which correspond to the Feynman diagram shown in Fig. 45 -- they are drawn in Fig. 47. The flow diagram in

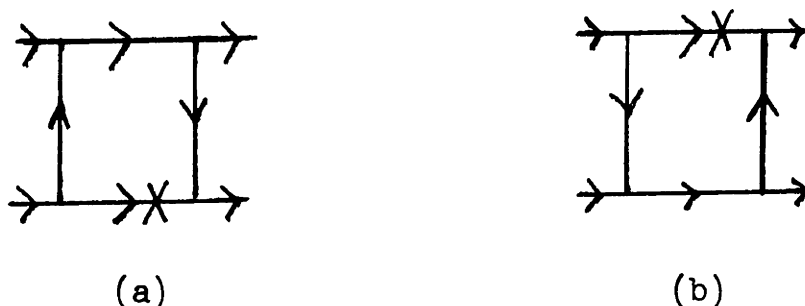


Fig. 47

Fig. 47(a) corresponds to the region (II.11b) and, as indicated in the diagram, the pole is given by (II.10b). The flow diagram in Fig. 47(b) corresponds to the region (II.11a), and does not contribute to the leading order. If $\Delta \neq 0$, there are still other flow diagrams none of which contribute to the leading order. In any calculation the flow diagram or diagrams which do contribute are always those which include the region where $q_- \gg p_{1-}$ -- so only such diagrams will be considered in the sequel. This is equivalent to assuming that the high-energy line at the top of a diagram carries no - momentum.

As an illustration of the flow-diagram technique,

consider the Feynman diagram in Fig. 48. The only contributing

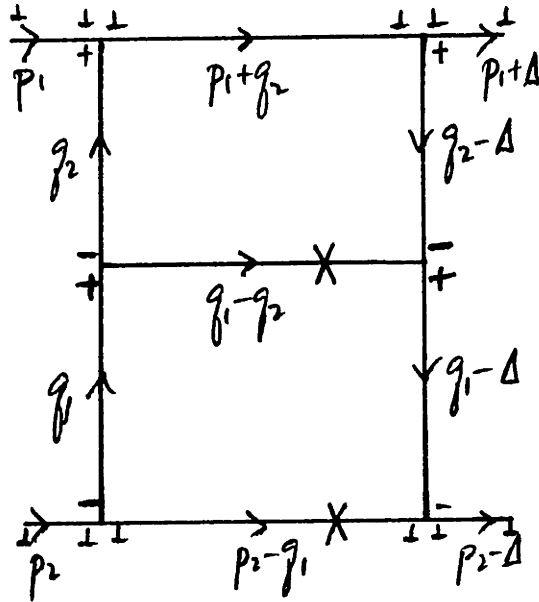


Fig. 48

flow diagram is the one with the arrows as given in that figure. The space-time amplitude is

$$\begin{aligned}
 M \sim & (-i)^{1+6+7} g^6 \frac{1}{2^2} (-2s)^2 \int \frac{d^2 \vec{q}_4}{(2\pi)^2} \frac{d^2 \vec{q}_2}{(2\pi)^2} \int \frac{dq_1}{2\pi} \frac{dq_2}{2\pi} \frac{dq_4}{2\pi} \frac{dq_2}{2\pi} N \\
 & \times \frac{1}{(p_1 + q_2 - \vec{q}_2^2 + i\varepsilon)(q_2 + q_2 - \vec{q}_2^2 - \lambda^2 + i\varepsilon)(q_2 + q_2 - (\vec{q}_2 - \vec{a}_1)^2 - \lambda^2 + i\varepsilon)(q_1 + q_1 - \vec{q}_1^2 - \lambda^2 + i\varepsilon)} \\
 & \times \frac{1}{(q_1 + q_1 - (\vec{q}_1 - \vec{a}_1)^2 - \lambda^2 + i\varepsilon)(q_4 - q_4)(q_1 - q_2) - (\vec{q}_4 - \vec{q}_2)^2 - \lambda^2 + i\varepsilon)(p_2 - q_1)(p_2 - q_1) - \vec{q}_1^2 - \lambda^2 + i\varepsilon} \\
 & \text{(II.18)}
 \end{aligned}$$

where the numerator

$$N \sim -(\vec{q}_{1+} + \vec{q}_{2+}) \cdot (\vec{q}_{1+} + \vec{q}_{2+} - 2\vec{A}_1) + \frac{(2q_{4+} - q_{2+})}{\sqrt{2}} \frac{(2q_{2-} - q_{1-})}{\sqrt{2}} + \frac{(2q_{2-} - q_{1-})}{\sqrt{2}} \frac{(2q_{4+} - q_{2+})}{\sqrt{2}} . \quad (\text{II.19})$$

Closing the contours as indicated in the figure we find, assuming $q_{1-} \ll p_{2-}$, that

$$q_{4+} = 0 \left(\frac{1}{p_{2-}} \right) \quad (\text{II.20a})$$

and

$$q_{2+} \sim - \frac{(\vec{q}_{1+} - \vec{q}_{2+})^2 + \lambda^2}{q_{1-} - q_{2-}} \quad (\text{II.20b})$$

so that

$$M \sim g^6 S^2 \int \frac{d^2 \vec{q}_{1+}}{(2\pi)^2} \frac{d^2 \vec{q}_{2+}}{(2\pi)^2} \int_0^{p_{2-}} \frac{dq_{1-}}{2\pi} \int_0^{q_{1-}} \frac{dq_{2-}}{2\pi} N \frac{1}{p_{1+} q_{2-} - \vec{q}_{2+}^2 + i\epsilon} \times \frac{1}{p_{2-} (q_{1-} - q_{2-})} \times \frac{1}{\left[- \frac{(\vec{q}_{1+} - \vec{q}_{2+})^2 + \lambda^2}{q_{1-} - q_{2-}} q_{2-} - \vec{q}_{2+}^2 - \lambda^2 \right] \left[- \frac{(\vec{q}_{1+} - \vec{q}_{2+})^2 + \lambda^2}{q_{1-} - q_{2-}} q_{2-} - (\vec{q}_{2+} - \vec{A}_1)^2 - \lambda^2 \right]} \times \frac{1}{(-\vec{q}_{1+}^2 - \lambda^2) [-(\vec{q}_{1+} - \vec{A}_1)^2 - \lambda^2]} . \quad (\text{II.21})$$

The leading contribution comes from the region

$p_{1-} \ll q_{2-} \ll q_{1-} \ll p_{2-}$, so that

$$M \sim g^6 s^2 \frac{1}{p_2^-} \int \frac{d^2 \vec{q}_{1\perp}}{(2\pi)^2} \frac{d^2 \vec{q}_{2\perp}}{(2\pi)^2} \frac{N}{(\vec{q}_{2\perp}^2 + \lambda^2) ((\vec{q}_{2\perp} - \vec{\Delta}_\perp)^2 + \lambda^2) (\vec{q}_{1\perp}^2 + \lambda^2) ((\vec{q}_{1\perp} - \vec{\Delta}_\perp)^2 + \lambda^2)}$$

$$\times \int_0^{p_2^-} \frac{dq_{1-}}{2\pi} \frac{1}{q_{1-}} \int_0^{q_{1-}} \frac{dq_{2-}}{2\pi} \frac{1}{p_2^- + q_{2-} - \vec{q}_{2\perp}^2 + i\epsilon} \quad (\text{II.22})$$

with

$$N \sim -(\vec{q}_{1\perp}^2 + \lambda^2) - (\vec{q}_{2\perp}^2 + \lambda^2) - [(\vec{q}_{1\perp} - \vec{\Delta}_\perp)^2 + \lambda^2] - [(\vec{q}_{2\perp} - \vec{\Delta}_\perp)^2 + \lambda^2]$$

$$+ 2(\vec{\Delta}_\perp^2 + \lambda^2) + \lambda^2. \quad (\text{II.23})$$

Finally,

$$M \sim g^6 s \left(\frac{\ln^2 s}{2(2\pi)^2} - i\pi \frac{\ln s}{(2\pi)^2} \right) \left(-4 \text{⊗} + 2 \text{⊗} + \lambda^2 \text{⊗} \right).$$

(II.24)

If we had calculated the crossed diagram (see Fig. 49) instead,

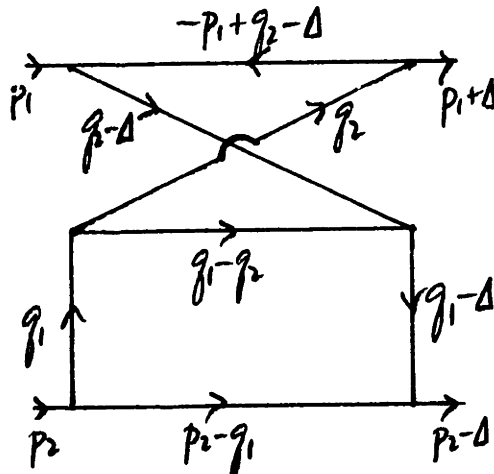


Fig. 49

the only difference would have been the propagator on the top horizontal line and this would lead to an extra minus sign and the lose of the imaginary part (see (2.11a)).

Now we will calculate the sum of the space-time amplitudes of all of the diagrams in Table V together with their four-vertex contributions. This equals (see Fig. 50 for notation)

$$\begin{aligned}
 & (-i)^{1+8+10} g^8 (-25)^3 \frac{1}{p_{1+}^2 p_{2-}^2} \frac{1}{2^3} \int \frac{d^2 \vec{q}_{1+}}{(2\pi)^2} \frac{d^2 \vec{q}_{2+}}{(2\pi)^2} \frac{d^2 \vec{q}_{3+}}{(2\pi)^2} \frac{d^2 \vec{q}_{1-}}{(2\pi)^2} \frac{d^2 \vec{q}_{2-}}{(2\pi)^2} \\
 & \times (2\pi)^2 \delta^{(2)}(\vec{q}_{1+} + \vec{q}_{2+} + \vec{q}_{3+} - \vec{\Delta}_1) (2\pi)^2 \delta^{(2)}(\vec{q}_{1-} + \vec{q}_{2-} - \vec{q}_{1-}' - \vec{q}_{2-}') \\
 & \times \int \frac{dq_{1+}}{2\pi} \frac{dq_{1+}'}{2\pi} \frac{dq_{2+}}{2\pi} \frac{dq_{2+}'}{2\pi} \frac{dq_{3+}}{2\pi} 2\pi \delta(q_{1+} + q_{2+} + q_{3+}) 2\pi \delta(q_{1+} + q_{2+} - q_{1+}' - q_{2+}') \\
 & \times \int \frac{dq_{1-}}{2\pi} \frac{dq_{1-}'}{2\pi} \frac{dq_{2-}}{2\pi} \frac{dq_{2-}'}{2\pi} \frac{dq_{3-}}{2\pi} 2\pi \delta(q_{1-} + q_{2-} + q_{3-}) 2\pi \delta(q_{1-} + q_{2-} - q_{1-}' - q_{2-}') \\
 & \times \left(\prod_{i=1}^3 \frac{1}{q_{i+} q_{i-} - \vec{q}_{i+}^2 - \lambda^2 + i\varepsilon} \right) \left(\prod_{i=1}^2 \frac{1}{q_{i+}' q_{i-}' - \vec{q}_{i+}'^2 - \lambda^2 + i\varepsilon} \right) \frac{1}{(q_{1+} - q_{1+}') (q_{1-} - q_{1-}') - (\vec{q}_{1+} - \vec{q}_{1+}')^2 - \lambda^2 + i\varepsilon} \\
 & \times \frac{1}{2} \left(\sum_{\sigma} \frac{1}{(q_{\sigma 11} - i\varepsilon)(q_{\sigma 11} + q_{\sigma 12} - i\varepsilon)} \right) \left(\sum_{\tau} \frac{1}{(-q_{\tau 11} + i\varepsilon)(-q_{\tau 11} - q_{\tau 12} + i\varepsilon)} \right) N.
 \end{aligned}$$

(II.25)

In (II.25) N is the numerator factor coming from the internal vertices plus the four-vector contribution (see Fig. 22) and equals

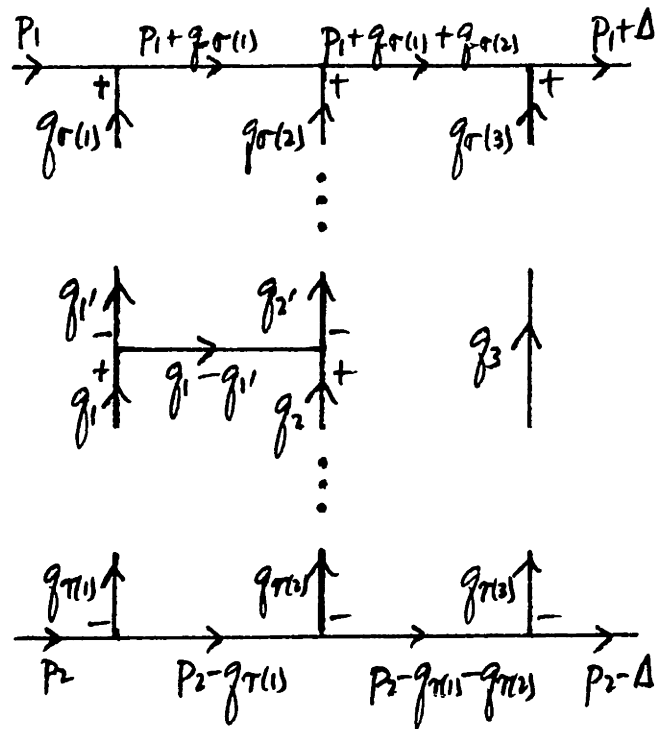


Fig. 50

$$\begin{aligned}
 & -(\vec{g}_{1+} + \vec{g}_{1-}) \cdot (-\vec{g}_{2+} - \vec{g}_{2-}) + \frac{2g_{1-} - g_{1+}}{\sqrt{2}} \frac{g_{1+} - g_{2+} - g_{1-}}{\sqrt{2}} \\
 & + \frac{2g_{1+} - g_{1-}}{\sqrt{2}} \frac{g_{1-} - g_{2-} - g_{1-}}{\sqrt{2}} + (g_{1-} - g_{1+})(g_{1+} - g_{1-}) - (\vec{g}_{1+} - \vec{g}_{1-})^2 - \lambda^2 \\
 = & g_{1+}g_{1-} - g_{2+}g_{1-} - \frac{1}{2}g_{1+}g_{1-} - \frac{1}{2}g_{1+}g_{1-} + \frac{1}{2}g_{2+}g_{1-} - g_{1+}g_{2-} + \frac{1}{2}g_{1+}g_{2-} \\
 & - (\vec{g}_{1+}^2 + \lambda^2) - (\vec{g}_{2+}^2 + \lambda^2) - (\vec{g}_{1-}^2 + \lambda^2) - (\vec{g}_{2-}^2 + \lambda^2) + 2[(\vec{g}_{1+} + \vec{g}_{2+})^2 + \lambda^2] + \lambda^2
 \end{aligned}$$

(II.26)

Each of the permutations σ and τ in (II.25) runs over the 3! ways of attaching the mesons to the high-energy lines, and

there is the product of the appropriate propagators from the high-energy lines for each permutation. Since $3! \times 3! = 36$, each of the 18 diagrams has been counted twice. To compensate for this there is an "overcounting factor" of $1/2$. From Appendix IV,

$$\delta(q_{1-} + q_{2-} + q_{3-}) \sum_{\sigma} \frac{1}{q_{\sigma(1)} - i\epsilon} \frac{1}{q_{\sigma(1)} + q_{\sigma(2)} - i\epsilon} = (-2\pi i)^2 \delta(q_{1-}) \delta(q_{2-}) \delta(q_{3-}) \quad (\text{II.27a})$$

and

$$\delta(q_{1+} + q_{2+} + q_{3+}) \sum_{\tau} \frac{1}{-q_{\tau(1)} + i\epsilon} \frac{1}{-q_{\tau(1)} - q_{\tau(2)} + i\epsilon} = (-2\pi i)^2 \delta(q_{1+}) \delta(q_{2+}) \delta(q_{3+}). \quad (\text{II.27b})$$

Thus (II.25) becomes

$$\begin{aligned} & \frac{1}{2} i g^8 \int \frac{d^2 \vec{q}_{1\perp}}{(2\pi)^2} \frac{d^2 \vec{q}_{2\perp}}{(2\pi)^2} \frac{d^2 \vec{q}_{1\perp}}{(2\pi)^2} \int \frac{dq_{1-}}{2\pi} \int_{-p_+}^{p_+} \frac{dq_{1+}}{2\pi} \prod_{i=1}^3 \frac{1}{q_{i\perp}^2 + \lambda^2} \\ & \times \prod_{i=1}^2 \frac{1}{q_{i\perp}^2 + \lambda^2} \frac{1}{-q_{1+} q_{1-} - (\vec{q}_{1\perp} - \vec{q}_{1\perp})^2 - \lambda^2} N \\ & \sim \frac{1}{4} g^8 \int \frac{d^2 \vec{q}_{1\perp}}{(2\pi)^2} \frac{d^2 \vec{q}_{2\perp}}{(2\pi)^2} \frac{d^2 \vec{q}_{1\perp}}{(2\pi)^2} \left(\prod_{i=1}^3 \frac{1}{q_{i\perp}^2 + \lambda^2} \right) \left(\prod_{i=1}^2 \frac{1}{q_{i\perp}^2 + \lambda^2} \right) \int \frac{dq_{1-}}{2\pi} \frac{N}{|q_{1-}|} \\ & \quad p_{2-} \rightarrow |q_{1-}| > p_{1-} \\ & \Rightarrow g^6 \frac{g^2 \ln s}{2\pi} \left(\bigcirc + \frac{1}{2} \lambda^2 \bigcirc \right) \quad (\text{II.28}) \end{aligned}$$

where the divergent terms have been dropped.

Appendix III. Transverse-Momentum Diagrams

Transverse-momentum diagrams stand for integrals over the transverse momenta. Each diagram consists of a series of vertices arranged vertically connected by line segments. Transverse momentum $\vec{\Delta}_\perp$ flows into the bottom vertex and out of the top vertex; and in between the momentum is conserved at each vertex. The integrals which the diagrams stand for are determined by the following rules:

- i) a factor of $\frac{1}{\vec{q}_\perp^2 + \lambda^2}$ for each line segment carrying momentum \vec{q}_\perp , unless there is a horizontal bar through that segment, in which case there is no factor;
- ii) $\int \frac{d^2 k_\perp}{(2\pi)^2}$ for each closed loop; and
- iii) for each horizontal bar through a vertex, a factor of $(\vec{q}_\perp^2 + \lambda^2)$ where \vec{q}_\perp equals the sum of the momentum coming into the vertex from below.

We give three examples in Fig. 51 which stand for

$$\int \frac{d^2 \vec{q}_\perp}{(2\pi)^2} \frac{1}{(\vec{q}_\perp^2 + \lambda^2) [(\vec{\Delta}_\perp - \vec{q}_\perp)^2 + \lambda^2]},$$

$$(\vec{\Delta}_\perp^2 + \lambda^2) \int \frac{d^2 \vec{q}_{1\perp}}{(2\pi)^2} \frac{d^2 \vec{q}_{2\perp}}{(2\pi)^2} \frac{1}{(\vec{q}_{1\perp}^2 + \lambda^2) [(\vec{\Delta}_\perp - \vec{q}_{1\perp})^2 + \lambda^2] [\vec{q}_{2\perp}^2 + \lambda^2]},$$

and

$$\int \frac{d^2 \vec{q}_{1\perp}}{(2\pi)^2} \frac{d^2 \vec{q}_{2\perp}}{(2\pi)^2} \frac{d^2 \vec{q}_{3\perp}}{(2\pi)^2} \frac{(\vec{q}_{1\perp} + \vec{q}_{2\perp})^2 + \lambda^2}{(\vec{q}_{1\perp}^2 + \lambda^2) (\vec{q}_{2\perp}^2 + \lambda^2) (\vec{q}_{3\perp}^2 + \lambda^2) [(\vec{q}_{1\perp} + \vec{q}_{2\perp} - \vec{q}_{3\perp})^2 + \lambda^2] [(\vec{\Delta}_\perp - \vec{q}_{1\perp} - \vec{q}_{2\perp})^2 + \lambda^2]}$$

respectively. Note that the second integral above is divergent.

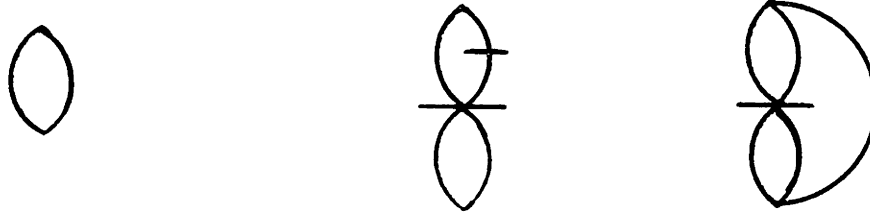


Fig. 51

Appendix IV. Identities Involving Sums
of Products of Propagators

In this appendix we will prove various formulas which express the sums of products of propagators on the high-energy lines in terms of delta functions. These sums are over various ways in which the exchanged mesons can be attached to the high-energy lines, weighted according to their isospin factors. The simplest example is when all diagrams have the same isospin factor so that their space-time amplitudes may be added together. In this case we wish to evaluate

$$\delta\left(\sum_{i=1}^n q_i\right) \sum_{\sigma} \frac{1}{(q_{\sigma(1)} + i\varepsilon)} \frac{1}{(q_{\sigma(1)} + q_{\sigma(2)} + i\varepsilon)} \cdots \frac{1}{\left(\sum_{i=1}^{n-1} q_{\sigma(i)} + i\varepsilon\right)} \quad (\text{IV.1})$$

where σ is the permutation of the integers $\{1, 2, \dots, n\}$ which takes i into $\sigma(i)$, and the sum in (IV.1) is over all $n!$ permutations. Consider the Fourier transform of a single term in (IV.1),

$$\begin{aligned} & \int \prod_{i=1}^n dq_i \prod_{i=1}^n e^{-ik_i q_i} \delta\left(\sum_{i=1}^n q_i\right) \frac{1}{q_1 + i\varepsilon} \frac{1}{q_1 + q_2 + i\varepsilon} \cdots \frac{1}{q_1 + q_2 + \dots + q_{n-1} + i\varepsilon} \\ &= \int \prod_{i=1}^{n-1} dq_i \prod_{i=1}^{n-1} e^{-i(k_i - k_n) q_i} \frac{1}{q_1 + i\varepsilon} \frac{1}{q_1 + q_2 + i\varepsilon} \cdots \frac{1}{q_1 + q_2 + \dots + q_{n-1} + i\varepsilon} \end{aligned} \quad (\text{IV.2})$$

If $k_n > k_{n-1}$ the contour may be closed in the upper half of the complex q_{n-1} plane to give zero; and if $k_{n-1} > k_n$, by closing in the lower-half-plane, (IV.2) equals

$$(-2\pi i) \int \prod_{i=1}^{n-2} dq_i \prod_{i=1}^{n-2} e^{-i(k_i - k_{n-1})q_i} \frac{1}{q_1 + i\epsilon} \frac{1}{q_1 + q_2 + i\epsilon} \dots \frac{1}{q_1 + q_2 + \dots + q_{n-2} + i\epsilon}. \quad (\text{IV.3})$$

Continuing in this manner we find that (IV.2) equals

$$\begin{cases} (-2\pi i)^n & \text{if } k_1 > k_2 > \dots > k_{n-1} > k_n \\ 0 & \text{otherwise.} \end{cases} \quad (\text{IV.4})$$

Therefore, summing over all permutations,

$$\int \prod_{i=1}^n dq_i \prod_{i=1}^n e^{-ik_i q_i} \delta\left(\sum_{i=1}^n q_i\right) \sum_{\sigma} \frac{1}{q_{\sigma(1)} + i\epsilon} \dots \frac{1}{\sum_{i=1}^n q_{\sigma(i)} + i\epsilon} = (-2\pi i)^{n-1}, \quad (\text{IV.5})$$

and taking the inverse Fourier transform, (IV.1) equals

$$(-2\pi i)^{n-1} \prod_{i=1}^n \delta(q_i). \quad (\text{IV.6})$$

This identity was first established by Cheng and Wu¹³ to show that the multi-photon exchange amplitudes in QED eikonalize. Particularized to the case $n = 2$, as in (2.15), it was used

above to show that the amplitudes in (2.8), (2.16), (2.17), (2.23), (2.24), (3.7), (3.8) and (3.9) are purely imaginary in the leading order.

Next we evaluate

$$\delta\left(\sum_{i=1}^3 q_i\right) \left(\frac{1}{(q_3+i\varepsilon)(q_3+q_2+i\varepsilon)} + \frac{1}{(q_3+i\varepsilon)(q_3+q_1+i\varepsilon)} + \frac{1}{(q_2+i\varepsilon)(q_2+q_3+i\varepsilon)} \right). \quad (\text{IV.7})$$

If we define

$$(k_1 k_2 \dots k_n) = \begin{cases} 1 & \text{if } k_1 > k_2 > \dots > k_n \\ 0 & \text{otherwise} \end{cases} \quad (\text{IV.8})$$

then the Fourier transform of (IV.7) is

$$(-2\pi i)^2 \left((321) + (312) + (231) \right) = (-2\pi i)^2 (31). \quad (\text{IV.9})$$

And the inverse transform of (IV.9) is

$$(-2\pi i)^2 \int_{k_3 > k_1} \frac{dk_1}{2\pi} \frac{dk_2}{2\pi} \frac{dk_3}{2\pi} e^{ik_1 q_1 + ik_2 q_2 + ik_3 q_3} = (-2\pi i) \frac{1}{q_3+i\varepsilon} \delta(q_3+q_1) \delta(q_2), \quad (\text{IV.10})$$

thus verifying (2.19), (3.18) and (3.38). This illustrates

the general idea: transform to k-space, simplify and transform back to q-space.

As another example, the Fourier transform of the term on the left-hand side of (2.26) is

$$\begin{aligned} (-2\pi i)^2 & \left(-3(321) - (213) - (132) - 2(312) - 2(231) \right) \\ & = (-2\pi i)^2 \left(-(21) - (31) - (32) \right). \end{aligned} \quad (\text{IV.11})$$

Inverting the transform verifies (2.26) and (3.22).

Other identities valid in the Fourier transform k-space are:

$$(123) + (132) + (312) - (213) - (231) - (321) = (12) - (21) \quad (\text{IV.12})$$

thus verifying (3.26);

$$(231) - (132) = (23) - (13) \quad (\text{IV.13})$$

thus verifying (3.29);

$$\begin{aligned} & 4(4321) + 4(3421) + 4(4312) + 4(4231) + (1423) + 3(3241) \\ & + (1342) + 3(2431) + (2314) + 3(4132) + (3124) + 3(4213) + (1432) \\ & + 3(2341) + (3214) + 3(4123) + 4(3412) + 2(2413) + 2(3142) \\ & = (42) + (31) + 2(41) \end{aligned} \quad (\text{IV.14})$$

thus verifying (3.54);

$$\begin{aligned}
 & -6(4321) - (1243) - 5(3421) - (2134) - 5(4312) - (1324) - 5(4231) \\
 & - 2(1423) - 4(3241) - 2(1342) - 4(2431) - 2(2314) - 4(4132) - 2(3124) \\
 & - 4(4213) - 3(1432) - 3(2341) - 3(3214) - 3(4123) - 2(2143) - 4(3412) \\
 & - 3(2413) - 3(3142) \\
 & = -(21) - (31) - (41) - (32) - (42) - (43) \qquad \text{(IV.15)}
 \end{aligned}$$

thus verifying (3.55);

$$\begin{aligned}
 & -(4321) - (3421) - (4312) - (4231) - (3241) - (2431) - (4132) - (4213) \\
 & - (2341) - (4123) - (3412) - (2413) \\
 & = -(41) \qquad \text{(IV.16)}
 \end{aligned}$$

thus verifying (3.58); and

$$\begin{aligned}
 & 7(4321) + 4(3421) + 4(4312) + 4(4231) + 2(3241) + 2(2431) + 2(4132) \\
 & + 2(4213) + (1432) + (3214) + (2143) + 2(3412) + (2413) + (3142) \\
 & = (321) - (341) - (413) + (421) + (432) \\
 & \quad + (21)(43) + (31)(42) + (41)(23) + 2(41)(32) \qquad \text{(IV.17)}
 \end{aligned}$$

thus verifying (3.59).

References

1. H. Cheng and T.T. Wu, Phys. Rev. Lett. 24, 1456 (1970) and references quoted therein.
2. B.M. McCoy and T.T. Wu, Phys. Rev. D 12, 3257 (1975); 13, 1076 (1976); L. Tyburski, Phys. Rev. D 13, 1107 (1976); H.T. Nieh and Y.-P. Yao, *ibid.* 13, 1082 (1976); C.Y. Lo and H. Cheng, *ibid.* 13, 1131 (1976). See also L.N. Lipatov, Yad. Fiz. 23, 642 (1976) (Sov. J. Nucl. Phys. 23, 338 (1976)).
3. H. Cheng and C.Y. Lo, Phys. Rev. D 15, 2959 (1977).
4. V.S. Fadin, E.A. Kuraev and L.N. Lipatov, Phys. Lett. 60B, 50 (1975).
5. M. Froissart, Phys. Rev. 123, 1053 (1961).
6. H. Cheng, J. Dickinson, C.Y. Lo, K. Olausen and P.S. Yeung, Phys. Lett. 76B, 129 (1978).
7. H. Cheng, J. Dickinson, C.Y. Lo and K. Olausen (to be published).
8. J. Dickinson, Phys. Rev. D 16, 1863 (1977).
9. C.Y. Lo, D.Sc. thesis, M.I.T. (1976).
10. For the Feynman rules, see G. 't Hooft and M. Veltman in "Renormalization of Yang-Mills Fields and Applications to Particle Physics," edited by C.P. Korthals-Altes (C.N.R.S., Marseille, France, 1972).
11. For a discussion of the infinite-momentum space technique see H. Cheng and T.T. Wu, Phys. Rev. 182, 1899 (1969).
12. For a reference on momentum-flow diagrams see B.M. McCoy and T.T. Wu, Phys. Rev. D 13, 379 (1976).
13. H. Cheng and T.T. Wu, Phys. Rev. 186, 1611 (1969).
14. T. Regge, Nuovo Cimento 14, 951 (1959).
15. N. Byers and C.N. Yang, Phys. Rev. 142, 976 (1966); T.T. Chou and C.N. Yang, *ibid.*, 170, 1591 (1968); Phys. Rev. Letts. 20, 1213 (1968).

16. R. P. Feynman, "Photon-Hadron Interactions", (Benjamin, Mass. 1972).
17. D. Amati, S. Fubini and A. Stanghellini, *Nuovo Cimento*, 26, 896 (1962).
18. C. N. Yang and R. Mills, *Phys. Rev.* 96, 191 (1954).
19. S. Weinberg, *Phys. Rev. Letts.* 19, 1264 (1967); A. Salam in "Elementary Particle Physics", ed. by N. Svartholm (Almqvist and Wiksells, Stockholm, 1968).
20. G. 't Hooft, *Nucl. Phys.* B33, 173 (1971); B. W. Lee, *Phys. Rev.* D6, 1188 (1972).
21. D. Gross and F. Wilczek, *Phys. Rev. Letts.* 26, 1343 (1973); H. D. Politzer, *ibid.*, 1346 (1973).
22. C. Y. Lo, Invariant Symmetric Tensors and the Generalized Leading Term Approximation in Yang-Mills Theories (unpublished). High-Energy Scattering Amplitudes of Yang-Mills Theory I (up to the eighth order perturbation) (unpublished). High-Energy Scattering Amplitudes of Yang-Mills Theories in Generalized Leading-Term Approximation and Eikonal Formulas (unpublished).
23. For references on these graphical methods, see R. Penrose in *Combinatorial Mathematics and Its Application*, ed. D. J. A. Welsh, Academic Press (N.Y., 1971), pp. 221-244; E. El-Baz and B. Castel, *Graphical Methods of Spin Algebras* (Dekkar, N.Y., 1972); G. P. Canning, *Phys. Rev. D* 8, 1151 (1973); G. P. Canning, Niels Bohr Inst. Report No. NBI-HE-24-2, 1974 (unpublished); G. P. Canning, *Phys. Rev. D* 12, 2505 (1975); P. S. Yeung, *Phys. Rev. D* 13, 2306 (1976); R. F. Cahalan and D. Knight, *ibid.* 14, 2126 (1976); P. Cvitanovic, *ibid.*, 14, 1536 (1976); J. Mandula, MIT course notes.